January 2019

Alpha1a-Adrenergic Receptor Modulation Of Epileptiform Activity And Seizures

Joseph Patrick Biggane

ALPHA1A-ADRENERGIC RECEPTOR MODULATION OF EPILEPTIFORM ACTIVITY AND SEIZURES

by

Joseph Patrick Biggane
Bachelor of Science, Mayville State University, 2013

A Dissertation

Submitted to the Graduate Faculty

of the

University of North Dakota

in partial fulfillment of the requirements

for the degree of

Doctor of Philosophy

Grand Forks, North Dakota

December
2019

This dissertation, submitted by Joseph P. Biggane in partial fulfillment of the requirements for the Degree of Doctor of Philosophy from the University of North Dakota, has been read by the Faculty Advisory Committee under whom the work has been done and is hereby approved.

Van Doze

Jane Dunlevy

Kumi Nagamoto-Combs

David Bradley

Donald Sens

This dissertation is being submitted by the appointed advisory committee as having met all of the requirements of the School of Graduate Studies at the University of North Dakota and is hereby approved.

Dr. Chris Nelson, Associate Dean
School of Graduate Studies

11/26/19
Date

PERMISSION

Title Alpha1A-Adrenergic Receptor Modulation of Epileptiform Activity and Seizures

Department Biomedical Sciences

Degree Doctor of Philosophy

In presenting this dissertation in partial fulfillment of the requirements for a graduate degree from the University of North Dakota, I agree that the library of this University shall make it freely available for inspection. I further agree that permission for extensive copying for scholarly purposes may be granted by the professor who supervised my dissertation work or, in his absence, by the Chairperson of the department or the dean of the School of Graduate Studies. It is understood that any copying or publication or other use of this dissertation or part thereof for financial gain shall not be allowed without my written permission. It is also understood that due recognition shall be given to me and to the University of North Dakota in any scholarly use which may be made of any material in my dissertation.

Joseph P. Biggane
November 01, 2019

TABLE OF CONTENTS

LIST OF FIGURES

LIST OF TABLES

Table Page

ACKNOWLEDGEMENTS

I wish to express my highest gratitude to Dr. Van Doze. Upon graduation from one of the smallest state universities in the country, Mayville State University, Van pointed me in the direction of graduate school and later offered me a technician role in his lab, where I matriculated as a graduate student. In addition to providing me with the opportunity of a lifetime, I appreciate the candid conversations that helped keep me out of, and occasionally get into, trouble during my time here at the University of North Dakota. I would especially like to thank Dr. Thomas Gonnella, whom provided me with an undergraduate research experience, which in my opinion, was second to none. Despite limited resources, we were able to do research which was not only published in highly regarded peer-reviewed journals, but even win an award for this research and present at regional and national conferences. My undergraduate research was probably the single most important factor that led me to be accepted at both major graduate universities in North Dakota, an aspect for which I will forever be appreciative. All of my early success would not have been possible had it not been for a chance encounter following a major injury during my college football career; while one career was in jeopardy, Dr. Gonnella and my undergraduate education advisor, Dr. Robert Miess, opened another career opportunity, which I attribute to my present situation. I would like to thank Mr. Joel Pierson, my high school chemistry teacher, whom sparked my interest in pursuing a bachelor's in chemistry during my formative years, and whom gave me a rock-solid introduction to the organization of the periodic table and, perhaps more pertinently, to

stoichiometry. Without such an enthusiastic teacher, I am not sure any of the aforementioned achievements would have been possible. I would like to thank my committee members, here at the University of North Dakota: Drs. Van Doze, Jane Dunlevy, Kumi Nagamoto-Combs, David Bradley and Don Sens. I am grateful for their acceptance to take me on as an advisee and who have all provided me with great guidance along the way. Importantly, I am lucky to have a committee that always made me feel welcome and were just as likely, if not more so, to strike up a casual conversation about how my day was going, or how my daughter was doing; for this I am especially appreciative. Although I wish to keep this section succinct, I would be remised to fail to mention my wife, best friend, and colleague, Dr. Emily Biggane. I would like to thank you for your unconditional love and support; also, the ability to have someone look at my work and listen to my presentations, from the perspective of a scientist, was invaluable to making my expressed thoughts coherent. I would like to thank my daughter Eleanor, who has given me infinitely more reasons to smile, and for always letting me know when my presentations are too boring, never failing to fall asleep during practice. I would like to thank my dogs, Jack and Jill, who always remind me what is most important in life, taking time to enjoy it…and belly rubs. I would like to thank my parents (Tim and Judy), sister (Holly), and the rest of the family (Jeremy, Skyler, Grace, and Caden) who were always supportive of my interests in science and breaking my toys to see how they worked. I would also like to thank them for continuing to support me throughout life, despite my incessant questioning (Why?) at every turn. Lastly, there are many others who supported my work and allowed me to pursue a career in science. I appreciate all those

who were supportive on this long and unexpected, but very enjoyable, journey; one which I hope is only beginning.

To my wife Emily, my daughter Eleanor, and my pups,

I have always had the will, but you showed me the way. No asymptotic limits!

ABSTRACT

The research herein aimed to increase our understanding about potential roles of adrenergic receptor subtypes in epileptic seizures and seizure-like (epileptiform) phenomena. Previous observations in our laboratory led us to hypothesize that the α_{1A}-adrenergic receptor is a critical component of the modulatory role of the α_1-adrenergic receptor, and more broadly, norepinephrine, on epileptiform and seizure activity. We utilized a combination of genetic and pharmacological manipulation to elucidate specific effects of the α_{1A}-adrenergic receptor subtype on altering hyperactivity in models of epilepsy, both in slice and *in vivo*. This research sought to address three main research questions: (1) What are the specific contributions of α_1-adrenergic receptor subtypes to alterations of epileptiform activity?; (2) Do any α_{1A}-adrenergic receptor alterations to epileptiform activity translate from tissue slices to *in vivo* models?; (3) Can we utilize genetically modified mice to identify possible candidate cell types of α_{1A}-adrenergic receptor expression? All of these questions are an attempt to circumvent historical difficulties with a lack of specificity of subtype-specific ligands and antibodies.

We found that α_{1A}-adrenergic receptor activation confers an antiepileptic effect, which was consistent with expectations formulated from previous observations of indirect neural circuit modulation. Specifically, previous observations from our laboratory strongly suggest that α_{1A}-adrenergic receptors confer hyperexcitation of hippocampal inhibitory interneurons. Interestingly, our approach also revealed that the α_{1A}-adrenergic receptor is important for maintaining optimal brain excitability, both *in vitro* and *in vivo*. This is exemplified by our characterization of unprovoked, recurrent seizures and exacerbated epileptiform burst frequency in α_{1A}-adrenergic receptor knockout mice.

Meanwhile, *in vitro* studies suggested little role for the other centrally expressed α_1-adrenergic receptor, the α_{1B}-adrenergic receptor, within our model systems. Our investigation of α_{1A}-adrenergic receptor expression used fluorescence microscopy and genetically-induced receptor reporter expression to better understand the observed phenomena. We show evidence for occasional α_{1A}-adrenergic receptor reporter co-localization on parvalbumin-expressing puncta and, more broadly, reporter localization consistent with inhibitory interneuron expression, within the mouse hippocampus.

Collectively, these findings suggest that the α_{1A}-adrenergic receptor contributes to demonstrated antiepileptic effects of the adrenergic system and that loss of this receptor subtype is demonstrably unfavorable to the maintenance of normal brain excitability and to the resistance of epileptiform activity. Additionally, our findings demonstrate the value of genetically modified animal models when chemical characterization is infeasible. These findings suggest that the α_{1A}-adrenergic receptor may represent a promising and unexplored therapeutic target and/or biomarker for epilepsy. Importantly, the proposed therapeutic pathway for α_{1A}-adrenergic receptor modulation is novel and may be used more broadly to evaluate the potential of interneuron-modulation in epilepsy. Even today, one-third of all people with epilepsy have no effective therapeutic option.

CHAPTER I
INTRODUCTION

Science is a sluggish beast of burden from which constant failure bestows the greatest knowledge. Science is a titillating gem whose sheen holds untold riches just out of reach. Today, much of the profound discoveries in science are incremental in nature. The significance of many findings are not well-understood for decades and sometimes lifetimes. The research herein represents the collaborative efforts of many researchers, past and present, working diligently to elucidate the puzzles of nature.

The interest of this dissertation was to investigate whether a receptor with roots in the origins of our laboratory could prove a novel and useful approach to treating a disease which has burdened humankind throughout much of our history and still represents a significant burden to modern-day medicine. More directly, we aimed to better understand the physiological mechanism for the actions of the noradrenergic system in epilepsy. Research of these mechanisms has led us to the hypothesize that the α_{1A}-adrenergic receptor (AR) is responsible for α_1-AR-mediated antiepileptic properties. Our research here explored this hypothesis by isolating α_1-AR subtype contributions; characterized potential translatability to an *in vivo* seizure model; and identified representative α_{1A}-AR expression patterns within the mouse hippocampus. Unexpectedly, our research also led to findings pertaining to the potential consequences of α_{1A}-AR loss-of-function.

Seizures, the functional consequence of epilepsy are thought to be the product of network dysfunction. Likewise, the noradrenergic system is thought to act in the brain as a large-scale modulator; thus, these concepts seemed to be a natural pairing. Unsurprisingly, there exists significant evidence to suggest a role for the noradrenergic system in epilepsy. However, for reasons we will discuss, the physiological participants in these antiepileptic effects remain poorly understood.

The Noradrenergic System

Norepinephrine and Epinephrine

Norepinephrine and epinephrine are endogenous catecholamine signaling molecules, which modulate diverse alterations in the periphery and in the brain. Both norepinephrine and epinephrine are produced within the adrenal medulla, sympathetic nervous system, and central nervous system (Molnoff *et al.*, 1971). Epinephrine is mostly synthesized in the medulla of the adrenal glands, where it is released into the bloodstream as a hormone, especially in the presence of stressful stimuli. Norepinephrine is also produced here and released to a lesser extent (Lymperopoulos, 2016; Currie, 2010). Norepinephrine is produced in large part by the sympathetic and central nervous systems. (Mollnoff *et al.*, 1971; Simpson *et al*., 2007). The production of norepinephrine within the central nervous system is discussed later, in detail.

Norepinephrine and epinephrine are derivatives of the amino acid tyrosine. The dominant pathway for norepinephrine and epinephrine synthesis is initiated by the conversion of tyrosine to DOPA, via the rate-limiting enzyme tyrosine hydroxylase (Nagatsu *et al*., 1964). DOPA is then converted to dopamine, which subsequently undergoes β-hydroxylation to form norepinephrine, via dopamine β-hydroxylase

(Kaufman, 1965; Weinshilboum1971). Finally, phenethanolamine-N-methyltransferase converts norepinephrine to epinephrine by methylation of the amine of norepinephrine (Molnoff *et al*., 1971). The synthesis of norepinephrine and epinephrine, as well as minor synthesis pathways are illustrated in Figure 1.

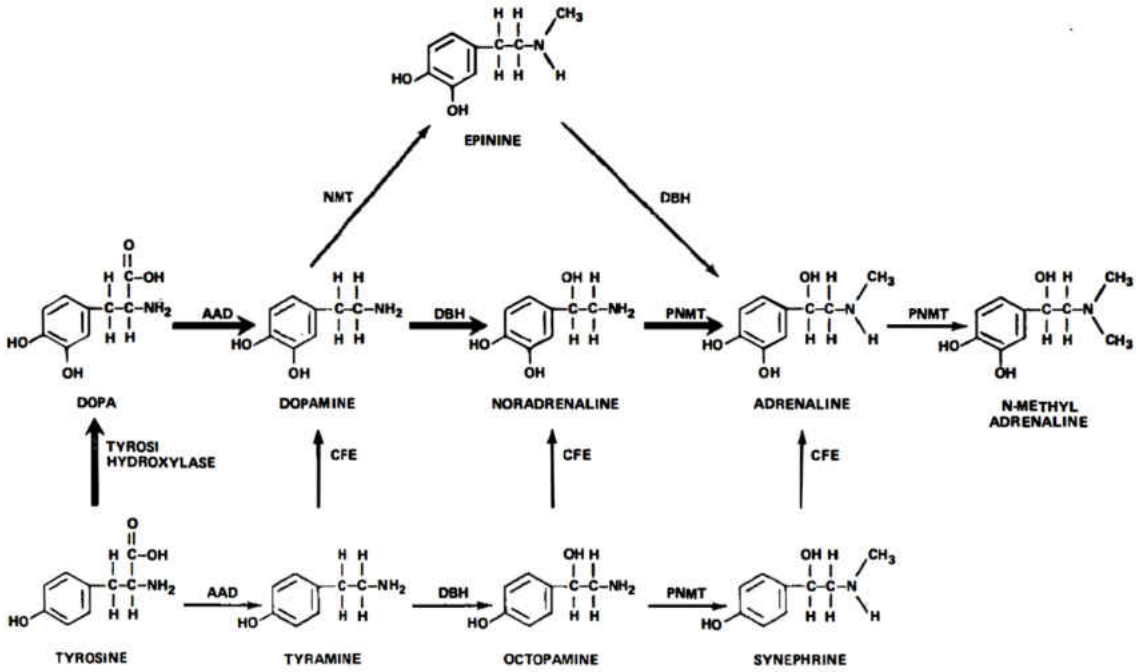

Figure 1. Biosynthesis of Catecholamines. DBH-dopamine-, β-hydroxylase; NMT-nonspecific methyltransferase; AAD-aromatic acid decarboxylase; PNMT - phenylethanolamine-N -methyltransferase; CFE-catecholamine-forming enzyme. Republished with permission of Annual Reviews, from *Biochemistry of Catecholamines*, P. Molinoff, and, and J. Axelrod, Volume 40, 1971; permission conveyed through Copyright Clearance Center, Inc.

Adrenergic Receptors

The ARs are the receptive elements to norepinephrine and epinephrine. ARs are a family of seven transmembrane-domain G-protein coupled receptors (GPCRs) (Lefkowitz, 2007; Rasmussen *et al*., 2007; Rasmussen *et al*., 2011; Westfield *et al*., 2011). There are nine known genetically-unique adrenergic receptor subtypes; these are the α_{1A}-, α_{1B}-, α_{1D}-, α_{2A}-, α_{2B}-, α_{2C}-, β_1-, β_2-, and β_3-ARs (Bylund *et al.,* 1994; Hieble *et*

al., 1995) (Fig. 2). These receptors are more generally classified as the α_1-, α_2-, or β-ARs and are differentiated based upon genetic similarities and differential affinities and responsiveness to various adrenergic agonists and antagonists (Bylund, 2006; Lefkowitz, 1979). An additional classification criteria is the most commonly associated heterotrimeric G-protein signaling protein; the α_1-ARs associate with $G_{q/11}$ proteins, the α_2-ARs with G_i proteins, and the β-ARs with G_s proteins (Finch *et al*., 2006). The classifications of G-proteins are based upon the characteristic α-subunit of the protein complex (Finch *et al*., 2006). $G_{q/11}$ signaling results in activation of phospholipase C with subsequent production of inositol triphosphate and diacylglycerol second messengers (Black, 2012). G_s and G_i signaling either activates or inhibits adenylyl cyclase function, respectively. Adenylyl cyclase produces cyclic adenosine monophosphate (cAMP), a second messenger important for many physiological processes (Halls, 2017).

Differences between the AR subtypes have been more difficult to delineate because a high degree of overlap between the binding sites leads to promiscuity towards many ligands (Finch *et al*., 2006); this is especially apparent in the α_1-ARs where only two residues differentiate primary ligand binding site to the α_{1A}-AR and α_{1B}-AR (Hwa *et al*., 1995; 1996). Demonstrated differences in efficacies in tissue and cell models are attributed to several factors. The most well-understood factors to contribute to observed differences in efficacies are cell-specific expression and localization and/or differences in G-protein subtype binding (Finch *et al*., 2006); Additionally, there are several lines of evidence suggesting AR alternative signal transduction pathways not associated with G-protein alpha subunits (Koch, 1994; Crespo, 1995), or signaling independent of G-protein second messenger pathways altogether (Tang *et al*., 1999; Xu *et al*., 1999; Pupo *et al*.,

2003; Wang, 2002; Lefkowitz, 2005). GPCRs sometimes also exhibit biased agonism, wherein a ligand binds prior to inactive second messenger coupling, allowing for other signal transducer couplings; this has been shown in several ARs (Wissler, 2018; DeGraff, 1999; Copik, 2015). A final layer of complexity to AR signaling is that these receptors exhibit a high degree of heterogeneous cellular localization; this is made particularly evident by the example of the α_{1D}-AR, which, for unknown reasons, are mostly localized to intracellular membranes. (McCune, 2000; Garcia-Sainz, 1999; Gisbert, 2000; Piascik *et al*., 2006). As a result of these and other potential factors, many AR subtypes exhibit disparate and sometimes opposing effects from other subtypes of that class when activated.

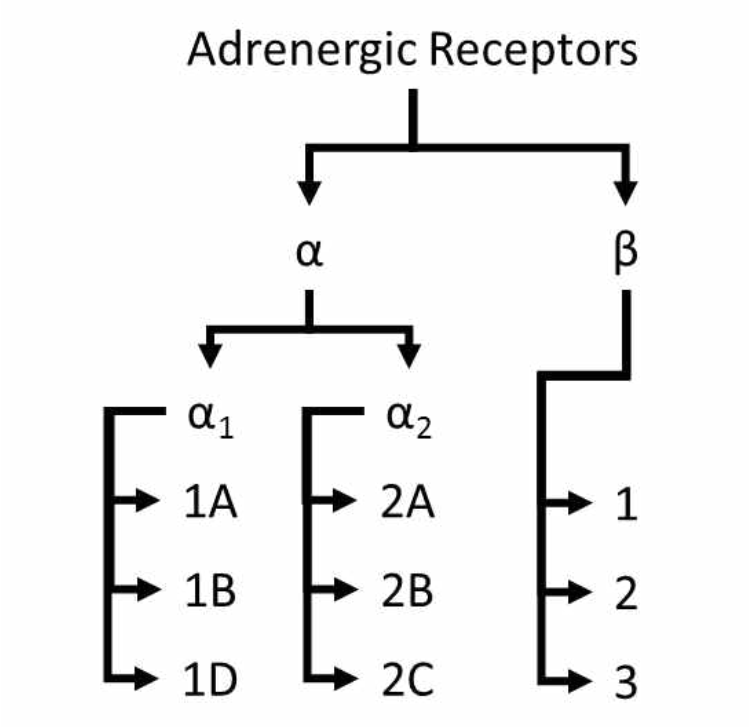

Figure 2. Current Classification of the Adrenergic Receptors. Representation of currently accepted adrenergic receptor classification based on successfully cloned

receptors. Hierarchical scheme divides each pharmacologically-unique class (α_1-, α_2-, or β-AR), followed by subtype division by pharmacological and genetic differentiations.

Our research has found functional evidence to suggest that the α_1-ARs seem to be expressed on inhibitory interneurons in the hippocampus (Bergles, 1996; Hillman, 2009). This seems to be unique to the α_1-ARs. Previous research in the Doze lab has identified clear evidence of excitatory (pyramidal) cell β-AR and α_2-AR function, but not of α_1-ARs (Jurgens *et al*., 2005; Jurgens *et al*., 2005b; Hillman *et al*., 2005; Hillman *et al*., 2007; Jurgens *et al*., 2007; Goldenstein *et al*., 2009). The focus of this dissertation research, α_1-ARs, are typically thought of as excitatory in nature, but due to the hypothesized expression on inhibitory interneurons, our findings show a counterintuitive inhibitory effect on brain excitability.

Central Noradrenergic Neuraxis

In mammals, the bulk of central NE is produced in the locus coeruleus, a dorsal pontine nuclear complex within the periventricular gray of the isthmus (Simpson *et al*., 2007; Giorgi *et al*., 2004). Noradrenergic fibers form both ascending and descending tracts, with the ascending tract exhibiting a high degree of collateralization, while the main fibers form a dorsal tegmental bundle that extends anterior and ventrally to join the medial forebrain bundle (Simpson *et al.,* 2007). The NE produced by these neurons is mainly released via volume transmission from non-synaptic varicosities (Aston-Jones, 2016). Noradrenergic fiber tracing suggests that each far-reaching, highly branched axon innervates the entire cerebral cortex (Giorgi *et al*., 2004). Despite this apparently unspecific and global innervation pattern, some areas, such as the hippocampus, receive

direct innervations from noradrenergic axon terminals (Foote *et al*., 1983; Blackstad, 1967).

Together, the anatomy of the noradrenergic fibers and the volume transmission of norepinephrine suggests a primary role for norepinephrine as a modulatory neurotransmitter. Many lines of evidence support this claim, including studies showing that norepinephrine alters neural oscillation patterns, which affects state of vigilance and the sleep-wake cycle (Aston-Jones, *et al*., 1981; 1991; 1994; Giorgi, 2004). Because of this broad action, region-specific actions of NE are thought to be conveyed by inherent differences in the expression of NE receptors, which are the ARs.

Historical Perspectives and Classification of the Noradrenergic System

Despite our relatively limited understanding of the complex nature of the noradrenergic system, it may be surprising that noradrenergic research underlies several important advances in our understanding of receptors and cellular signaling. Around the turn of the 20th century, John Abel published his work describing the isolation of the first hormone, epinephrine (Abel, 1899; Bylund, 2006). However, it is worth noting that others disputed his claim, especially Jokichi Takamine, who was working to extract the hormone around the same time as early work by Abel and was the first to publish his discovery of the pure crystalized form, which he referred to as Adrenalin (Arthur, 2015; Takamine, 1901; Parascandola, 2010). Interestingly, it was not realized until later that neither scientist had isolated pure epinephrine, though Takamine was closer, as his crystal isolation only contained norepinephrine impurities (Parascandola, 2010). Interestingly, though the controversy has mostly faded, remnants of this tumult exists in the regional differences in terminology and inconsistencies of receptor nomenclature. Specifically,

while much of the world refers to the endogenous catecholamines, noradrenaline and adrenaline, researchers and medical practitioners in the United States refers to the same chemicals as norepinephrine and epinephrine, in recognition of Abel. However, interestingly, the receptive elements are called adrenergic receptors, perhaps, as a concession to recognize both Abel and Takamine. Regardless of the true discoverer, the work of these researchers, as well as that of Thomas Aldrich, firmly placed noradrenergic research at the forefront of many discoveries to come.

Shortly thereafter, Sir Henry Dale utilized epinephrine in his work describing the effects of ergot alkaloids on epinephrine in the sympathetic nervous system, on the nature of receptive mechanisms (Bylund, 2006; Schild, 1997; Dale, 1906). Norepinephrine was discovered shortly after this initial flurry of discoveries. In the late 1940s, the laboratory of Raymond Ahlquist furthered our understanding of receptors when his laboratory utilized several norepinephrine and epinephrine synthetic analogs to demonstrate the presence of multiple classes of receptors by showing that variable responses could be elicited from the same agonist depending on the tissue studied (Ahlquist, 1948; Ahlquist, 1973). This work was a great advancement in our understanding, which provided the antecedents of Receptor Theory. More generally, these findings provided a much greater understanding of the physiology underlying the responses of our cells to stimuli.

Our current classification of the 9 distinct AR subtypes is the result of studious pharmacological characterization and cloning studies. The pharmacological characterizations of the ARs occurred in the decades after the discoveries of Ahlquist and used this same basic approach to define several AR subtypes. The cloning studies which followed implemented techniques to isolate purified receptors using affinity

chromatography. The purified proteins were digested and underwent amino acid sequencing. From these crude sequences, the researchers would create hybridization probes of the reverse-engineered potential DNA sequences, which were subsequently used to create cloned DNA fragments. Finally, this DNA library was expressed and pharmacologically characterized to cross-reference the newly cloned protein to known pharmacological isolates (Lefkowitz, 2007; Bylund, 2006). These experiments have thus far resulted in 9 distinct AR subtypes. Interestingly, only the α_{1D}-AR was cloned prior to pharmacological characterization, making the identity of this receptor difficult to confirm, initially (Bylund, 2006).

Subsequent analyses have found tissue-specific AR subtypes, such as the α_{1L}-AR, as well as potential subtypes which are pharmacologically distinct but deemed likely variants of existing subtypes or which have not been successfully cloned, including the α_{1C}-AR and the β_4-AR, respectively (Bylund, 2006; Granneman, 2001; Muramatsu *et al*., 1998). This work recently culminated in the published crystal-structure of the β_2-AR and β_2-AR-G_s complex by the laboratory of Brian Kobilka in 2007 and 2011, respectively, for which he was awarded the Nobel Prize (Rasmussen *et al*., 2007; Rasmussen *et al*., 2011; Westfield *et al*., 2011). While sequence similarities with rhodopsin and site-directed mutagenesis studies had largely predicted some of the characteristics of the AR structure, this represented an important milestone in our understanding of these G-protein coupled receptors, especially of the ARs. Much of the work on the structure and signaling of GPCRs was done be the Lefkowitz laboratory, which pioneered many of the techniques for cloning of the ARs and found the structure of rhodopsin (Lefkowitz, 2013).

Lefkowitz and Kobilka shared the 2012 Nobel Prize for Chemistry for their work (Lefkowitz, 2013; Kobilka, 2013).

Epilepsy

Epilepsy is the 4th most common neurological disorder, with a lifetime incidence probability of 1-in-26 (Hirtz *et al.*, 2007; Shafer, 2015). No current therapies halt the etiological progression of epilepsy (epileptogenesis), but rather antiseizure medications are used as palliative care measures; these therapies are only 50-70% successful in seizure control (Hirtz *et al*, 2007; Giorgi *et al.*, 2004; Yin *et al.*, 2013; Shafer, 2015). Unfortunately, most current antiseizure drugs are associated with many side-effects on memory and mood (Szilagyi, 2014; Petersen, 1998; ILAE, 2003). Most current epilepsy therapies decrease global neuronal excitability and so these side-effects are inherent to the very mechanism utilized to prevent, or limit, seizure occurrence.

Clinical Descriptions of Epilepsy

Epilepsy is diverse in clinical presentation but shares a measurable electrophysiological manifestation. Epilepsy is hallmarked by recurrent and unprovoked, transient disruptions of brain function by abnormal and excessive electrical activity (seizures) (Fisher, 2017). The initial diagnosis criteria for epilepsy is the confirmation of two or more seizures in a period of more than 24-hours; the observation of one seizure with a determined high likelihood for subsequent seizures; or the diagnosis of a seizure disorder. The second criterion is typically used in cases where a seizure is observed with a known co-morbidity associated with acquired epilepsy, such as stroke or high fever (Fisher, 2017).

While epileptic seizures share a common underlying pathophysiology, the clinical presentation or seizures is diverse and, in most cases, cause is poorly understood. Roughly 60-70% of seizures are idiopathic, meaning the cause is unknown (AES, 2019). Some factors likely influence predisposition to epilepsy include genetic, brain structure, metabolic, and immune abnormalities and/or deficiencies (Wirrell, 2019). Additional factors especially relevant to acquired epilepsy include brain trauma or infection.

Classically, seizures were categorized by a combination of two clinical presentations, simple or complex and partial or generalized (Bancaud *et al*, 1981). These terms describe the level of consciousness and location of activity during a seizure. However, the clinical classifications for seizure types were updated in 2017 to include the following types: focal onset, generalized onset, or unknown onset, with awareness or impaired awareness (focal onset only), and by motor involvement (Fisher, 2017). Generally, the changes in classification allow for more accuracy in clinical descriptions and do not generally change the presentations being measured; those are the level of consciousness and nature of the seizure.

Current Treatments and Antiepileptic Drug Discovery

Current antiepileptic therapies include pharmacological approaches, dietary alterations, and electrical stimulation therapy. Currently, in the United States, there are over 30 clinically-approved unique pharmacological agents (Vossler *et al*., 2018). While there are new and emerging therapies, no current treatment is antiepileptogenic; rather, current drugs are more accurately antiseizure drugs. The first known effective treatment for epilepsy was the use of lithium. Though epilepsy was described in the earliest medical texts (e.g. “The Sacred Disease” by Hippocrates) and suggested in even more

ancient texts, it was only relatively recently that much progress had been made beyond attempts at surgical ablation of the epileptic foci, or herbal remedies (Magiorkinis *et al*., 2014; Wolf, 2014). Around the turn of the last century, the first known chemical treatments with real success, the bromides (e.g. potassium bromide), were discovered to be relatively reliable treatments for seizures. Bromides are no longer used as treatments in epilepsy, due to a relative lack of efficacy and toxicity (Shorvon, 2009b)

The first breakthrough antiepileptic drug was phenobarbital in 1909 (Shorvon, 2009). Phenobarbital is a barbiturate which acts as a positive allosteric modulator of ionotropic $GABA_A$ receptors to enhance the inhibitory actions of GABA. Phenobarbital, and other barbiturates are extremely useful for treatment of *status epilepticus* and remains useful to this day (Shorvon, 2009). However, barbiturates are notorious for pronounced sedative side-effects, making their usefulness in everyday treatment limited.

The next major step in antiepileptic drug therapeutics came in 1939, from the work of Merritt and Putnam who utilized drug-screening techniques by implementing known chemoconvulsants in animal models and testing clinically-used drugs. The most famous, phenytoin, a purified constituent of an earlier hypnotic drug was found to be highly efficacious in screening and was quickly adopted for clinical use (Shorvon, 2009). The mechanism of action for phenytoin is not well-understood, but is believed to enhance inactivation of sodium channels (AES "Summary of Antiepileptic Drugs"). Phenytoin and subsequent similar drugs were found to be useful in many types of epilepsies and was not associated with as severe of sedative effects (Shorvon, 2009). Much of the next decade or two saw the production of several new derivative drugs, some of which sought to combine the molecular constituents of phenytoin and phenobarbital (Shorvon, 2009).

The final major class of antiepileptic drugs still in use today are the benzodiazepines (Wick, 2013). Like barbiturates, the benzodiazepines were found to be effective for treatment acute seizure clusters and *status epilepticus* (Riss *et al*., 2008; Shorvon, 2009b). Diazepam, and other benzodiazepines act similarly to the barbiturates, but act directly upon $GABA_A$ receptors as agonists (Vossler *et al*., 2018). The benzodiazepines were developed mainly as anxiolytics and sedatives, but were also found to be useful in epilepsy (Shorvon, 2009b). This class of drugs presented an alternative to barbiturates in acute epilepsy crisis. Notably, both the barbiturates and benzodiazepines are associated with a high likelihood for dependency and abuse, so these classes of antiseizure drugs are typically limited to acute crisis within the clinic.

Most recently implemented antiepileptic drugs are derived from, or similar to phenytoin, barbiturates, and benzodiazepines (Vossler *et al*., 2018). Other potential avenues have explored aspects of glutamatergic signaling, but have not found much success (Shorvon, 2009b). Rather, most novel therapies, in recent years, have aimed at reduction of side-effects, or combinatorial therapies to find greater treatment success in drug-resistant epilepsies (Shorvon, 2009b). A recent novel avenue for epilepsy, as well as pain, are the cannabinoids, specifically cannabidiol. This class of drugs has shown exciting potential for treatment of several epilepsies. However, this is still an emerging area of research and the mechanism of action is poorly understood. For example, cannabidiol is not thought to interact through the known cannabinoid receptors, type 1 or type 2 (Vossler *et al*., 2018).

Other than drug therapies, there remain several other therapies of interest in epilepsy, including surgery, electrical stimulation, and diet. Brain surgery techniques

have come a long way from the days of H.M. and temporal lobectomies (Augustinack *et al*., 2014); current surgical ablation techniques implement intracranial EEG and MRI (Chan *et al*., 2018; Englot *et al*., 2017). Surgery is still common in drug-resistant epilepsies, especially in cases with well-defined epileptic foci (Choi *et al*., 2008; Engel *et al*., 2003). Ketogenic diet is another alternative therapy, which has prevailed as an epilepsy therapy since the 1930's (Shorvon, 2009). The ketogenic diet replaces most dietary carbohydrates with fats, encouraging a shift in metabolism towards ketogenesis and the production of ketone bodies from fatty acids (Ulamek-Koziol *et al*., 2019; Sampaio, 2016). The brain is able to use ketones as an effective alternative energy source and seems to reduce seizure prevalence effectively for some patients; however, the mechanism is poorly understood (Ulamek-Koziol *et al*., 2019; Sampaio, 2016). A final established alternative antiepileptic therapy is vagus nerve stimulation. Vagus nerve stimulation works by electrically stimulating the vagus nerve, sending impulses to several sites within the brain (Ramani, 2008). Interestingly, as we will discuss in later chapters, several studies have found that in-tact noradrenergic signaling is requisite for the efficacy of both the ketogenic diet and vagus nerve stimulation (Giorgi, and Ramani, 2008).

A much more specific variant of electrical stimulation has recently gained traction called responsive neurostimulation (Englot *et al*., 2017). The concept of this therapy is similar to that of deep-brain stimulation used in diseases like Parkinson's. Responsive neurostimulation acts by sending electrical pulses when unusual activity is detected (Englot *et al*., 2017; Jobst *et al*., 2017). The most cutting-edge among these stimulators are programmed to specifically quench the activity with frequencies antidromic to the main seizure frequency (Englot *et al*., 2017). Current pre-clinical research is attempting

to develop closed-loop algorithms to predict seizure onset in real-time and provide proactive prevention of seizure activity (Nagaraj *et al*., 2015; Krook-Magnuson *et al*., 2015; Berenyi *et al*., 2012). Development of such predictive tools could be revolutionary for focal seizure treatment, but may be extremely difficult for reasons described in the next sections.

Neuron Physiology and Seizures

As previously mentioned, seizures are unprovoked, transient disruptions of brain function by abnormal and excessive electrical activity. The brain is an electrical organ which forms dynamic circuits locally and with the periphery (Swanson, 2008; Comin *et al*., 2013; Buzsaki *et al*., 2004). The functional units of the brain, neurons, are cells which conduct charges and generate an electrical potential via a precise balance of ions within the cell. The electric potential is formed by an imbalance in charges, mostly of sodium, potassium, and chloride, present within the cells and in the extracellular environment (McCormick, 2008). Ion pumps actively curate an environment in neurons whereby the intracellular environment contains more anions and less cations than the extracellular environment (McCormick, 2008). The resulting imbalance of charge creates an electrical potential, with the cell membrane serving as a selectively permeable barrier. The resulting electrical potential makes the neuron polarized.

When a neuron becomes sufficiently depolarized by transient, selective opening openings in the cell membrane, it discharges an electrical pulse during an event dubbed the action potential (Hodgkin *et al.*, 1952; Bean, 2007). Depolarization mostly occurs due to the opening of ligand-gated ion channels, while voltage-gated ion channels dominate during the action potential (Bean, 2007). Generally, this electrical potential is

carried from the cell body (soma) of the neuron to the axon terminal(s), where it stimulates the release of neurotransmitters. Prototypic neurons release glutamate or γ-aminobutyric acid (GABA) to excite or inhibit the next cell(s) in the circuit, respectively (McCormick, 2008). Within a neural circuit, there exists both excitatory and inhibitory neurons. Excitatory neurons carry information, while inhibitory neurons regulate the conveyance of the information (Kepecs *et al.*, 2014).

During a seizure, there is an imbalance between excitatory and inhibitory neuronal activity. During a seizure, excitatory, or glutamatergic, neurons are not correctly inhibited, and thus, there is excessive and abnormal electrical activity within the circuit (Traub *et al*., 2014; Bernard *et al*., 2000; Stief *et al*., 2007). Initiation of seizure activity is poorly understood, but brain regions with highly recurrent circuitry, such as the hippocampus, are common areas of seizure foci. Feedback pathways, such as recurrent synapses, are common within the brain, but in this context the feedback causes excitation of neighboring cells, rather than regulatory inhibition. Within a recurrent circuit electrical signals are amplified as a depolarizing neuron excites neighboring neurons (Le Duigou *et al*., 2014; Traub *et al*., 1982; Miles *et al*, 1983; Miles *et al*., 1986).

The recruitment phase of a seizure is also a poorly understood phenomenon but may involve non-synaptic conduction (i.e. action at a distance) from growing electrical fields (Weiss *et al*., 2013; Isaev *et al*., 2012; Zhang *et al*., 2014). The inability of the inhibitory circuitry to cease, or limit, recruitment leads to the eventual overwhelming of the inhibitory circuitry (Shevon *et al*., 2012; Trevelyan *et al*., 2006; Steif *et al*., 2007). One line of thinking posits that this likely because excitatory neurons outnumber inhibitory neurons by as much as a factor of 30, and functionally, by a factor of about 10;

meaning that inhibitory circuitry may be overwhelmed when typically-silent neurons become recruited to depolarize, such as in a seizure (Shoham *et al*., 2006; Ovsepian, 2019; Miles *et al*., 1987).

One may wonder why the brain is prone to seizures in the first place. In most cases (6-out-of-10), seizures are idiopathic, meaning the cause of is not associated with any obvious structural or functional abnormalities (Schachter). It has been suggested that even normal brain operation occurs in a highly entropic state, meaning that even minute dysfunction can lead to profound consequences (Beggs *et al*., 2008; Beggs *et al*., 2012; Roberts *et al*., 2015; Hesse *et al*., 2014). This highly chaotic and energetic system is typified by well-known neural oscillation patterns, sometimes known colloquially as brain waves or EEG patterns (Werner, 2007; Poil *et al*., 2008; Buzsaki, *et al* 2004). Normal brain oscillation patterns exemplify the necessity for signal amplification in a dynamic brain, but the commonality of seizures demonstrates the fragility of such a system.

Noradrenergic System in Epilepsy

Studies over several decades have revealed that norepinephrine exhibits antiepileptic properties, both in vitro and in vivo. Further, ablation of noradrenergic fibers exacerbates several models of epilepsy (Giorgi *et al*., 2004). The literature suggests that noradrenergic participation is especially efficacious in progressive models of epilepsy, such as kindling (Cochran, 1980; McIntyre, 1981, 1986). The effect of NE in epilepsy models was first assessed by methods for chemical ablation on noradrenergic neurons in the locus coeruleus; These approaches included direct injection of the non-selective catecholminergic neurotoxin 6-hydroxydopamine into the locus coeruleus, or

alternatively, systemic administration of the noradrenergic-selective neurotoxin N-(-2-chloroethyl)-N-ethyl-2-bromobenzylamine (Giorgi, 2004). These studies characterized the loss of brain norepinephrine in several epilepsy models. The conclusions drawn from these studies were robust and recognized NE as possessing antiepileptic potential; however, due to limitations of the methodology, these studies did little to elucidate the receptor subtypes mediating these effects (Mishra, P, 1994; Arnold, P., 1973; McIntyre D., 1979). These experiments also provided great insight into the importance of the locus coeruleus noradrenergic fibers; because these methods largely left lateral tegmental noradrenergic fibers in-tact, this revealed that the locus coeruleus fibers were the predominant fibers responsible for the antiepileptic effects of NE (Giorgi, 2004; Weinshenker *et al*., 2004) Experiments stimulating the release of NE, or blocking reuptake, found the opposite effects of the ablation studies; thus, supporting the theory that NE is an antiepileptic neurotransmitter (McIntyre, 1982; Jimenez-Rivera, 1986).

Studies have been done to attempt to elucidate the receptor subtypes responsible for the antiepileptic effects of NE, but current adrenergic ligands lack subtype selectivity and/or do not readily cross the blood-brain barrier (Weinshenker *et al*., 2004). This review looked extensively through the literature and found that no one receptor class is solely antiepileptic or proepileptic. The authors attribute the conflicting findings to the lack of ligand specificity and likely differences in the roles of subtypes within the AR classes.

This aspect of elucidating the AR subtype roles is explored further in Chapter II. Briefly, we have developed a system for pharmacologically isolating AR subtypes by utilizing combinations of antagonists and agonists in hippocampal slices. A major novel

implementation of this research was the utilization of AR subtype knockout mice to more confidently assess contributions of a particular subtype of interest, the α_{1A}-AR. Our interests in the α_{1A}-AR, besides antiepileptic potential, are based on findings which suggested that, in healthy mice, constitutive α_{1A}-AR activation results in increased learning and memory, improved mood, and increased synaptic plasticity (Doze *et al*., 2011). Thus, α_{1A}-AR activation could prove dually beneficial for epilepsy patients, since epilepsy is associated with elevated incidence in mood; and because most current therapies are detrimental to memory formation, general cognitive function, and can exacerbate mood abnormalities.

CHAPTER II

α_{1A}-AR, BUT NOT α_{1B}-AR, ACTIVATION ATTENUATES EPILEPTIFORM FREQUENCY AND RECEPTOR KNOCKOUT EXACERBATES EPILEPTIFORM FREQUENCY

Introduction

As previously discussed, noradrenergic fiber ablation in rodent seizure models led to the conclusion that norepinephrine confers an antiepileptic phenotype. Additionally, both the ketogenic diet and vagus nerve stimulation therapies rely upon an intact noradrenergic system (Giorgi *et al*., 2004). Such an apparent role in epilepsy raised the question of which AR subtypes confer these antiepileptic effects and whether they can be selectively targeted.

Previous studies within our laboratory have shown that α_1-AR activation increases the excitatory potential of interneurons, including a direct depolarization of the membrane potential of interneuron subpopulations (Bergles *et al.* 1996; Hillman, *et al.*, 2009). This research also suggested that the increased activity of the interneurons, ostensibly achieved by decreasing basal potassium conductance and increasing inwardly rectifying hyperpolarization-activated conductance, was powerful enough to decrease the excitability of pyramidal neurons in the hippocampus (Bergles, 1996). The latter study by Hillman suggested the importance of the α_{1A}-AR to this effect and that these effects

carry to a broader circuit-level effect, to increase hippocampal inhibitory tone (Hillman 2009). Attempts to identify AR subtypes in neuronal populations to elucidate the physiological mechanism underlying these actions has been largely limited to functional isolation via genetic and pharmacological manipulation; currently, no selective antibodies exist for targeting the α_{1A}-AR for immunofluorescence identification (Jensen *et al.,* 2009). Further, we have found that overexpressed reporter-tagged α_{1A}-AR mutant mice show expression in cell types where no function can be found (Papay *et al*., 2006; Hillman *et al*., 2005; Hillman *et al*., 2007).

In this study, we investigated the specific role of α_{1A}-AR activation in epileptiform frequency by utilizing a combination of α_1-AR subtype knockout mice and selective ligands. The low-magnesium model of epileptiform burst generation was used in this study to study the effect of α_{1A}-AR stimulation on epileptiform burst frequency in the mouse hippocampus. Reducing magnesium results in the loss of magnesium-block to NMDA glutamate receptors. This alteration results in the generation of rhythmic, seizure-like bursts associated with an overwhelming of inhibitory signaling (Trevelyan *et al.*, 2006). In order to circumvent the limitations of previous pharmacological characterizations, we transitioned our research from rats to mice and implemented the use of genetically modified knockout mice. We investigated the effect of α_1-AR activation using the selective agonist, phenylephrine, in normal control mice, as well as knockout mice lacking functional expression of either the α_{1A}-AR or α_{1B}-AR. Also, we assessed the potential for differential effects dependent upon the agonist activating the α_{1A}-AR, using pharmacological isolation techniques. Finally, we present a previously unknown phenomenon suggesting that loss of α_{1A}-AR expression leads to exacerbation of

hippocampal epileptiform frequency. We discuss the importance of these findings and the potential to explain phenomena seen *in vivo*.

Materials and Methods

Reagents

Sodium chloride, calcium chloride, potassium chloride, dextrose, sodium bicarbonate, sodium pyruvate, and sodium phosphate monobasic were from Fisher Scientific. (-)-Phenylephrine hydrochloride, timolol maleate, (-)-epinephrine-(+)-bitartate, and were from Sigma Aldrich. Atipamezole hydrochloride, picrotoxin, and cirazoline hydrochloride were from Tocris Bioscience. Magnesium sulfate and sodium L-ascorbate were from JT BAKER and Pfaltz and Bauer, respectively.

Animal Use

Mice were housed in an AAALAC-accredited facility at the University of North Dakota. All experiments involving mice were performed under IACUC-approved protocols. C57BL/6J mice were obtained from Jackson Laboratories. Knockout background mice (in-bred C57BL/6 mice), α_{1A}-AR knockout mice, and α_{1B}-AR knockout mice were generously provided by the lab of Dianne Perez at the Cleveland Clinic Foundation (Lerner Institute, Cleveland, OH).

α_{1A}-AR Knockout Mouse Generation

α_{1A}-AR knockout reporter mice were generated as previously described (Rokosh *et al.*, 2002). Briefly, a plasmid vector containing 1.1 Kb from the 5' arm and 6.5 Kb from the 3' arm, sequence retrieved from the 129/SvJ genomic library, targeted portions

of critical exon 1 and the adjacent intron for excision from the α_{1A}-AR gene. This vector also contained a LacZ operon and conferred resistance for neomycin.

The plasmid vector was transfected into RW-4 129/SvJ embryonic stem cells using electroporation. Positive transfections were identified with neomycin resistance. Positive cells were cultured and analyzed for correct insertion. A small fraction of transfected samples contained the correct insertion with no additional random insertions. These embryonic stem cells were subsequently chosen for insertion into C57BL/6 blastocysts. Blastocysts were implanted into a 129SvJ x FVB/N female; subsequently, pups were assessed for germ-line expression of the correct mutation.

Finally, heterozygous mutant mice were bred up and back-crossed with C57BL/6 and FVB mice for several generations. These mice are considered congenic to C57BL/6 mice, the stain for which we utilize as "normal" controls (Simpson PC, 2006).

α_{1B}-AR Knockout Mouse Generation

The α_{1B}-AR knockout was previously generated as described in a similar fashion to the α_{1A}-AR knockout mouse (Cavalli *et al*., 1997). A portion of exon 1 was replaced with a vector conferring neomycin resistance. Blastocysts were selectively injected into pseusopregnant female 129Sv x C57BL/6J mice. Mice were subsequently back-crossed for several generations and is congenic to the C57BL/6 background strain (Simpson, 2006).

Hippocampal Slice Preparation

Isoflurane (Isothesia, Henry Schein Animal Health) was used to deeply anesthetize mice, which were then decapitated. The brain was quickly removed and

immediately placed in ice-cold artificial cerebrospinal fluid (aCSF) for dissection, containing (in mM): choline chloride 110, dextrose 25, sodium bicarbonate 25, magnesium sulfate 7, sodium pyruvate 3.1, sodium ascorbate 11.6, calcium chloride 0.5, potassium chloride 2.5, sodium phosphate monobasic 1.25.

Hippocampi were isolated and sectioned into 450 μm coronal slices. Upon sectioning, slices were immediately transferred to 33-35^{o}C aCSF, containing (in mM): Sodium chloride 119, dextrose 11, sodium bicarbonate 26.2, magnesium sulfate 1.3, calcium chloride 2.5, potassium chloride 5, sodium phosphate monobasic 1. After 30 minutes, slices were removed from incubation and allowed to equilibrate at room temperature for at least an additional 60 minutes. All solutions were continually perfused with 95% O_2/ 5% CO_2.

Electrophysiological Local Field Potential Recordings

Extracellular local field potential recordings were performed using a borosilicate glass pipet, pulled using a Narishige vertical puller. Pipettes contained a silver/silver-chloride recording filament, and were filled with 3 M sodium chloride. Freshly sanded silver wire was chloride to minimize the rate of oxidation and provide minimal baseline drift during recording (Grubbs *et al*., 1983). Recording electrodes were placed deep into the *stratum pyramidale* of the CA3 region of the hippocampus, where epileptiform bursts were measured in changes of electrical potential at the electrode. Specifically, the border of the CA3a-b sub-regions were targeted. Recordings were measured in bridge-clamp mode by an Axoclamp 2B data acquisition and amplification system (Axon Instruments), set to 10x gain. Signals were further amplified by a Brownlee Precision 440 amplifier (AutoMate Scientific), set to 100x gain. Signals were transformed from direct current to

alternating current by a DigiData 1322a digitizer (Axon Instruments). Signals were recorded using pClamp 9 (Axon Instruments) software package. Line transmission interference was selectively reduced on-line with a dedicated band-pass filter unit (Digitimer). Extraneous environmental interference was reduced or eliminated via Faraday cage and strategic grounding procedures. Vibration was isolated minimized by an air table (TMC).

Epileptiform Activity Generation in Hippocampal Slices

Individual slices were transferred to a recording chamber filled with aCSF bath solution flowing at a rate of 4-5 mL/min. Bath solution was input to the recording chamber via gravity-driven flow, which was regulated by a common intravenous therapy flow regulator. Bath flow rate was determined by hand-timed measurements of solution reservoir volume. Epileptiform activity was generated using aCSF with no magnesium added and increased potassium concentration, 5 μM adjusted from 2.5 μM. If slices did not produce regular synchronized activity within 45 minutes after introduction of no magnesium aCSF slices were determined to be non-responsive and discarded. Further, after generation of regular epileptiform activity slices were recorded for baseline activity for at least 30 minutes, or until the rate of spiking had become stable. Regularity was determined by comparisons of burst frequency at 5-minute intervals.

Dose-Response and Pharmacological Manipulation

Characterization of receptor response was achieved by the application of various AR agonists at increasing dosages. Specifically, initial experiments (data not shown) were performed to determine likely efficacious range. After initial determination of efficacious range, and collection of baseline epileptiform burst frequency, increasing

concentrations of drug were added to the bath solution in 8-minute intervals. This interval was chosen based on time-course interval studies of time to maximal effect, with additional time added to compensate for dead volume of bath solution inlet lines. Drug concentration was increased at half-logarithmic increases based on the assumption that the generated dose response relationship would be sigmoidal on a logarithm-transformed axis for drug concentration. This logarithm-transformed sigmoidal curve fit is the most common dose-response relationship observed in biology and is modeled from mass-action equations which describe the non-linear interaction probabilities between dissimilar molecules due to volume and molecule prevalence (i.e the probability of interaction between dissimilar molecules is negligible until concentrations of each are sufficiently high, whereupon interactions suddenly become much more common) (Kenakin, 2016; Guldberg *et al.,* 1879).

We evaluated dose-response relationships for both endogenous AR agonists, norepinephrine and epinephrine, as well as the α_1-AR specific agonist, phenylephrine (Furchgott, 1967). Comparison of dose-response curves allowed us to assess the relative efficacy of phenylephrine to the full agonist endogenous ligands norepinephrine and epinephrine. Comparison of α_1-AR specific effects were made possible by constant blockade of α_2-ARs and β-ARs by constant bath application of saturating concentrations of atipamezole and timolol, respectively. Specific contributions of α_1-AR subtypes found in the central nervous system were investigated by generating phenylephrine dose-response curves in hippocampal slices from α_{1A}-AR and α_{1B}-AR knockout mice. Contribution of GABAergic signaling was assessed in phenylephrine dose-response experiments in the presence of 100 μM picrotoxin, a GABA-A receptor blocker.

Analysis

Epileptiform bursts were identified in Clampfit 10 by threshold and waveform analysis, then exported to Microsoft Excel 2016 or Google Sheets for sorting of epileptiform spikes. Spikes were sorted into 150-second or 300-second bins, depending on the baseline epileptiform frequency, to allow for enough data collection to differentiate epileptiform frequency changes of at least a 10%. The last bin associated with each concentration was then exported for further analysis. Only the last bin was selected to accurately assess the effects of each dose, allowing adequate time for perfusion and receptor signaling, while also providing adequate data for normalization of outliers. Graphs and dose-response curves were prepared with GraphPad Prism 7.x or 8.x. The dose-response relationship for these experiments was generated by a non-linear regression analysis. These data were best fit using [Agonist] vs. response (three-parameters) Dose-Response – Stimulation non-linear regression parameters. Predicted values reported from the non-linear regression functions include the drug concentration of half-maximal response (EC_{50}), or potency, and maximum drug response, or efficacy. The values shown within this chapter are typically shown in figures as negative responses. However, these responses are mediated by agonists and would not be reported correctly by antagonist dose-response values, such as an IC_{50}. While potentially counter-intuitive, this representation provides the reader with a clear representation of the nature of the effect (i.e. excitation of receptors results in decreased epileptiform burst frequency. Any relevant statistical tests are discussed within the text, as appropriate.

Results

Agonist-mediated α_1-AR Stimulation Attenuates Mouse Hippocampal CA3 Slice Epileptiform Frequency in a Magnesium-depletion Model of Seizure-like Activity

Magnesium is an important regulator of neural excitability. Magnesium ions are divalent cations, which imitate many chemical properties of calcium. In normal cerebrospinal fluid (CSF) magnesium concentrations are between 1-2 mM and block N-methyl-D-Aspartate (NMDA) glutamatergic channels. When magnesium is removed from artificial CSF (aCSF) the result is dysregulated glutamatergic channel activity and spontaneous neuronal hyperactivity. At room temperature, spontaneous epileptiform bursts from mouse hippocampal CA3 area occurred at regular intervals with a mean frequency of approximately 0.1 Hz (Fig. 3A). Our experiments investigated the effects of AR agonists on the epileptiform burst frequency, which we measured as a function of the baseline frequency (Fig. 3B). A dose-response curve was utilized to characterize the potencies and efficacies of agonists by plotting the frequency of the final time bin associated with each dose and performing a non-linear regression curve fit analysis (Fig. 3C).

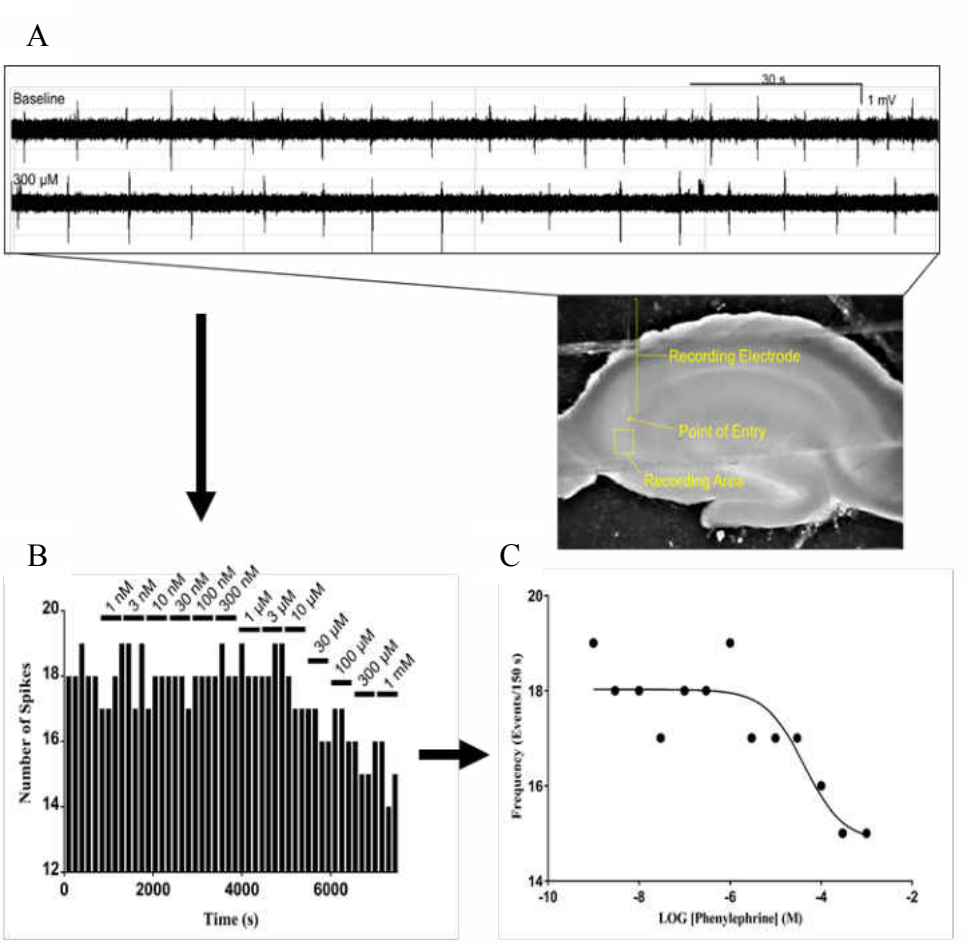

Figure 3. Epileptiform Activity Recording and Dose-Response Relationship Analysis. (A) Example electrophysiological hippocampal field activity recording trace of epileptiform bursts and (outset) image of hippocampal slice showing recording electrode in the *stratum pyramidale* of the CA3a subregion. (B) Example graphic illustrating the plotting of time and number of spikes into discrete bins, with tracking of dose applied during each time. (C) Example graphic illustrating the transformation of the time axis to concentration of ligand (dose) and the non-linear curve fit to the last discrete bin associated with each dose. Note that the typical dose-response curve is sigmoidal on a logarithmic scale and is customary to present it as such.

Characterization of Endogenous and Synthetic AR Agonists Effects on Hippocampal CA3 Epileptiform Burst Frequency

We investigated the potential of endogenous and synthetic AR agonists to alter spontaneous epileptiform burst frequency by assessing dose-response relationships for

several agonists. NE (Fig. 4A) exhibited a slightly higher maximum attenuation than Epinephrine (EPI) (Fig. 4B), with efficacies estimated to be 16.88±2.87% (n=5 Slices) and 12.78±2.49% (n=5 Slices), respectively. EPI exhibited a slightly higher potency, 1.85 μM, than NE, 6.29μM, but as predicted by binding values they were within the same order of magnitude for the α_{1A}-AR. Additionally, we investigated the α_1-AR-selective agonist, phenylephrine (PE). The efficacy value for PE, 16.08±1.89% (n=5 Slices), was similar to the endogenous catecholamines and suggested that our pharmacological blockade of α_2-AR and β-AR contributions was functioning as expected. The potency for PE, approximately 2.31 μM, was similar to NE and EPI. In the presence of α_2-AR and β-AR blockers, and with evidence from α_1-AR-selective agonist, PE, there is an apparent attenuation of epileptiform burst frequency mediated by α_1-AR activation.

Although it has been done previously in rats, we also assessed the contributions of GABAergic signaling to the observed effects by investigating phenylephrine response in the presence of 100 μM picrotoxin. Picrotoxin is potent $GABA_A$ receptor blocker and common chemoconvulsant used to generate epileptiform burst activity in disinhibitory animal models of epilepsy. We observed an abolishment of phenylephrine-mediated decreases in epileptiform burst frequency in the presence of 100 μM picrotoxin (n=2 slices) (Fig. 5). This data suggested that phenylephrine-mediated effects are GABA-dependent, which had been shown previously in rat hippocampus (Hillman *et al*., 2009). Additionally, we noted that at all doses of phenylephrine the response measured was greater than the baseline frequency. However, this is likely representative of inherent differences in baseline epileptiform frequency from the addition of picrotoxin, rather than effects representative of phenylephrine-mediated alterations. Unfortunately, we did not

collect an additional baseline frequency measurement following introduction of picrotoxin to the low-magnesium aCSF.

A

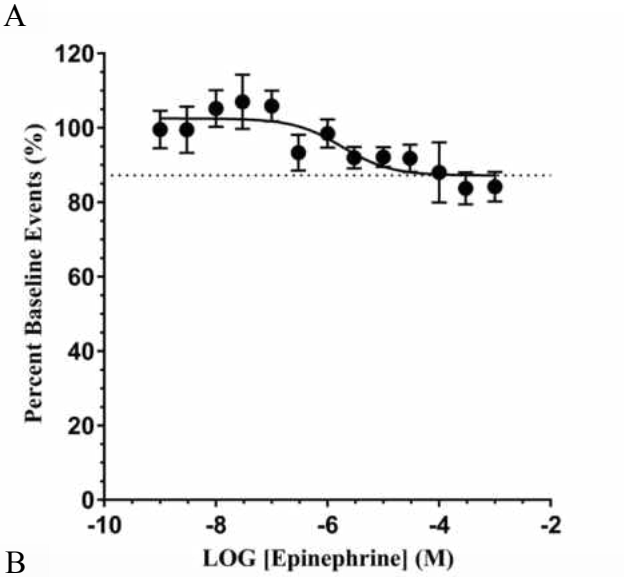
Percent Baseline Events (%)
120
100
80
60
40
20
0
-10
-8
-6
-4
-2
LOG [Epinephrine] (M)

B

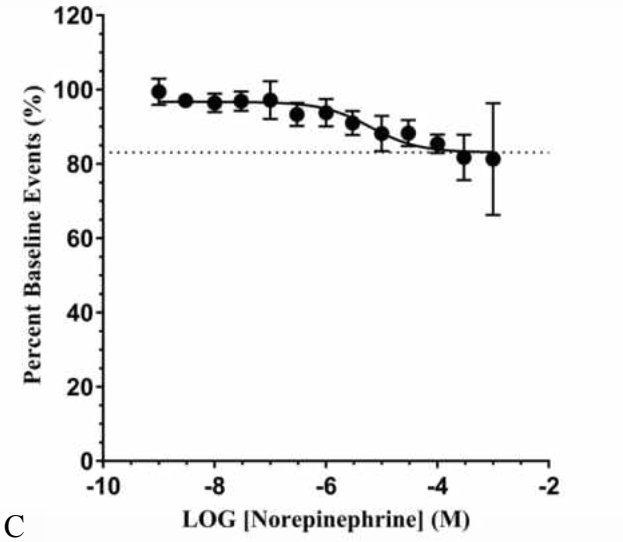
Percent Baseline Events (%)
120
100
80
60
40
20
0
-10
-8
-6
-4
-2
LOG [Norepinephrine] (M)

C

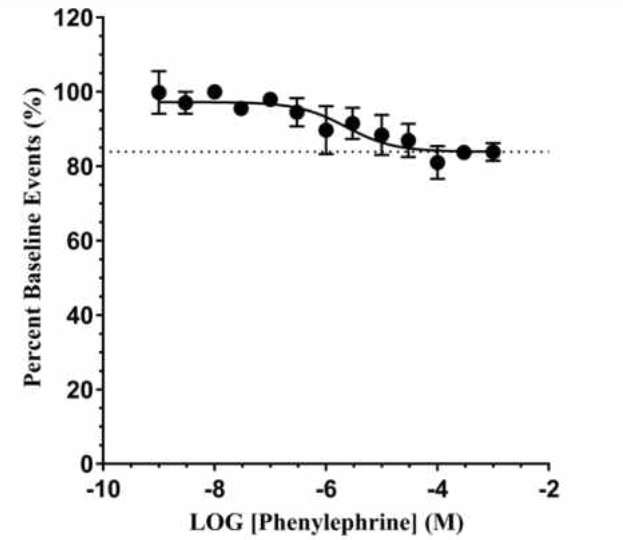
Percent Baseline Events (%)
120
100
80
60
40
20
0
-10
-8
-6
-4
-2
LOG [Phenylephrine] (M)

Figure 4. Dose-Response Relationships of Endogenous and Synthetic Agonists. (A) Epileptiform burst frequency in response to increasing doses of the endogenous agonist epinephrine. (B) Epileptiform burst frequency in response to increasing doses of the endogenous agonist norepinephrine. (C) Epileptiform burst frequency in response to increasing doses of the α_1-AR-selective agonist phenylephrine. All dose-response curves are normalized to the baseline epileptiform burst frequency.

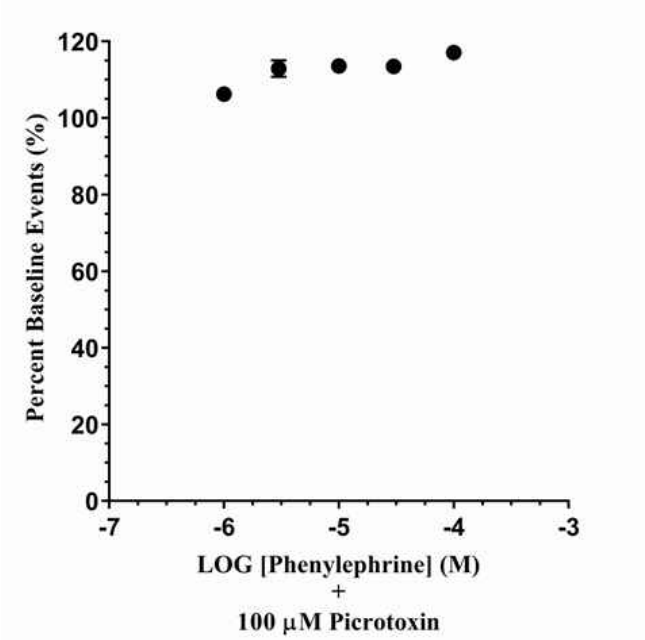

Figure 5. Dose-Response Relationships Phenylephrine in the Presence of Picrotoxin. Epileptiform burst frequency in response to increasing doses of the α_1-AR-selective agonist phenylephrine in the presence of 100 μM picrotoxin. Dose-response curve was normalized to the baseline epileptiform burst frequency without picrotoxin.

α_{1A}-AR, but not α_{1B}-AR, Knockout Abolishes α_1-AR Activation-mediated Attenuation of Hippocampal CA3 Epileptiform Burst Frequency

We further assessed the nature of the α_1-AR activation-mediated attenuation of epileptiform burst frequency using α_{1A}-AR and α_{1B}-AR constitutive knockout mice. In the presence of α_1-AR-selective agonist, PE, we observed that α_1-AR activation-mediated attenuation of epileptiform burst frequency was completely abolished in hippocampal slices from α_{1A}-AR knockout mice (efficacy= N.D., n=8 Slices) (Fig. 6A). Conversely,

PE attenuation was similar to wild-type control slices in slices from α_{1B}-AR knockout mice (efficacy=16.83±2.23%, n=12 Slices) (Fig. 6B). Interestingly, the potency was approximately an order of magnitude weaker, 21.94 μM, than PE in slices from wild-type control mice; however, it is worth noting that there was variability in all potency estimates and the value for this group was estimated from several partial dose-response curves. Together, these experiments showed that α_{1A}-AR knockout results in a complete abolishment of α_1-AR activation-mediated attenuation of hippocampal epileptiform burst

frequency, whereas hippocampal slices from α_{1B}-AR knockout mice exhibited little variation from effects observed in slices from wild-type control mice.

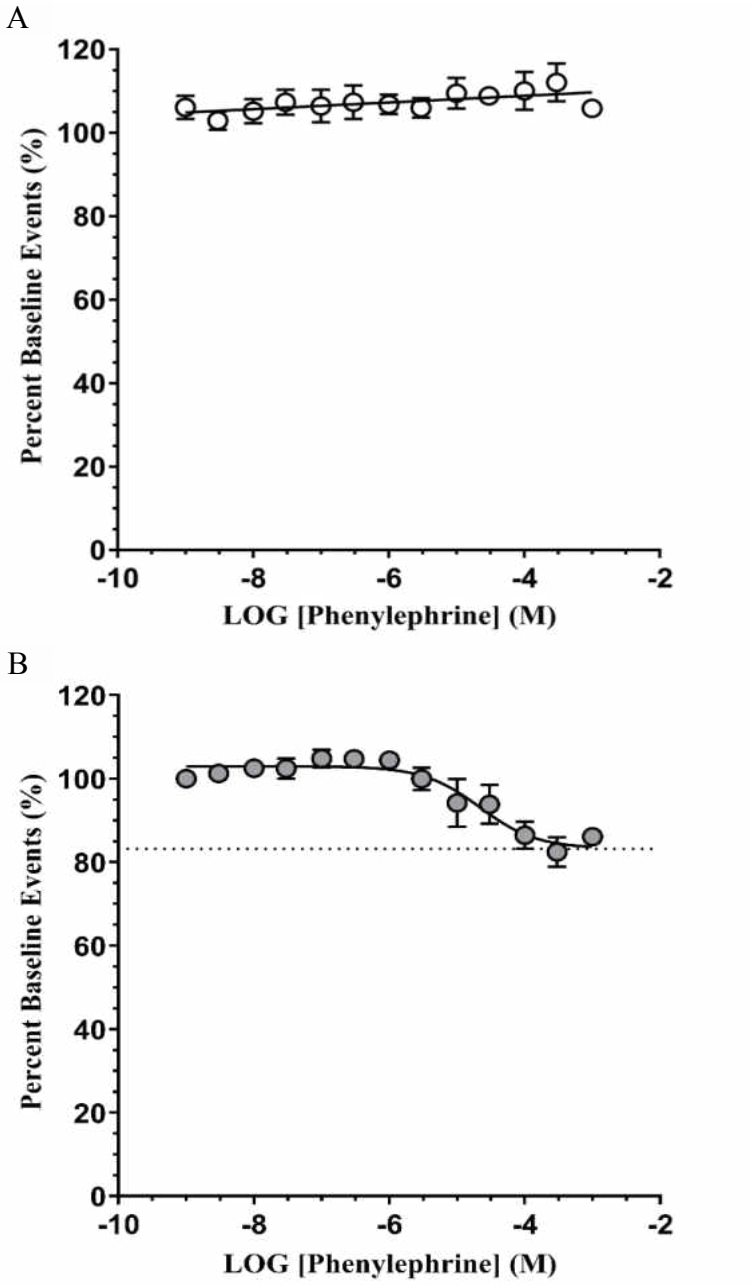

Figure 6. Dose-Response Relationships of Phenylephrine in Hippocampal Slices from α_1-AR Subtype Knockout Mice. (A) Epileptiform burst frequency in response to increasing doses of phenylephrine in hippocampal slices from α_{1A}-AR knockout mice. (B) Epileptiform burst frequency in response to increasing doses of phenylephrine in hippocampal slices from α_{1B}-AR knockout mice. All dose-response curves are normalized to the baseline epileptiform burst frequency.

Hippocampal Slices from α_{1A}-AR knockout mice, but not α_{1B}-AR knockout mice, Exhibit Higher Baseline Epileptiform Burst Frequency

We observed an interesting phenomenon when testing dose-response relationships in hippocampal slices from wild-type control and α_1-AR subtype knockout mice. The baseline frequencies for each mouse strain were determined after spontaneous burst frequencies were determined to be stable for at least 15-minutes (Fig. 7). ANOVA (P=0.0064) suggested that there was a significant difference in the baseline frequencies between slices from wild-type controls, α_{1A}-AR knockouts, and α_{1B}-AR knockouts. Dunnett's Multiple Comparisons (P=0.0068) test revealed that the baseline frequency of hippocampal slices from α_{1A}-AR knockout mice (0.16±0.01 Hz, n=12 Slices) was significantly higher than the baseline frequency of wild-type control slices (0.10±0.01 Hz, n= 11 Slices). In contrast, no significant difference (P=0.8416) was observed between the baseline epileptiform burst frequency of hippocampal slices from wild-type control mice and slices from α_{1B}-AR mice (0.11±0.02 Hz, n=13 Slices). The mean difference in hippocampal epileptiform burst baseline frequencies from wild-type control mice and α_{1A}-AR knockout mice (0.60±0.02 Hz) is equivalent to a baseline frequency 158.7% greater in slices from α_{1A}-AR knockout mice than that of slices from wild-type control mice.

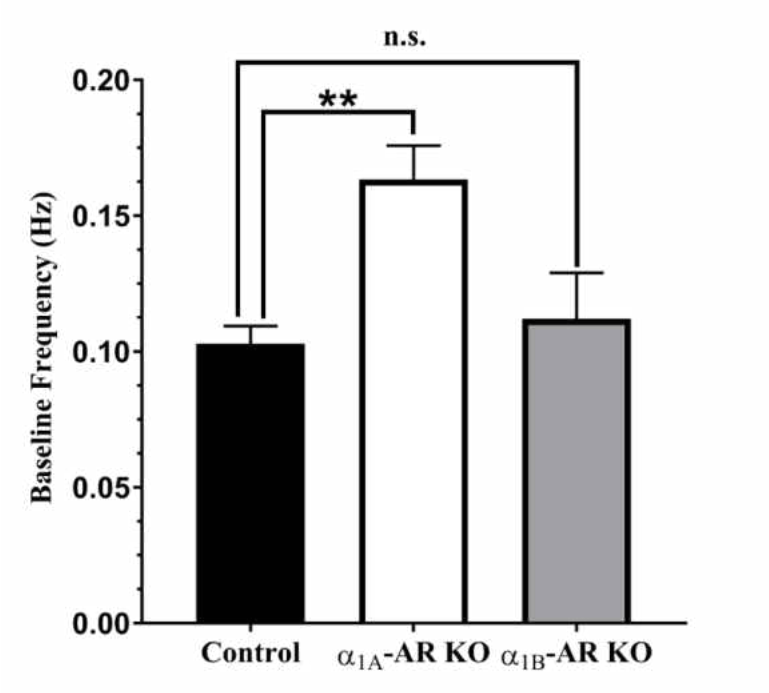

Figure 7. Comparison of Baseline Epileptiform Burst Frequencies in Hippocampal Slices from Control and α_1-AR Subtype Knockout Mice. Baseline epileptiform burst frequency in each mouse line as observed from the Hippocampal CA3 region. Statistical analyses are representative of one-way ANOVA and Dunnett's post-hoc multiple comparisons test. Statistical significance is represented as follows: No statistical significance (n.s.), $P < 0.05$ (*), $P < 0.01$ (**), $P < 0.001$ (***).

Discussion

Our results have produced several exciting findings: 1) α_1-AR activation by several AR agonists elicited a moderate decrease in epileptiform frequency from the mouse hippocampus; 2) These effects were observed within the hippocampal CA3 region; 3) knockout of the α_{1A}-AR abolished the previously observed phenomenon, while α_{1B}-AR knockout resulted in no observable difference from AR activation in hippocampal slices from wild-type control mice; 4) α_{1A}-AR knockout results in a significant increase in baseline hippocampal epileptiform burst frequency.

An important observation and potential caveat to our results, is that we consistently observed a positive baseline drift at sub-efficacious doses and in α_{1A}-AR knockout mice, which may suggest that our dose-response relationships are artificially less-efficacious than that should be. A potential remedy for this observation would be to implement baseline observations between doses or to observe each dose-response individually. However, the first remedy would require the assumption that there is no desensitization to the agonist, an unlikelihood. The second remedy would be wasteful in terms of mice needed. Since these baseline drift is on the order of 0-5%, over time, a third potential remedy would be to normalize the baseline over time with by performing no agonist controls for several hours and implementing this normalization factor prior to the time-dose transformation step in our analysis. Here, it was our preference to present the data with no normalization and instead allow the reader to make their own assessment.

These results were especially interesting within the context of previous experiments. Previously, the effect of α_1-AR activation was only known to decrease epileptiform burst frequency in the rat hippocampus. Our findings support our previous work and show that the characteristics of α_1-AR activation in the epileptic hippocampus are not limited to the rat, increasing the robustness and increasing the translational potential of these results. Additionally, our findings present the first time that this α_1-AR antiepileptic effect has been observed in the CA3 region. All previous studies focused in the CA1 region of the hippocampus. This further suggests a robust phenomenon. Out implementation of hippocampal slices from α_1-AR subtype knockout mice allowed us to investigate the specific contributions of the subtypes with known expression in the central

nervous system, the α_{1A}-AR and α_{1B}-AR. From our experiments with these knockout strains, we concluded that the α_{1A}-AR is the predominant α_1-AR subtype responsible for previously observed antiepileptic characteristics. While previous experiments by Hillman suggested this finding with α_{1A}-AR-selective antagonists, the unpredictable nature of AR cross-reactivity left doubt. Perhaps, the most unexpected and novel finding from this study were our results which showed that α_{1A}-AR knockout increased the baseline epileptiform burst frequency by over 1.5-fold. This finding is especially exciting because it suggests that α_{1A}-AR knockout results in a significant compromise of the circuitry responsible for preventing epileptiform activity within the hippocampus. Interestingly, this finding may suggests a potential mechanism and method for elucidating our observations discussed in the next chapter.

To our knowledge, very few studies have implemented AR knockout mice to study receptor subtype contributions in models of epilepsy. A notable exception is the work by Pizzanelli and colleagues, which identified that loss of α_{1B}-AR expression resulted in significant protective effects against the onset of chemoconvulsant-induced seizures, in mice. While our own results do not support a role for the potential proconvulsant effects of α_{1B}-AR activation, it cannot be ruled out. In fact, the results by Pizzanelli are extremely compelling and, taken together, may support a hypothesis for a compensatory effect in α_{1B}-AR knockout mice. However, no reciprocal increase in α_{1A}-AR or α_{1B}-AR was observed in either receptor knockout mouse strain, as would be expected if there were a compensatory mechanism at work. Thus, the exact mechanism of α_{1A}-AR and α_{1B}-AR contributions remains unclear, but both studies utilizing knockout mice have revealed potential anticonvulsant properties of the α_{1A}-AR (in vivo findings

discussed in subsequent chapters) and a proconvulsant or no role for the α_B-AR in epilepsy models. Further, these experiments show exciting progress towards understanding the specific contributions of AR subtypes to the demonstrated antiepileptic nature of NE.

CHAPTER III

α_{1A}-AR ACTIVATION INCREASES THE LATENCY TO EPILEPTIC SEIZURE EMERGENCE, WHILE RECEPTOR KNOCKOUT INCREASES PREVALENCE OF SPONTANEOUS AND RECURRENT EPILEPTIC SEIZURES

Introduction

While previous research in our laboratory and the results from Chapter 2 provide ample evidence that α_{1A}-AR activation, specifically, is capable of attenuating epileptiform burst frequency in hippocampal slices, measured in both CA3 and CA1 regions, of both mice and rats, there has been little investigation into the translational potential of these findings. To investigate the effects of α_{1A}-AR activation on seizures *in vivo*, we set out to establish a model of chemoconvulsant-induced seizures, utilizing the sea weed-derived glutamate analog, kainic acid, a potent glutamatergic kainic acid receptor agonist. Importantly, kainic acid induces seizures by creating a hyperexcitatory environment, rather than altering inhibitory circuitry (Ben-Ari *et al*., 2000). The mechanism of this chemoconvulsant was important because we have hypothesized that the effects of α_{1A}-AR on seizure threshold is due to its excitation of inhibitory interneurons. Thus, ablation of inhibitory circuitry would likely mask the efficacy of receptor activation.

The experiments herein, utilized relatively high doses of kainic acid to induce a state of acute *status epilepticus*. While our previous results suggest that NE antiepileptic

characteristics are most efficacious in progressive (chronic) insult models of epilepsy, we wanted to investigate the effects of α_{1A}-AR activation in an acute seizure model. Our reasoning for this choice was an effort to maintain consistency with the experiments performed in hippocampal slices and we were interested in the robustness of any observed effects. Our hippocampal slice model of epilepsy is an acute model, in that magnesium deprivation is constant throughout our experiment and that the short-term nature of our recordings provides little time for changes to hippocampal circuitry, as would be expected in chronic seizure/epilepsy models.

In addition to kainic acid-induced seizures, we investigated anecdotal and initial investigations into spontaneous seizures observed in α_{1A}-AR knockout mice. Unfortunately, this propensity for seizures means that the α_{1A}-AR knockout mice are a poor candidate for induced seizure models. Instead, we observed α_{1A}-AR knockout mice over a period of 48-hours to investigate several lingering questions about these spontaneous seizures; do α_{1A}-AR knockout mice only exhibit seizures when exposed to aversive, stressful stimuli (such as handling or bright, open spaces)? Can these seizures be considered chronic, possibly indicating α_{1A}-AR knockout mice as a candidate epilepsy model? What are the nature of these seizures? We make observations of these questions and we establish a protocol for electroencephalographic characterizations of seizures in these mice.

Our investigation of α_{1A}-AR activation in kainic acid-induced *status epilepticus* is an important step towards evaluating the translation potential of an α_{1A}-AR antiepileptic therapy. Further, our use of kainic acid, other than being advantageous, was very purposeful. Kainic acid is a versatile chemoconvulsant that can be used in low doses to

induce a model of temporal lobe epilepsy which exhibits some similarities to kindling-induced epilepsy; a model which has shown ARs to be particularly efficacious (Tse *et al*., 2014; Hellier *et al*., 1998).

The results presented herein lay the framework for future investigations of the α_{1A}-AR antiepileptic modality in chronic models of epilepsy. However, for the first time, these results directly elucidate the translational potential of our findings in hippocampal slices *in vivo* and suggest applicability of α_{1A}-AR activation characteristics outside of the hippocampus. Additionally, our investigations of the spontaneous seizures exhibited by α_{1A}-AR knockout mice may suggest that this receptor subtype may be a viable and novel animal model of epilepsy.

Materials and Methods

Animal Use and Drug Treatment

Mice were housed in an AAALAC-accredited facility at the University of North Dakota. All experiments involving mice were performed under IACUC-approved protocols. C57BL/6J mice were obtained from Jackson Laboratories. Knockout background mice (in-bred C57BL/6 mice) and α_{1A}-AR knockout mice were generously provided by the lab of Dianne Perez at the Cleveland Clinic Foundation (Lerner Institute, Cleveland, OH).

All kainic acid experiments used male and female C57BL/6J mice, aged 80-95 days. Following general health assessments, mice were randomly and evenly distributed to into untreated control or treated groups. In treatment groups, mice were administered 40μM cirazoline hydrochloride (Tocris Bioscience), in drinking water, *ad libitum*.

Importantly, treated drinking water was prepared using only water from the same source as untreated mice. Cirazoline treatment continued for a period of 4-weeks prior to experimentation.

α_{1A}-AR Knockout Mouse Generation

α_{1A}-AR knockout reporter mice were generated as previously described (Rokosh *et al*., 2002). Briefly, a plasmid vector containing 1.1 Kb from the 5' arm and 6.5 Kb from the 3' arm, sequence retrieved from the 129/SvJ genomic library, targeted portions of critical exon 1 and the adjacent intron for excision from the α_{1A}-AR gene. This vector also contained a LacZ operon and conferred resistance for neomycin.

The plasmid vector was transfected into RW-4 129/SvJ embryonic stem cells using electroporation. Positive transfections were identified with neomycin resistance. Positive cells were cultured and analyzed for correct insertion. A small fraction of transfected samples contained the correct insertion with no additional random insertions. These embryonic stem cells were subsequently chosen for insertion into C57BL/6 blastocysts. Blastocysts were implanted into a 129SvJ x FVB/N female; subsequently, pups were assessed for germ-line expression of the correct mutation.

Finally, heterozygous mutant mice were bred up and back-crossed with C57BL/6 and FVB mice for several generations. These mice are considered congenic to C57BL/6 mice, the stain for which we utilize as "normal" controls (Simpson PC, 2006).

Seizure Generation

Following a 30-minute cage acclimation period, seizures were generated in mice following intraperitoneal injection of the chemoconvulsant kainic acid (Tocris

Bioscience), at 25 or 35 mg/kg. The doses we used, 25 mg/kg and 35 mg/kg, resulted in about 40% mortality and greater than 70% mortality, respectively, across all treatment groups. Additionally, 35 mg/kg kainic acid resulted in nearly all mice reaching severe seizure stages, including generalized tonic-clonic seizures. Due to its relatively short half-life in solution, kainic acid was prepared fresh daily, several hours prior to experiments, at a stock concentration of 2.0 mg/mL, in 1x phosphate buffered saline. Kainic acid solutions were prepared from the same chemical stock batch for each experiment to maintain maximal consistency. Mice were observed for a total of 2-hours post-injection.

Behavioral Scoring

Seizures were scored according to a modified Racine's scale for characterizing rodent seizures. Briefly, seizure activity was scored grades 1-6 according to the following criteria: (1) Sudden and prolonged cessation movement with orofacial spasms, (2) prolonged and exaggerated hunched posture with head bobbing, (3) emergence of pronounced forelimb clonus, (4) emergence of forelimb clonus and rearing, (5) progression to rearing and falling, (6) loss of postural control with full body involvement tonic-clonic activity. Grade 1 activity was not characterized in experiments without electroencephalographic confirmation. Seizure activity was recorded for later analysis. Videos were blinded by persons uninvolved with the experiments and unaware of the treatment groups for scoring by a trained observer.

Video Synchronized Electroencephalography

Kainic acid response was further characterized using video-EEG. Briefly, a four-channel EEG head-stage (Pinnacle Technologies) was surgically attached to the mouse

skull (Fig. 8). Leads were placed strategically to capture frontal cerebral, caudal cerebral, and cerebellar activity. Cerebellar activity was recorded as a negative control channel. The final EEG channel was embedded within the dental cement, used to attach the head-stage, and detected any movement-related or intrinsic noise. Transcranial electrodes were jewelry screws with a soldered silver wire lead attached to a dedicated head-stage terminal. All solder was electrically conductive in case of loose attachments.

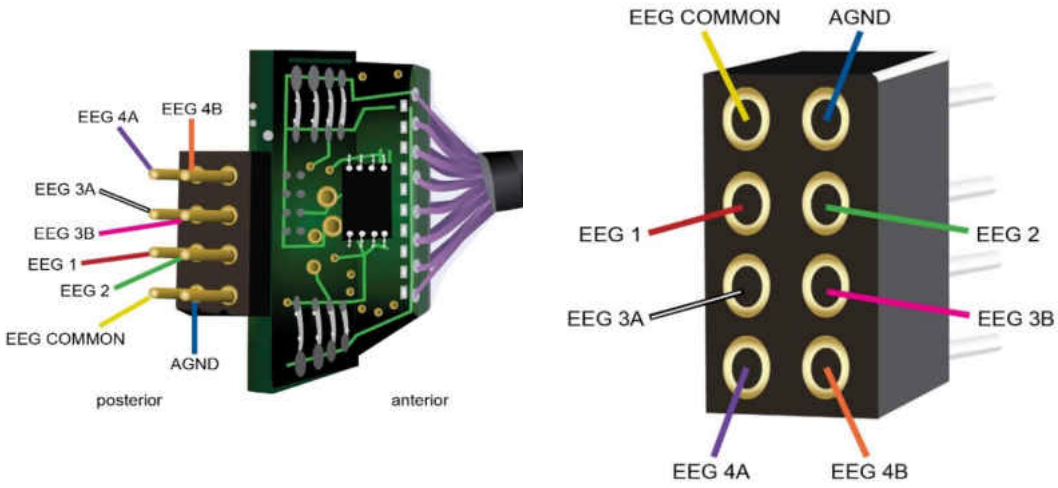

Figure 8. Electrode Pinout Diagram. Illustration showing the electrode configurations on the data acquisition plug (Left), with attached amplifier and filter, and EEG head-stage (Right), showing the receptacle. Permission for publication was obtained directly from representatives with the manufacturer, Pinnacle Technologies. Image credit: Pinnacle Technologies, Lawrence, KS.

Surgery

Mice were given a pre-operative subcutaneous dose of buprenorphine sustained release (SR) analgesic at 0.5 mg/kg at least one-hour prior to anesthesia. Following buprenorphine acclimation, mice were deeply anesthetized via intraperitoneal injection of ketamine [12.5 mg/mL]/xylazine [2.0 mg/mL] cocktail. Consciousness was tested by toe

pinch. Once fully unconscious, mice were mounted in stereotaxic unit with ear and bite bar. The area of incision was prepared by shaving and sanitization while lubricating gel (Bausch & Lomb) was applied to the eyes. A midline incision was made to expose the surface of the skull and any remaining superficial fascia was removed from the surface. Electrode pilot holes were drilled at the following stereotaxic coordinates (to Bregma, to Midline): +2.0 mm, ±1.5 mm for EEG #1; -2.75 mm, ±1.5 mm for EEG #2; -7.0 mm, ±1.5 mm for EEG #3; and non-specific placement in dental cement for reference EEG #4. All Electrode screws were inserted to a depth of approximately 1.0 mm to contact the cortical or cerebellar surface. All surgeries were performed according to standard recommendations by the hardware manufacturer, Pinnacle Technologies. Dental cement was utilized to ensure stable electrode placement and head-stage attachment. Mice were given an additional dose of buprenorphine SR 72-hours post-surgery. Additionally, mice were observed for signs of pain, excessive inflammation, and infection daily for at least one-week post-surgery. Mice were promptly euthanized if they had not eaten in 24-hours, showed greater than 20% weight loss, or showed more than three symptoms of pain and distress (self-mutilation, increased/decreased movement, unkempt appearance, dehydration, tremor, etc.).

Recording

Mice began treatment phase following 1-week of recovery. For more information about cirazoline treatment refer to "Animal Use and Treatment" within this section. Following completion of the treatment phase, mice were allowed to acclimate to EEG tether for at least 24-hours. An additional 24-hours was allowed for the recording of baseline observations and comparison between untreated and treated groups. Then,

mice were injected with kainic acid as outlined above and observed for seizure activity for 2-hours post-kainic acid injection. Synchronized video or video-EEG data was collected for later analysis. Video feed was captured by two cameras (Arecont Vision) opposed at 45-degree angles to maximize probability of optimal viewing angle (Fig. 9). Video feeds and EEG data were transferred to a custom-built Dell computer workstation (Pinnacle Technologies) after being passed through a power-over-ethernet switch for synchronization of feeds. Data was captured internally using Pinnacle Acquisition software (Pinnacle Technologies) and later transferred to external SATA HDDs (Western Digital), via hot swap hard drive bay (ThermalTake) for data transfer and archival.

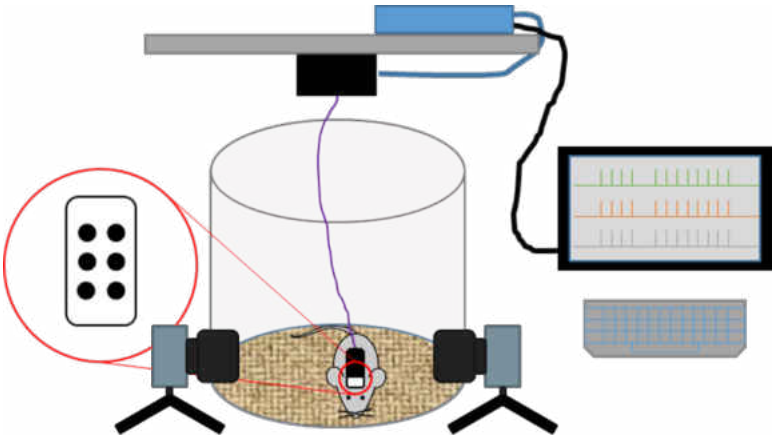

Figure 9. Video and Video-EEG Apparatus. Image generated using Microsoft PowerPoint 2016. Credit: Pinnacle Technologies, illustration adapted from image on pinnaclet.com.

Analysis

Data files were blinded as previously described for analysis in Seizure Pro software (Pinnacle Technologies). Video data was manually scored as previously outlined. Data was analyzed for manifestation of sub-behavioral threshold seizure activity. EEG data was assessed for seizures by threshold analysis and line length

measurement. Additionally, short-time Fourier transformation analysis was utilized to compare cortical neural oscillatory frequency band intensities between untreated and treated groups preceding, during, and between seizures. While not implemented here, basic spatiotemporal mapping was achieved by comparing electrode intensities between the frontal and caudal cerebral EEG channels.

Statistics

Latency to behaviorally progressive seizures was compared individually by t-test comparisons. Multiple comparisons were not weighted due to the inevitable and expected increases variance when measuring separate seizure parameters. Additionally, the sample of each subsequent latency are representative of subsets of the same population, measured for different characteristics, no attempt was made at inter-stage comparisons. A probability of insignificance alpha threshold of $P<0.05$ was set for rejection of the null hypothesis. All data are graphically presented as mean±SEM, while alpha levels are presented as follows: 0.05 (*), 0.01 (**), 0.001 (***).

Results

High Doses of Kainic Acid Show a Consistent Trend of Increased Latency to Seizure Formation and Intensification in Mice Treated with Cirazoline

In our initial efforts to establish a kainic acid-induced seizure model, a 35 mg/kg dose of the chemoconvulsant was utilized to assess the potential antiepileptic effects of long-term α_{1A}-AR activation, with cirazoline. We observed a consistent trend of increased latency to emergence of seizure activity and intensification in cirazoline-treated mice (Fig. 10). Specifically, latency to the emergence of grades 2-6 for non-treated

control mice were as follows: [2] 963.0±149.5 seconds (n=8), [3] 1580.3±310.7 seconds (n=8), [4] 1771.0±301.5 seconds (n=8), [5] 2101.1±409.1 seconds (n=8), and [6] 2928.6±749.7 seconds (n=8). In comparison, the latency to each stage was somewhat greater in cirazoline-treated mice: [2] 1753.8±515.8 seconds (n=12), [3] 2337.9±482.5 seconds (n=12), [4] 2556.7±491.9 seconds (n=12), [5] 2748.7±496.1 seconds (n=12), and [6] 3539.0±692.0 seconds (n=12). Multiple t-test comparisons did not reveal any statistical differences between cirazoline-treated and non-treated control groups at any seizure stage. However, the consistent trend of lower values for the emergence of every stage warranted further investigation. Specifically, we hypothesized that the dosage of kainic acid may have overpowered inhibitory circuitry and a lower dose may reveal important differences unobserved at 35 mg/kg kainic acid. Further, we seeked to increase the number of animals used from each sex in order to investigate any differences in efficacy.

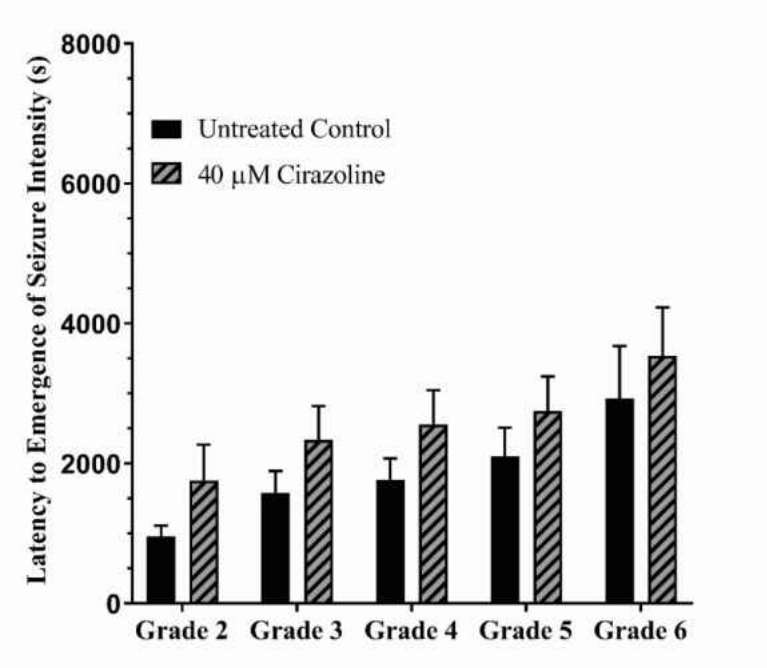

Figure 10. Effect of Cirazoline Treatment on Latency to Emergence and Progression of Seizures in Response to High Dose Kainic Acid. Mice were administered intraperitoneal injections of 35 mg/kg kainic acid following an acclimation period of at least one-half hour. Grades on X-axis are indicative of the presence of the following behavioral seizure characteristics: (2) prolonged and exaggerated hunched posture with head bobbing, (3) emergence of pronounced forelimb clonus, (4) emergence of forelimb clonus and rearing, (5) progression to rearing and falling, (6) loss of postural control with full body involvement tonic-clonic activity. Being that each measured stage was from largely the same sample population, and not all mice achieved higher than grade 2 seizures, we did not account for multiple comparisons in our T-test comparisons. No statistical significance was observed.

Cirazoline-treated Mice Exhibit Increased Latency to Initial Emergence of Low-dose Kainic Acid-induced Seizures

Next, we assessed the effect of cirazoline treatment on the latency to emergence and progression of chemoconvulsant-induced seizures by utilizing a lower, 25 mg/kg, dose of kainic acid. As illustrated in Figure 11, latency to the emergence of grades 2-6 for non-treated control mice were as follows: [2] 816.3±92.6 seconds (n=24), [3]

3104.5±408.7 seconds (n=24), [4] 4020.8±505.8 seconds (n=24), [5] 5157.5±533.9 seconds (n=24), and [6] 5656.4±495.7 seconds (n=24). In comparison, the latency to initial stage emergence was somewhat greater in cirazoline-treated mice: [2] 1616.3±382.2 seconds (n=23), [3] 3188.9±523.8 seconds (n=23), [4] 3583.4±524.5 seconds (n=23), [5] 4447.5±608.1 seconds (n=23), and [6] 4914.4±572.8 seconds (n=23). Because each category represented a separate measurement of the same samples, with drastically different expected variances, we utilized multiple t-test comparisons, without correcting for multiple comparisons. This analysis showed a significant difference in the emergence of grade 2 seizure activity (P=0.04) when comparing non-treated controls and cirazoline-treated groups. The latency for grade 2 activity was 799.9±385.8 seconds greater in cirazoline-treated mice, or 198.0±51.9% of control latency.

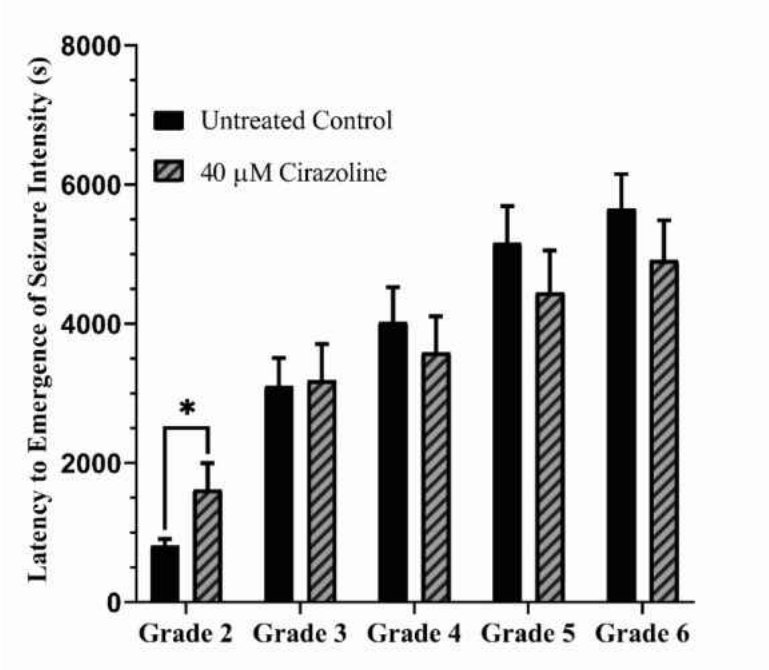

Figure 11. Effect of Cirazoline Treatment on Latency to Emergence and Progression of Seizures in Response to Low Dose Kainic Acid. Mice were administered intraperitoneal injections of 25 mg/kg kainic acid following an acclimation period of at least one-half hour. Grades on X-axis are indicative of the presence of the

following behavioral seizure characteristics: (2) prolonged and exaggerated hunched posture with head bobbing, (3) emergence of pronounced forelimb clonus, (4) emergence of forelimb clonus and rearing, (5) progression to rearing and falling, (6) loss of postural control with full body involvement tonic-clonic activity. Being that each measured stage was from largely the same sample population, and not all mice achieved higher than grade 2 seizures, we did not account for multiple comparisons in our T-test comparisons. No statistical significance was observed. Statistical significance is presented, as follows: $P < 0.05$ (*), $P < 0.01$ (**), $P < 0.001$ (***).

There were no apparent differences between untreated controls and cirazoline-treated groups between males and females (Fig. 12). However, it was apparent that female mice were apparently more vulnerable to the kainic acid insult than were male mice, regardless of treatment. While this is an interesting finding, it was not a primary goal of this study, and so no statistical assessment was performed on this data.

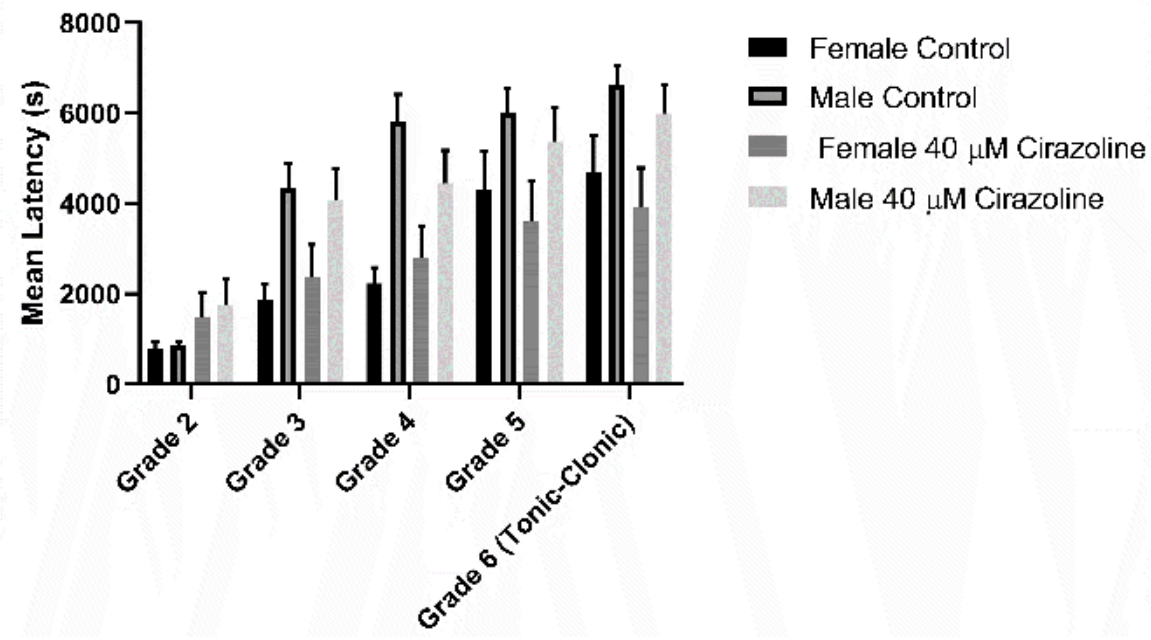

Figure 12. Effect of Cirazoline Treatment on Latency to Emergence and Progression of Seizures in Response to Low Dose Kainic Acid, Separated by Sex. Mice were administered intraperitoneal injections of 25 mg/kg kainic acid following an acclimation period of at least one-half hour. Grades on X-axis are indicative of the presence of the following behavioral seizure characteristics: (2) prolonged and

exaggerated hunched posture with head bobbing, (3) emergence of pronounced forelimb clonus, (4) emergence of forelimb clonus and rearing, (5) progression to rearing and falling, (6) loss of postural control with full body involvement tonic-clonic activity. No statistical assessments were performed.

Video-electroencephalography Characteristics of Seizure Activity in Non-Treated Control and Cirazoline-Treated Mice

Analysis of the previously discussed methods with electroencephalography confirmed the electrographic nature of the seizures we were characterizing using the method of Racine. Additionally, we were able to confirm the existence of prominent EEG seizure activity corresponding with behavioral manifestation, i.e. Racine's scoring (Fig. 13).

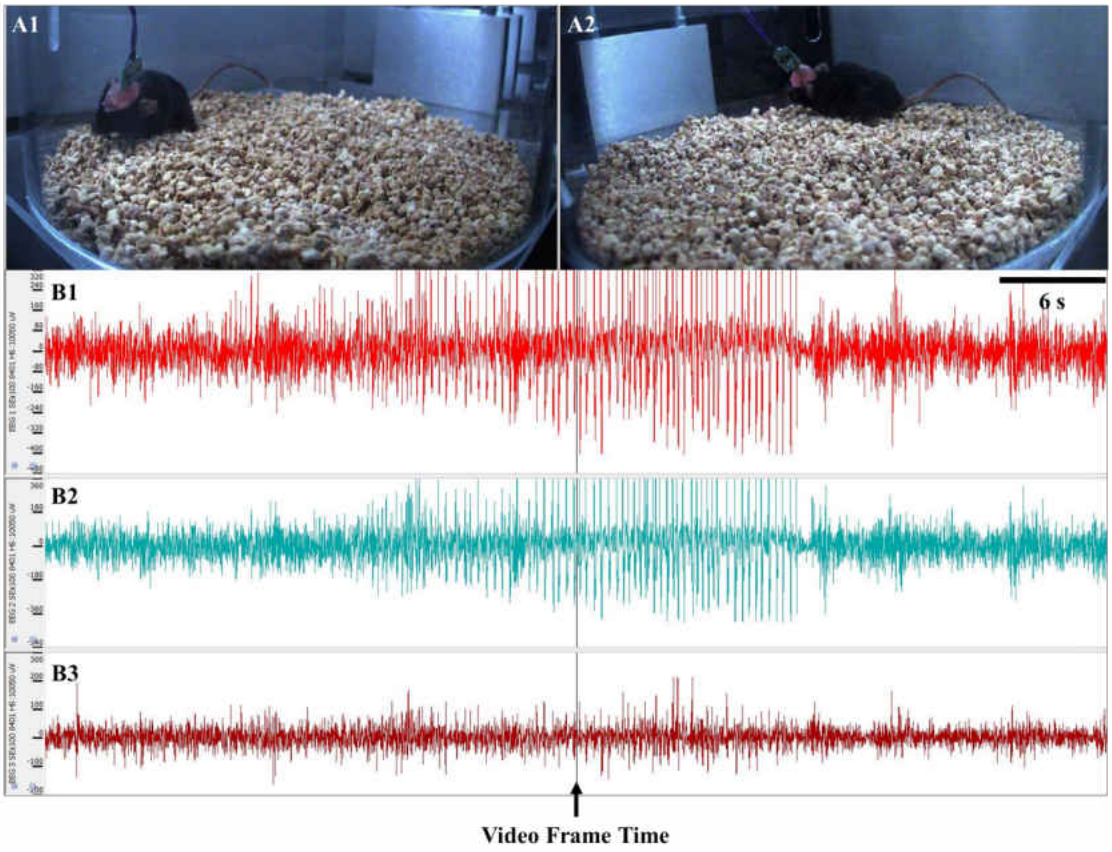

Figure 13. Example Video-EEG of Confirmed Seizure Following Intraperitoneal Kainic Acid Injection. In the EEG trace there is a clear apparent increase in EEG electrical potential amplitude (mV) and corresponding video indicates Racine's Grade 2 motor seizure. (A) Still frames from synchronized video recording of seizure, from both camera perspectives, showing hunched posture, forelimb tonus, nuchal clonus (head bobbing, not apparent in still), and tail rigidity. (B) EEG trace activity excessive and hypersynchronized EEG electrical potential (mV) (i.e. a seizure) measured from multiple electrodes. [1] Trace of left parietal area electrode (to Bregma, to Midline): -2.75 mm, -1.5 mm; [2] Trace of right parietal area electrode (to Bregma, to Midline): -2.75 mm, +1.5 mm; [3] Trace of combined left-right frontal electrodes (to Bregma, to Midline): +2.0 mm, ±1.5 mm; (not shown) Trace of acrylic-embedded electrode to capture noise and movement artifacts. Labelled indicator shows the time point shown in (A).

As summarized in Figure 15, we observed a mean latency to the first EEG-confirmed seizure of 813.5±188.4 seconds (n=4) in untreated control mice and a mean latency of 912.5±44.2 seconds (n=3) in mice treated with 40 μM cirazoline. These results seem to suggest a very similar onset latency for initial seizure activity with a slight delay observed in cirazoline-treated mice; however, a confounding variable is that only 3/5 cirazoline-treated mice exhibited any level of seizure activity. In all kainic acid studies, we attempted to control for variance in the kainic acid solutions from day-to-day by performing experiments with both groups, alternating which treatment group underwent early versus later injections.

Despite attempts to control for any differences in kainic acid doses have noticed in each set of experiments (35 mg/kg kainic acid, 25 mg/kg kainic acid, and 25 mg/kg kainic acid with EEG) that there were several mice which did not exhibit any seizure activity. Specifically, across all kainic acid experiments, 36/36 control mice exhibited at least low-grade seizure activity, while only 35/40 cirazoline-treated mice exhibited at least low-grade seizure activity. This phenomenon is interesting considering the findings of Pizzanelli *et al*. (2009), which found this to be a very common occurrence in α_{1B}-AR

knockout mice. However, it is difficult to rule out the possibility of a missed injection, so we have chosen to present this data without making definitive conclusions.

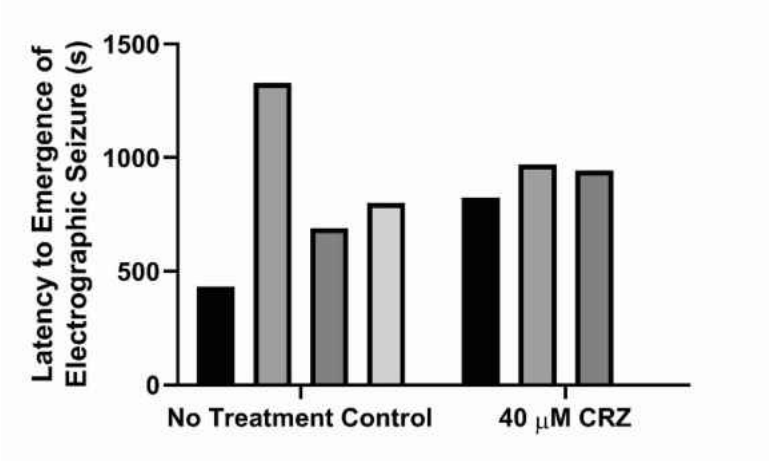

Figure 14. Latency to Initial Kainic Acid-Induced Electrographic Seizure in Untreated Control and Cirazoline-Treated Mice. Latency values are presented separately due to relatively low sample size and high variance. Similarly colored bars are not corresponded in any way. Each electrographic seizure was identified in Pinnacle Seizure Pro software by threshold analysis and confirmed with line length analysis, being defined as at least 2 times greater than background for ≥10 seconds. Noise and movement artifacts were controlled via a dedicated acrylic-embedded electrode.

Given our previous observations that cirazoline treatment delays the initial onset of behaviorally-manifested motor seizures, we hoped to characterize the nature of this sub-behavioral seizure activity in non-treated and cirazoline treated mice (Fig. 15). Unfortunately, we were unable to collect sufficient data due to the difficult nature of the electrode implantation surgeries. Interestingly, we noticed a nearly instantaneous spike in EEG activity following kainic-acid injection. While the high doses of kainic acid were useful for separating seizure initiation and progression in the treatment groups from a behavioral perspective, it indicates that we may need to significantly lower the dose of kainic acid used when assessing sub-behavioral seizure activity.

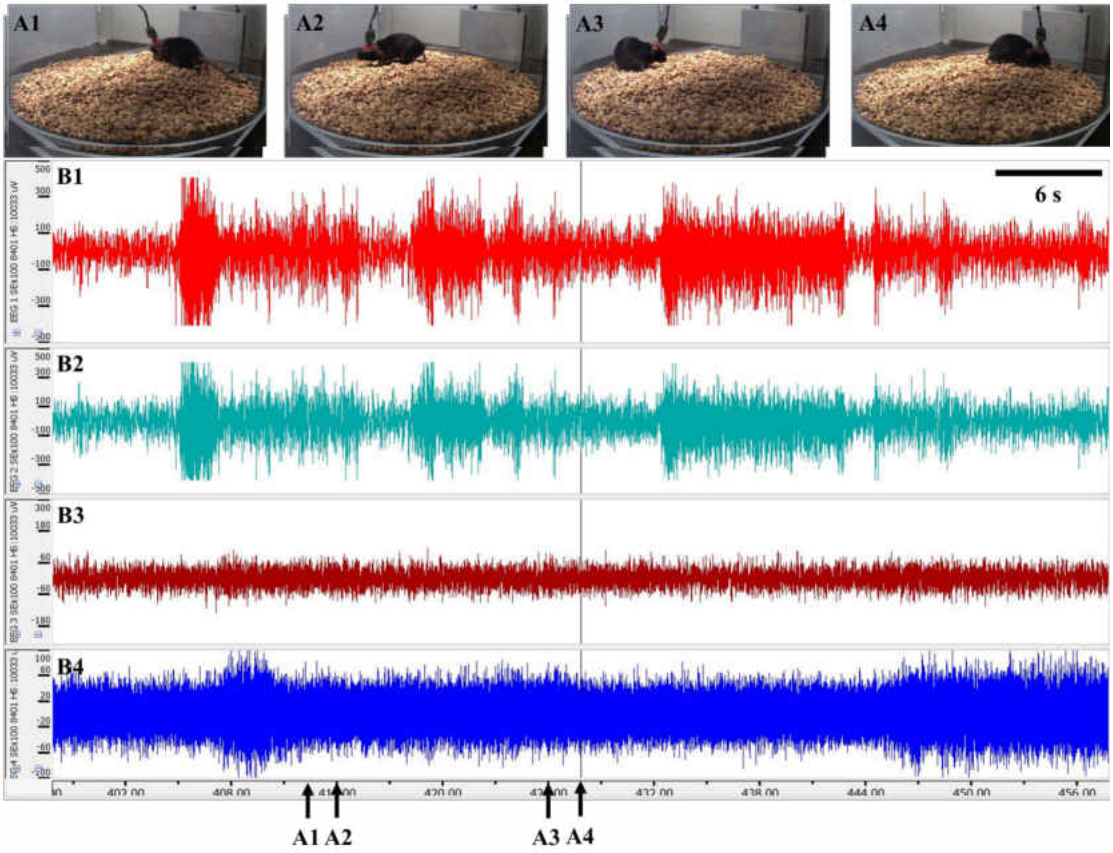

Figure 15. Example Video-EEG of Initial Activity Following Intraperitoneal Kainic Acid Injection. In the EEG trace there is a clear apparent increase in EEG electrical potential amplitude (mV), but corresponding video shows does not indicate generalized cognitive impairment. (A) Still frames from synchronized video recordings of possible mouse seizure activity; [1-4] correspond to the indicators at the bottom of B4. (B) EEG trace activity showing increased EEG electrical potential (mV) measured from multiple electrodes. [1] Trace of left parietal area electrode (to Bregma, to Midline): -2.75 mm, -1.5 mm; [2] Trace of right parietal area electrode (to Bregma, to Midline): -2.75 mm, +1.5 mm; [3] Trace of combined left-right frontal electrodes (to Bregma, to Midline): +2.0 mm, ±1.5 mm; [4] Trace of acrylic-embedded electrode to capture noise and movement artifacts.

Spontaneous Epileptic Seizures in α_{1A}-AR Knockout Mice, As Assessed by Behavioral-Scoring and Electroencephalography

Previous work led by a former Doze lab member, Dr. Katie Collette, observed a high incidence of seizures in α_{1A}-AR knockout mice. In these observations, 55.8%

(19/34) α_{1A}-AR knockout mice exhibited seizure activity after handling and during 15-minute observations in an open field apparatus. It was noted that all seizures observed were Racine's grade 1 or 2. This high incidence was in comparison to wild-type controls and α_{1B}-AR knockout mice, where no seizures were observed. Interestingly, there was anecdotal evidence of these seizures for years. During normal cage changes, both members of our laboratory and members of the CBR staff frequently noted seizures in these mice. From these anecdotal observations and seizure incidence measurements, we became interested about the nature of these seizures.

We utilized custom video recording apparatuses to capture behavior of α_{1A}-AR knockout mice; each recording was for a period of 48-hours. Additionally, we attempted to minimize stressful stimuli, via the following steps: (1) Each mouse was individually caged in an observational cylindrical cage lined with normal home cage bedding; (2) mice received *ad libitum* access to food and water; (3) a white noise machine was utilized to decrease extraneous jarring sounds in the environment; (4) Room lights were automatically timed to mimic home cage light-dark cycles (07:00 on/19:00 off); (5) mice were allowed to acclimate to observation cages for at least 24-hours before observations began. We observed 8 α_{1A}-AR knockout mice (4 females, 4 males) for both seizure incidence and severity, while noting information about time-of-day and activity level prior to seizure occurrence.

All mice exhibited unusual activity that could have been interpreted as a motor seizure (e.g. prolonged freezing), but only progressive and obvious seizures were counted towards analyses. Our observations revealed a confirmed motor seizure incidence of 75% (6/8) during 48-hour of observation. The number and severity of observed seizures

ranged widely. A total of 26 motor seizures were observed, with a mean prevalence of 3.25±1.65 (Range: 0-14) seizures per mouse. The mean Racine's grade of observed seizures was 3.12±0.30, Range: 2-6 (Fig. 16).

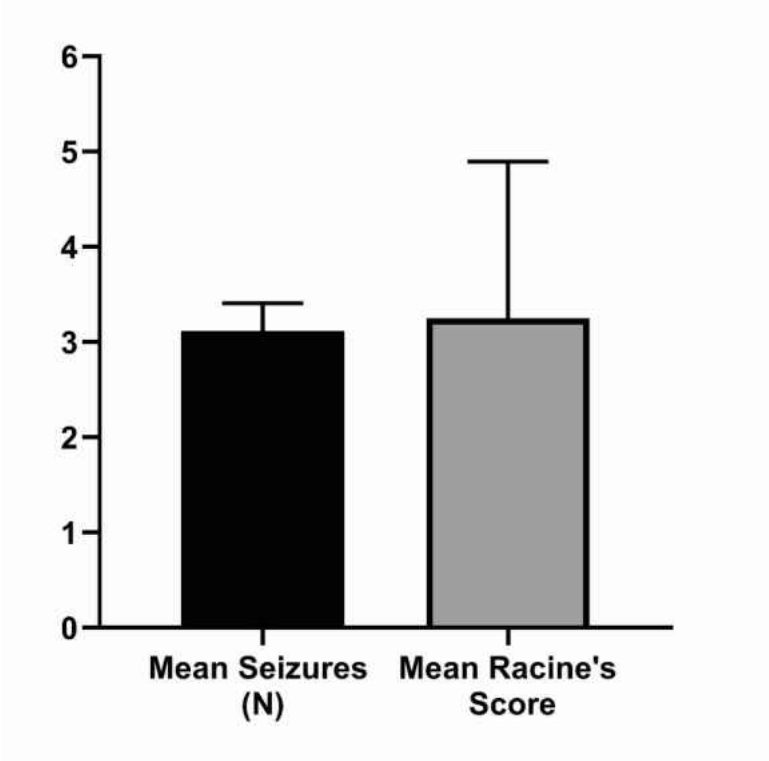

Figure 16. Mean Number of Seizures Observed per Mouse, with Mean Seizure Severity, in α_{1A}-AR Knockout Mice. The mean number of seizures included all mice, including those which did not exhibit any motor seizure activity. The mean Racine's Score was estimated from the aggregated score of all seizures and was not weighted. Information about seizures in individual mice can be found in Table 1. All values are represented as mean±SEM.

The majority of seizures were exhibited by one individual, with14 confirmed motor seizures over the 48-hour recording period. However, the maximum grade assigned to these seizures was a 3-out-of-6. Two other individuals exhibited several high grade seizures (grades 4-6), which involve intense tonus and/or clonus, usually involving the entire body. Finally, the two remaining mice exhibited only one, low-grade motor

seizure each. A description of individual seizure characteristics, as well as information about activity level preceding seizure, time-of-day, and sex and age are listed in Table 1. While seizure start and end times were noted, we did not estimate seizure duration because of the difficult making an assessment of when a seizure ends without EEG confirmation. Following the main seizure, there is typically a period of ictal tonic immobility or normal EEG period with no movement, which are difficult to discern.

		Seizure Start -- End (s)	Activity Level	Time of Day	Racine's Grade
ID:	Mouse 1				
Sex:	Male				
Age (days)	469				
Confirmed Seizure?	No				
Notes:	None				
ID:	Mouse 2				
Sex:	Male				
Age (days)	616				
Confirmed Seizure?	No				
Notes:	None				
ID:	Mouse 3				
Sex:	Male				
Age (days)	616				
Confirmed Seizure?	Yes				
Notes:		11838 -- 11934	Active	Night	2
		15801 -- 15919	Active	Night	3
		98337 -- 98399	Active	Day	2
		104569 -- 104584	Active	Day	2
		104617 -- 104665	Active	Day	2
		105227 -- 105332	Active	Day	3
		106778 -- 106811	Active	Day	2
		107504 -- 107559	Active	Day	2
		108300 -- 108409	Active	Day	3
		111934 -- 111972	Active	Day	2
		114836 -- 114909	Active	Day	2
		117319 -- 117424	Active	Day	2
		121482 -- 121542	Active	Day	2
		134139 -- 134571	Sleeping	Night	3
ID:	Mouse 4				
Sex:	Male				
Age (days)	616				
Confirmed Seizure?	Yes				
Notes:		89237 -- 89245	Sleeping	Day	4
		113437 -- 113488	Active	Day	2
		131366 -- 131371	Sleeping	Night	5
ID:	Mouse 5				
Sex:	Female				
Age (days)	473				
Confirmed Seizure?	Yes				
Notes:		212355 -- 212476	Sleeping	Night	6
		228552 -- 228591	Sleeping	Day	6
		228606 -- 228765	Active	Day	2
		253645 -- 253744	Sleeping	Day	6
		269338 -- 269473	Sleeping	Day	6
ID:	Mouse 6				
Sex:	Female				
Age (days)	473				
Confirmed Seizure?	Yes				
Notes:		132181 -- 132187	Active	Day	4
		150262 -- 150274	Sleeping	Day	4
ID:	Mouse 7				
Sex:	Female				
Age (days)	473				
Confirmed Seizure?	Yes				
Notes:		171985 -- 171995	Active	Day	2
ID:	Mouse 8				
Sex:	Female				
Age (days)	473				
Confirmed Seizure?	Yes				
Notes:		179856 -- 179916	Sleeping	Night	2

Table 1. Long-term Motor Seizures Recordings in α_{1A}-AR Knockout Mice. Notes of individual, unprovoked motor seizures in α_{1A}-AR knockout mice. Information about sex, age, and the nature of each seizure is listed. Seizure characteristics include motor seizure initiation time, estimated time of cessation, activity level, time of day, and Racine's Grade for severity.

In order to assess the validity of our motor seizure assessments, two α_{1A}-AR knockout mice were fitted with EEG head-stages which measured brain electrical activity at two leads placed on the left and right hemispheres over the cerebrum. One α_{1A}-AR knockout exhibited spontaneous seizures over several days of recording, including a Racine's grade 5 seizure event (Fig. 17).

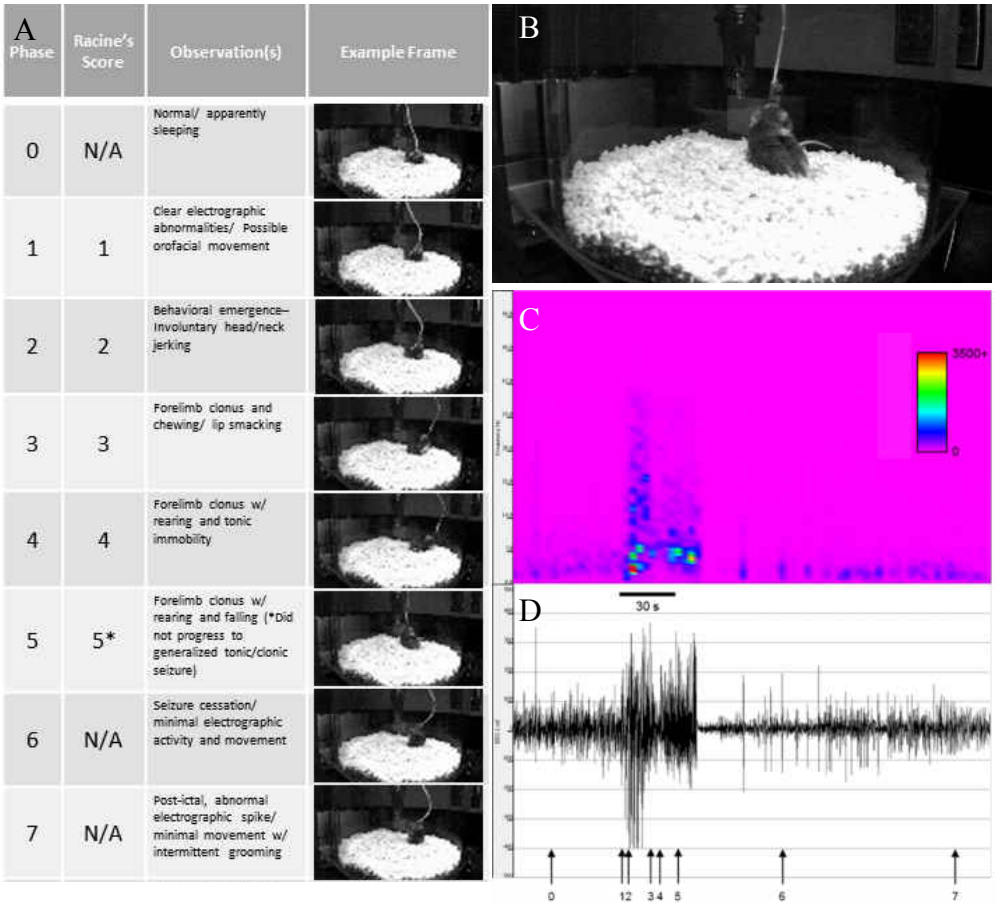

Figure 17. Example of Unprovoked Racine's Grade 5 Seizure, with EEG, in α_{1A}-AR Knockout Mouse. (A) Description of seizure phases, including initation, progression, and cessation. (B) Enlarged image of camera view of Racine's Grade 5 seizure activity; shows mouse in unaturally reared posture due to hindlimb tonus prior to exhibiting

multiple falls. (C) Time-course power spectrum analysis via Short-time Fourier Tansformation; shows the increase in prevalency of EEG activity throughout all frequency bands, but especially in low frequencies (<10 Hz; green, yellow, and red on heat map). (D) EEG trace showing relative amplitude of electrical potential (mV) as measured from an electrode (other not shown for simplicity). Numbered indicators correspond with seizure phases described in (A).

Discussion

These experiments represented a new foray for our laboratory into understanding the role of α_{1A}-AR activity in in vivo models of epilepsy; an essential step to understanding the translational potential of this receptor. Cumulatively, these experiments have shown a propensity for α_{1A}-AR activation to increase the latency to initial seizure onset after kainic acid chemoconvulsant insult, as well as the necessity for in-tact α_{1A}-AR signaling for maintenance of normal seizure threshold.

Interestingly, the effect size for the latency to initial seizure onset was similar to that seen in dose-response experiments in hippocampal slices. Unfortunately, the current experiments would not allow for the resolution necessary to attribute hippocampal α_{1A}-AR contributions to the observed difference. However, Pinnacle Technologies has recently begun offering custom-fitted head-stages with depth electrodes, which are capable of simultaneously measuring cortical and deep brain EEG. Ultimately, these results suggest a broader role for α_{1A}-AR activation in the resolution of abnormal brain activity and seizures. However, more EEG experiments and refinement of surgical procedures is necessary before definitive statements can be made.

Results in α_{1A}-AR knockout mice revealed interesting findings surrounding the nature of seizures in these mice. First, we observed that α_{1A}-AR knockout mice indeed exhibit significant seizure activity devoid of obvious provocation. This suggests that the seizures observed are spontaneous, but may be worsened with aversive stimuli.

Additionally, we found that half of the mice observed exhibited multiple seizures over a 48-hour period. Interestingly, this rate of seizure occurrence is similar to guidelines for epilepsy diagnosis. This may suggest α_{1A}-AR knockout mice as an animal model of spontaneous epilepsy. Likewise, constitutively active mutant α_{1B}-AR mice have been described to develop a Parkinsonian phenotype in aged mice and have been documented to exhibit seizures (Zuscik *et al.*, 2000). Finally, we report that some mice exhibited Racine's grade 4-6 seizures (Convulsive, 3-6). This is evidence for potential severe epilepsy phenotypes in some α_{1A}-AR knockout mice. Our findings, that of the constitutively active mutant α_{1B}-AR mouse, and previously mentioned findings by Pizzanelli (2009) suggest a role for the α_1-ARs in seizures and epilepsy and a potential of opposing roles of the α_{1A}-AR and α_{1B}-AR.

Taken together, our results in this study show a clear importance for α_{1A}-AR function in maintaining normal brain excitability and preventing abhorrent seizure activity. These data fit well with our findings in hippocampal slices and support our hypothesis which suggests antiepileptic characteristics of the α_{1A}-AR. However, these results, in slice and *in vivo*, suggest a modest or moderate effect elicited from α_{1A}-AR activation. However, the most significant findings revolve around seizure activity prevention. Interestingly, previous studies which ablated NE signaling also found the greatest efficacy in delaying seizure or epilepsy onset, rather than acute differences on seizure cessation (Giorgi *et al.,* 2004). Future research may find interesting results when assessing the efficacy of α_{1A}-AR activation in chronic, rather than acute, models of epilepsy.

CHAPTER IV
ENDOGENOUS PROMOTER-DRIVEN REPORTER EXPRESSION SUGGESTS THAT α_{1A}-AR IS OCCASIONALLY CO-LOCALIZED WITH PARVALBUMIN, BUT IS ALSO MODERATELY EXPRESSED ELSEWHERE IN THE MOUSE HIPPOCAMPUS

Introduction

Electrophysiological studies in the rat hippocampus and our work, in the mouse hippocampus, both indirectly suggest that the α_{1A}-AR modulates hippocampal alterations via actions in inhibitory interneurons (Bergles *et al.*, 1996; Hillman *et al.*, 2007; Hillman *et al.*, 2009). However, substantiating this hypothesis has proven difficult because of the lack of any commercially-available antibodies which reliably target the α_{1A}-AR (Jensen *et al.*, 2009). Thus, in order to circumvent this issue several transgenic mouse models have been generated which produce reporter proteins, either tagged to the α_{1A}-AR gene or under the α_{1A}-AR promoter, that can be reliably labelled with immunohistochemical or immunofluorescence assays. Evidence from reporter imaging and single-cell gene expression studies have supported this hypothesis and further suggested that the α_{1A}-AR was expressed on parvalbumin- and somatostatin-expressing interneurons, both common interneuron subtypes, with implications in epilepsy.

Hillman & colleagues first suggested prevalent α_{1A}-AR co-expression with somatostatin using single-cell real-time polymerase chain reaction (RT-PCR) (Hillman

et al., 2005). Subsequent fluorescence imaging of green fluorescence protein (GFP)-labelled α_{1A}-AR transgenic mice supported these findings, observing GFP co-localization on interneurons, identified by markers for glutamic acid decarboxylase (Papay *et al.*, 2006). Further investigation suggested GFP co-localization with both somatostatin and parvalbumin (Knudson, 2007). While supportive of the earlier RT-PCR findings, both the Papay and Knudson experiments identified GFP labelling on hippocampal pyramidal neurons. These results produced questions because our laboratory was unable to illicit an α_{1A}-AR response on any pyramidal cells. Ultimately, these results were attributed to the purposeful overexpression of GFP-labelled α_{1A}-AR. Thus, with the limited scope of single-cell PCR and the questions surrounding the likely false-positive expression of the α_{1A}-AR on hippocampal pyramidal neurons, in the GFP-tagged α_{1A}-AR transgenic mouse, we aimed to investigate α_{1A}-AR reporter expression in a non-overexpressed model system.

We utilized the α_{1A}-AR knockout mouse, developed by Simson & colleagues, to investigate α_{1A}-AR reporter immunofluorescence labelling and co-labelling with parvalbumin-expressing cells in the hippocampus. This knockout mouse has a knock-in LacZ gene, expressed under the endogenous α_{1A}-AR gene promoter, which allows for reliable labelling of cells which would normally express the α_{1A}-AR. Further, the advantage of utilizing LacZ as a reporter is that it allowed for the investigation of functional characterization of β-Galactosidase enzyme, the protein product of the LacZ gene, using the X-Gal colorimetric assay.

Ultimately, the goal of identifying the expression patterns of the α_{1A}-AR in the hippocampus is aimed at determining the mechanisms by which the α_{1A}-AR alters interneuron excitability. Current evidence suggests that α_{1A}-AR activation modulates the excitability of hippocampal interneurons by altering the conductance of outwardly-rectifying potassium channels and hyperpolarization-activated cyclic nucleotide-gated channels, the so-called "funny current", and in some circumstances by modulating sodium channel conductance (Bergles *et al.*, 1996; Hillman *et al.*, 2007). However, these apparently circumstance-specific mechanisms suggests that there may be several mechanism by which the α_{1A}-AR modulates effects on brain excitability; therefore it is important to develop a model to better understand this complex system.

Materials and Methods

Animal Use

Mice were housed in an AALAC-approved facility and all experiments had IACUC approval. All tissues used in immunofluorescence experiments were prepared and fixed at the Cleveland Clinic Foundation, under the supervision of Dr. Dianne Perez. All mice were generated in the Perez laboratory and each mouse is genotyped to ensure correct mutations.

α_{1A}-AR Knockout Reporter Mouse Generation

α_{1A}-AR knockout reporter mice were generated as previously described (Rokosh *et al*., 2002). Briefly, a plasmid vector, containing 1.1 Kb from the 5' arm and 6.5 Kb from the 3' arm, sequence retrieved from the 129/SvJ genomic library, targeted portions

of critical exon 1 and the adjacent intron for excision from the α_{1A}-AR gene. This vector also contained a LacZ operon and conferred resistance for neomycin.

The plasmid vector was transfected into RW-4 129/SvJ embryonic stem cells using electroporation. Positive transfections were identified with neomycin resistance. Positive cells were cultured and analyzed for correct insertion. A small fraction of transfected samples contained the correct insertion with no additional random insertions. These embryonic stem cells were subsequently chosen for insertion into C57BL/6 blastocysts. Blastocysts were implanted into a 129SvJ x FVB/N female; subsequently, pups were assessed for germ-line expression of the correct mutation.

Finally, heterozygous mutant mice were bred and back-crossed with C57BL/6 and FVB mice for several generations. These mice are considered congenic to C57BL/6 mice, the stain for which we utilize as "normal" controls (Simpson, 2006).

Tissue Preparation

Adult α_{1A}-AR knockout reporter mice were placed in an empty chamber and carbon dioxide gas was slowly released, from a compressed gas cylinder, into the chamber until respiratory arrest was apparent. Mice were quickly transferred out of the contained where the thoracic cavity was opened and the heart exposed. Mice were then intracardially perfused with 37^{o}C PBS through the left ventricle, while a small incision was made to the right atrium. PBS was perfused until the effluent from the right atrium was completely clear. Following clearance of blood, the perfusion solution was switched to ice-chilled (2-4^{o}C) 4% paraformaldehyde (Fisher Scientific). Successful fixation was assessed by rigor of the appendages.

Next, the head was decapitated and the skull was exposed via an incision down the midline. The brain was exposed by carefully removing the remainder of the cervical vertebra, and subsequently, using a scissor to cutting the skull, posterior to anterior, initiated from the foramen magnum. After careful removal of the skull, a spatula was used to slowly remove the brain. Isolated brains were post-fixed in 4% paraformaldehyde (Fisher Scientific) for 4 hours, at 4^{o}C. After 4 hours, brains were washed in and transferred to fresh PBS. Finally, in preparation for sectioning, brains were transferred 15% sucrose (Fisher Scientific) in PBS, then twice transferred to fresh 30% sucrose in PBS, each time equilibrating at 4^{o}C.

Functional β-Galactosidase Visualization

For functional expression experiments, brains fixed according to the previously outlined parameters and sent to the Bergles laboratory, at the Johns Hopkins University, where they were sectioned and stained with X-Gal reagent. Briefly, brains were sectioned in the coronal or sagittal planes, at 35-μm intervals, using a vibrating microtome (Leica VT1000S). Next, tissue slices underwent β-Galactosidase-X-Gal enzymatic reaction, according to an optimized protocol (Bergles Laboratory). Finally, tissue was mounted and visualized using a light microscope.

Sectioning for Immunofluorescence

For immunofluorescence experiments, brains were trimmed and flash frozen with dry ice-cooled isopentane (Fisher Scientific) in optimal cutting temperature compound (OCT)(Leica) and transferred to a refrigerated cryostat (Leica) cooled to at least -20^{o}C. 14-μm thick coronal sections were made and individual slices were transferred to room temperature glass slides (VWR) subbed in gelatin. Slides were evaluated for the presence

of the hippocampi and transferred to a -80^{o}C freezer (So-Lo) until ready for immunostaining.

Immunofluorescence Labelling

Slides were removed from the freezer and allowed to desiccate at room temperature for at least 2-hours prior to proceeding with the immunostaining procedure. Slides were inserted into a copplin jar with 1xPBS to dissolve OCT and then laid flat and marked with a pap-pen (Fisher Scientific) to form a hydrophobic barrier.

Tissue was blocked and permeabilized by applying a sufficient volume of Incubation Solution, consisting of Block-Aid Blocking Solution (ThermoFisher) and 0.1% Triton X-100 Surfact-Amps Detergent Solution (ThermoFisher), over the sample to completely immerse the sample. Tissue samples were incubated in this solution, at room temperature, for 1-hour. A subset of samples underwent an antigen retrieval procedure prior to blocking. This procedure consisted of the following steps: A 1-hour incubation in zinc-formalin (10%) buffer (ThermoFisher), at room temperature; followed by thorough rinsing and an incubation in 1:100 citrate buffer (Vector Labs), pH 6, at 90-95^{o}C, for 10 minutes. Then, samples underwent the normal blocking and permeablization procedure outlined above.

Following blocking and permeablization, slides were incubated with a primary antibody mixture, Rabbit anti-β-Galactosidase (mouse epitope) 1^{o} Polyclonal Antibody [Novus, NB600-305] and Goat anti-Parvalbumin (rat epitope) 1^{o} Antibody [Swant, PVG213], diluted in incubation solution. Slides were coverslipped and incubated overnight, in a moistened box, at 4^{o}C. After overnight incubation with primary antibodies, slides were rinsed at least 3 times with 1xPBS for 5-minutes. Then, slides

were incubated with secondary antibodies, Donkey anti-Rabbit IgG (H+L) Highly Cross-Adsorbed 2^{o} Antibody, Alexa Fluor 568 (ThermoFisher, A-10042) and/or Donkey anti-Goat IgG (H+L) Cross-Adsorbed 2^{o} Antibody, Alexa Fluor 488 (ThermoFisher, A-11055), mixed or separately, for 1-hour, at room temperature, in a foil-covered box. Following secondary antibody incubation, slides were again rinsed at least 3 times, for 5-minutes, in 1xPBS. Finally, slides were mounted with 2-3 drops per slice of ProLong Gold Antifade Moutant with DAPI (ThermoFisher) and a #1 glass coverslip was carefully applied to avoid trapping of air bubbles. Coverslip mountant was allowed to cure for at least 24- to 48-hours, in darkness, prior to proceeding to imaging.

Imaging

Slides were carefully cleaned and placed onto the stage of a Leica TCS SPE DM5500 Scanning Confocal Microscope for imaging. Slides were imaged with laser lines at 405 nm, 488 nm, and 594 nm and corresponding emission filters. Slides were imaged with 10x, 20x, 40x, or 63x objectives, with a 1.5x digital zoom. The 20x, 40x, and 63x objectives were oil-immersion objectives. Images were captured using Leica LAS X imaging software.

Analysis

Images were analyzed using Leica LAS X image analysis software. No statistical analyses were performed in these experiments since the outlined goal of the study was to perform a qualitative assessment.

Results

Functional α_{1A}-AR Reporter Distribution in the Mouse Brain

Our initial efforts in assessing α_{1A}-AR distribution within the mouse brain entailed utilizing the α_{1A}-AR knockout mouse line, which expresses a LacZ operon under the endogenous α_{1A}-AR gene promoter to produce β-Galactosidase protein. We investigated the broad brain expression patterns and fuctionality of the β-Galactosidase reporter protein using X-Gal staining, a synthetic galactose substitute, which undergoes a colorimetric shift when cleaved by β-Galactosidase**.** The product of this reaction stains the puncta containing this protein a dark blue hue and is indicative of the presence of functional protein expression, under the endogenous gene promoter. As shown in in Figure 18, there was broad expression of fucntional β-Galactosidase throughout the brain, with localized areas of high density expression. Particularly, we noted dense expression within the deep layers (layers 4/5) of the cortex and moderate expression within the hippocampus.

While expression patterns within the cortex were interesting and unexpected, little is known about the function of the α_{1A}-AR on the cells within this area, so our analysis going forward focused on the expression within the hippocampus. Broadly speaking, we observed stained puncta distributed fairly evenly throughout the hippocampal regions and layers. The density of stained puncta was somewhat greater within the dentate gyrus and were prevalent in the *stratum lacunosum-moleculare*, a layer of less cell density. Next, we sought to investigate the laminar and regional distribution of puncta using immunofluorescence labeling because this technique allows more specificity when estimating laminar margins and allowed us to investigate the hypothesis that the α_{1A}-AR is predominantly expressed on parvalbumin-positive cells; this is a group of cells,

expressed in the hippocampus and elsewhere in the brain, previously shown to be almost exclusively indicative of a sub-population of inhibitory interneurons

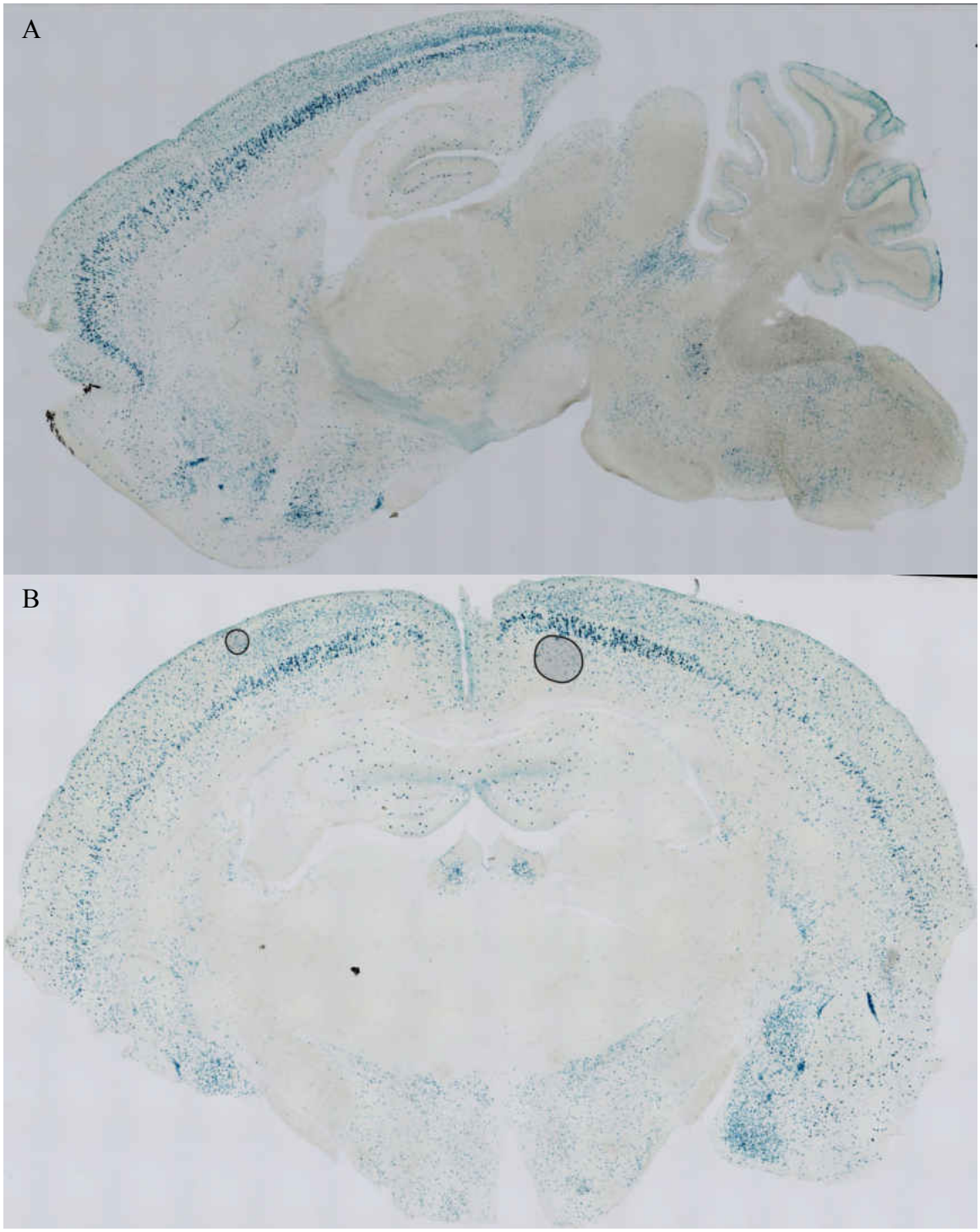

Figure 18. X-Gal Staining of Puncta Expressing Functional α_{1A}-AR Reporter, β-Galactosidase. Low (4x) magnification of the brain, showing the hippocampus, in (A) parasagittal plane (B) coronal plane.

Evaluation of Hippocampal Laminar and Regional Distribution of DAPI-Stained Cell Nuclei Using Confocal Fluorescence Microscopy in Mouse Brain

Laminar distribution of cells-of-interest were characterized based on relative position to the tightly organized and densely packed pyramidal layer of Ammon's Horn (*cornu ammonus*) and granule layer of the dentate gyrus (*fascia dentata*), within the hippocampus. These layers are readily apparent in fluorescence imaging with DAPI nuclear stain. Margins of other hippocampal layers were generally estimated based upon regions of intermediate or sparsely dense nuclear-stained puncta superficial and deep to the readily apparent pyramidal and granule layers. Further, we estimated the regional distribution of the cells of interest. Generally, in addition to the identifying positioning within the dentate gyrus (DG) or Ammon's Horn (CA), it is important to differentiate between regions of Ammon's Horn due to discrete fiber innervation patterns in this reticulated structure. These laminar separations and regions can be visualized in Figure 20, which is a low (20 by 1.5x) magnification stitching of several imaging fields from the same hippocampal slice. This magnification was utilized, rather than a lower magnification, because it allows high enough resolution to see individual punctum.

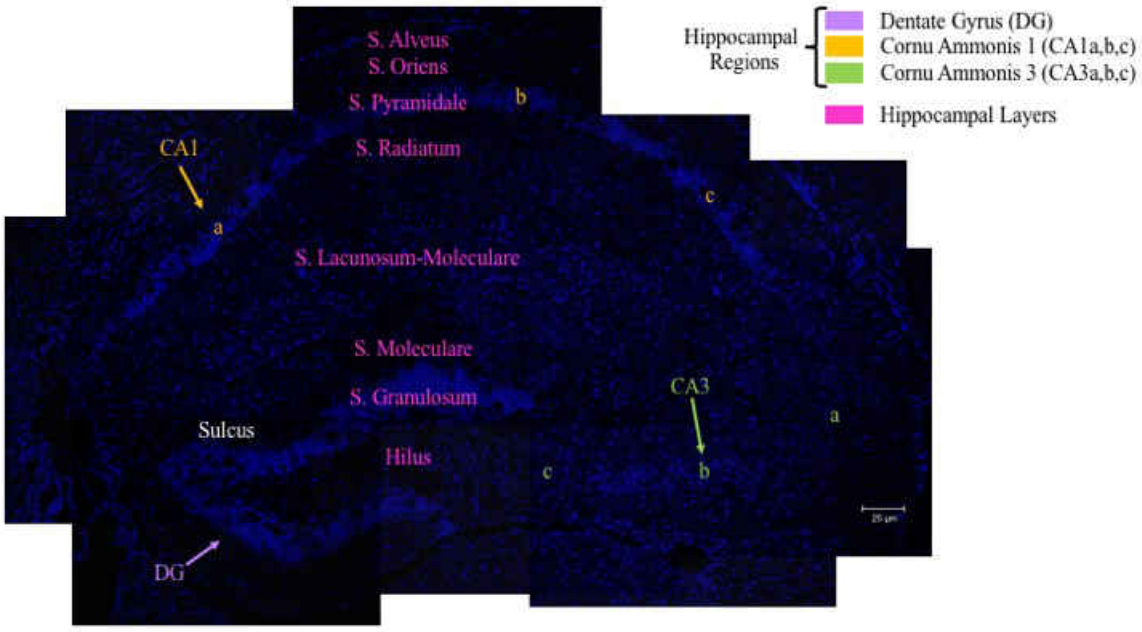

Figure 19. Panoramic Stitch of DAPI-stained Puncta Throughout the Mouse Hippocampus. Several low (20-by-1.5x) magnifications imaging fields were stitched together to form an overview of puncta organization throughout the entirety of the mouse hippocampus. These particular images are from negative 2^{o} only control slice, showing a dorsomedial slice of the left hippocampus. All apparent immunofluorescence was indicative of DAPI. The legend of the figure illustrates the color-coding scheme used to approximate the various hippocampal regions and strata.

The layers, or strata, we estimated, in order from superficial to deep, were as follows: (in Ammon's horn) *stratum oriens*, *stratum pyramidale*, *stratum radiatum*, and stratum *lacunosum-moleculare*; (in dentate gyrus) *stratum moleculare*, *stratum granulosum*, and hilus. Additional layers, *stratum alveus* and *stratum lucidum*, are sometimes differentiated, but are region specific and were not readily identifiable the sections observed, with fluorescence nuclear staining; nor were the *strata lacunosum* and *moleculare*, of Ammon's Horn easily differentiated, though this is less commonly done in the literature. Most generally, the value of this laminar assignment is to give the reader an idea of what type of cell may be expressing the marker-of-interest; although this is only circumstantial in nature, the existence of excitatory neurons almost solely within the

densely packed *stratum pyramidale* and *stratum granulosum* is well-known and provides preliminary evidence for future imaging studies and provides insight into observations made in electrophysiological experiments performed in the hippocampal slice.

The regions we estimated include the DG, CA1, and CA3. The CA2 is a small region between the CA1 and CA3 which is not easily differentiated using these methods and is typically not associated with the main signaling pathway of the hippocampus, the perforant path. In the case of a cell-of-interest being expressed between the estimated distal margin of the CA1 and the proximal margin of the CA3, where the CA2 likely exists, this was noted and the puncta were assigned to the closer of the CA1 or CA3. It is also noteworthy that unlike in humans and other mammals, there is not generally a CA4 region and instead the CA3 is directly adjacent to the hilus of the dentate gyrus. As previously alluded to, we also estimate sub-regions for the CA1 and CA3, which are divided as a, b, and c, based on being proximal, middle, or distal to the entorhinal cortex, for the CA1, or to the CA1, for the CA3.

While this characterization methodology is highly subjective, it allows for a much more contextual description when the cells are imaged at higher magnification and the larger, more apparent structures are not observable. Ultimately, it was often necessary to image at high (63-by-1.5x) magnification because of relatively weak immunofluorescence signal-to-noise ratios. The provision of the low magnification stitched image should lend to greater reproducibility and enable other observers to calibrate their assessments to their own margins.

Antigen Retrieval

The immunofluorescence staining methods used were generally successful for identifying cells expressing the α_{1A}-AR reporter and/or parvalbumin. Initially, fluorescence signal intensity was especially low for the α_{1A}-AR reporter, but we were confident that we were observing cells that were showing fluorescence. To address this issue, a protocol for antigen retrieval was implemented. This antigen retrieval was successful (Fig. 20); however, it did seem to intensify the background signal intensity, especially apparent with the parvalbumin-indicated puncta. As shown below, the fluorescence intensity was great enough to make qualitative conclusions about the nature of α_{1A}-AR reporter expression and its propensity for co-labelling with parvalbumin-positive cells, in the mouse hippocampus.

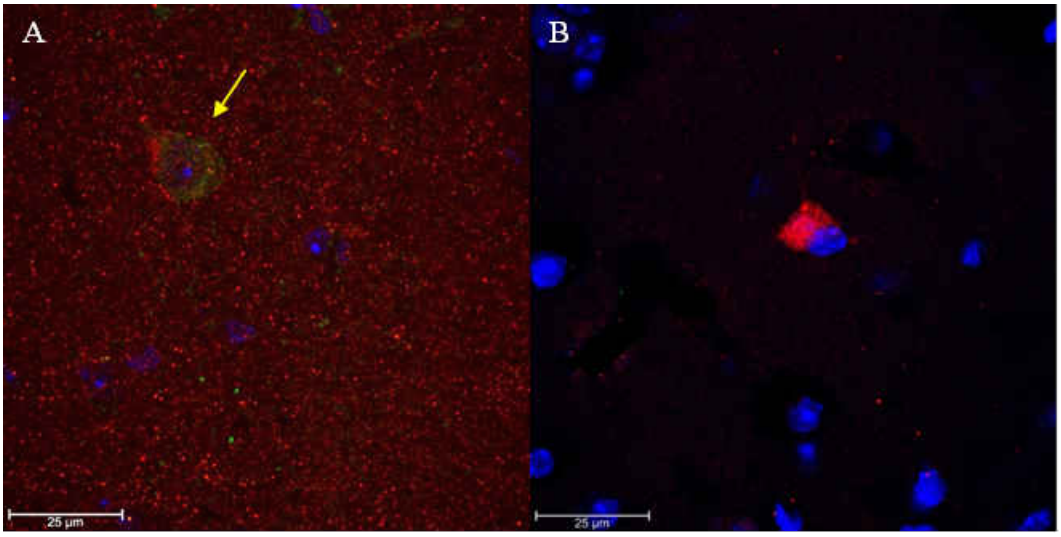

Figure 20. Effect of Antigen Retrieval on Typical Fluorescence Signal Intensity (a) High, 63-by-1.5x, magnification image of a punctum with weak β-Gal immunofluorescence and possible parvalbumin immunofluorescence without antigen retrieval. This punctum was imaged within the *stratum radiatum* layer of the CA1a region of the mouse hippocampus. (b) High, 63-by-1.5x, magnification image of a punctum exhibiting good β-Gal fluorescence. This image was captured form the *stratum oriens* layer of the CA1b region, near the upper blade of the *stratum granulosum* of another mouse hippocampus.

Hippocampal Puncta α_{1A}-AR Reporter Immunofluorescence

Immunofluorescence imaging of the α_{1A}-AR reporter, β-Gal, suggested a low-to-moderate rate of expression, which was consistent with the hippocampal expression of the same reporter exhibited in X-Gal functional protein colorimetric staining. As seen in Figure 21, β-Gal was not exclusively colocalized with parvalbumin-positive puncta. While this finding partially refuted our hypothesis about α_{1A}-AR expression on hippocampal interneurons, it also provided an opportunity for additional qualitative comparisons of expression patterns on this elusive receptor. Specifically, we observed that relative to parvalbumin-positive puncta, there were far fewer (less than half) puncta positive for β-Gal. Further, although there were instances where β-Gal and parvalbumin fluorescence did colocalize, it was on the minority of β-Gal positive puncta, estimated to be about one-fourth to one-third of total puncta observed. However, it is worth noting that because of our utilization of coronal brain slices, the CA3 region of the hippocampus tended to be less developed and organized, than can be observed in the middle and ventrolateral portions; therefore, it remains possible that our sampling could be under-representative of the expression of the α_{1A}-AR reporter. However, we did find several examples of β-Gal positive puncta in the CA3 region, so we did not section along other axes.

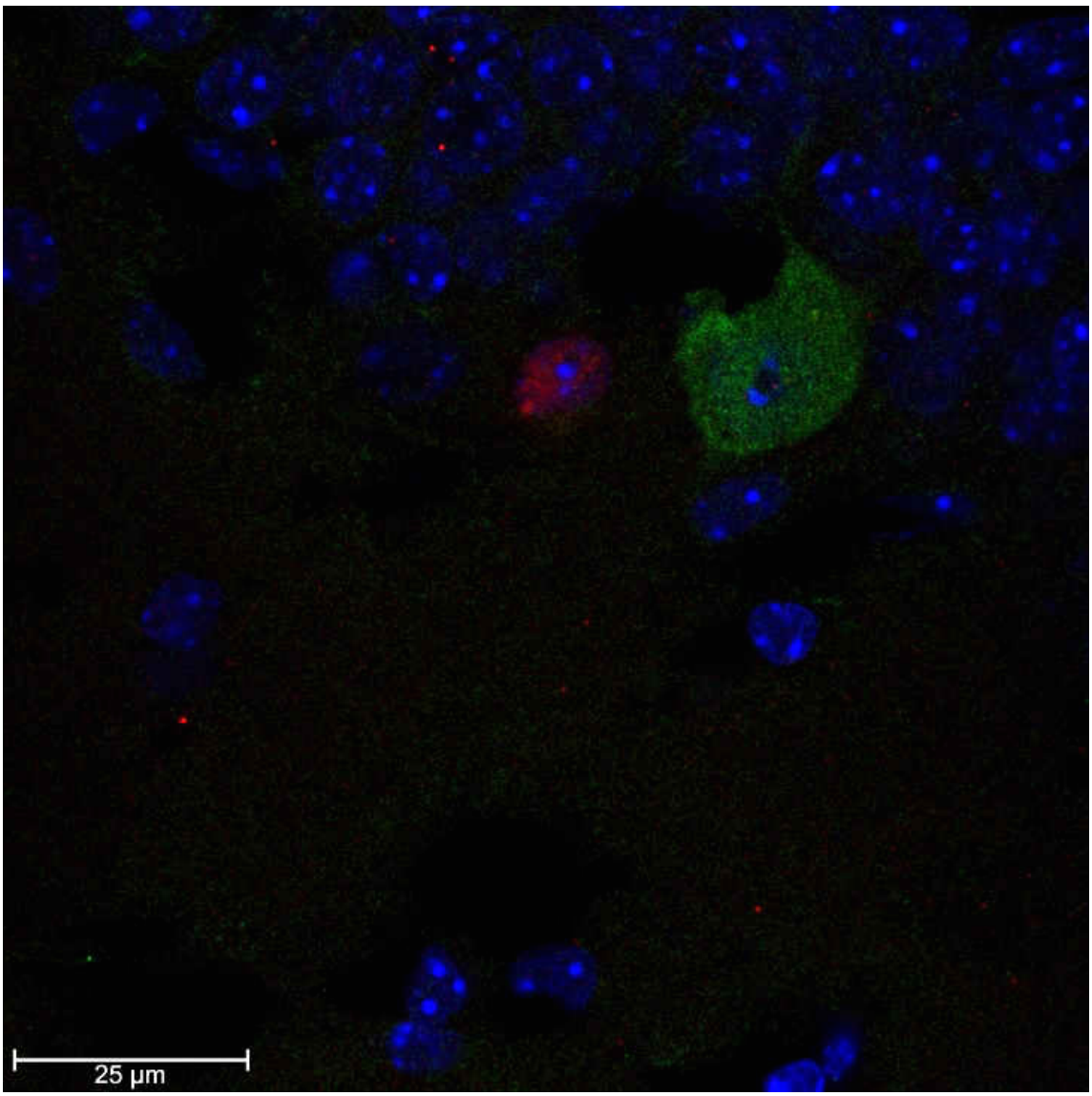

Figure 21. Example Image Showing Non-exclusive β-Gal-Positive and Parvalbumin-Positive Puncta in the Mouse Hippocampus. High, 63-by-1.5x, magnification image of a β-Gal-positive punctum (red) and a parvalbumin-positive punctum (green) near the *stratum granulosum* of the dentate gyrus.

In comparison to parvalbumin-positive puncta, we estimated the β-Gal positive puncta to be more uniformly distributed throughout the hippocampus. We found examples of β-Gal positive puncta present within every region of the hippocampus and the expression within the *stratum lacunosum-moleculare* seemed especially noteworthy

(Fig. 22). While parvalbumin-positive puncta were most dense in the *stratum oriens*, β-Gal positive puncta were found about as often in the *stratum oriens* and *stratum lacunosum-moleculare*, and did seem to be more prevalent than β-Gal positive puncta in the stratum *lacunosum-moleculare*. Additionally, β-Gal positive puncta were commonly found in the area of the subgranular zone and hilus of the dentate gyrus (Fig. 22F).

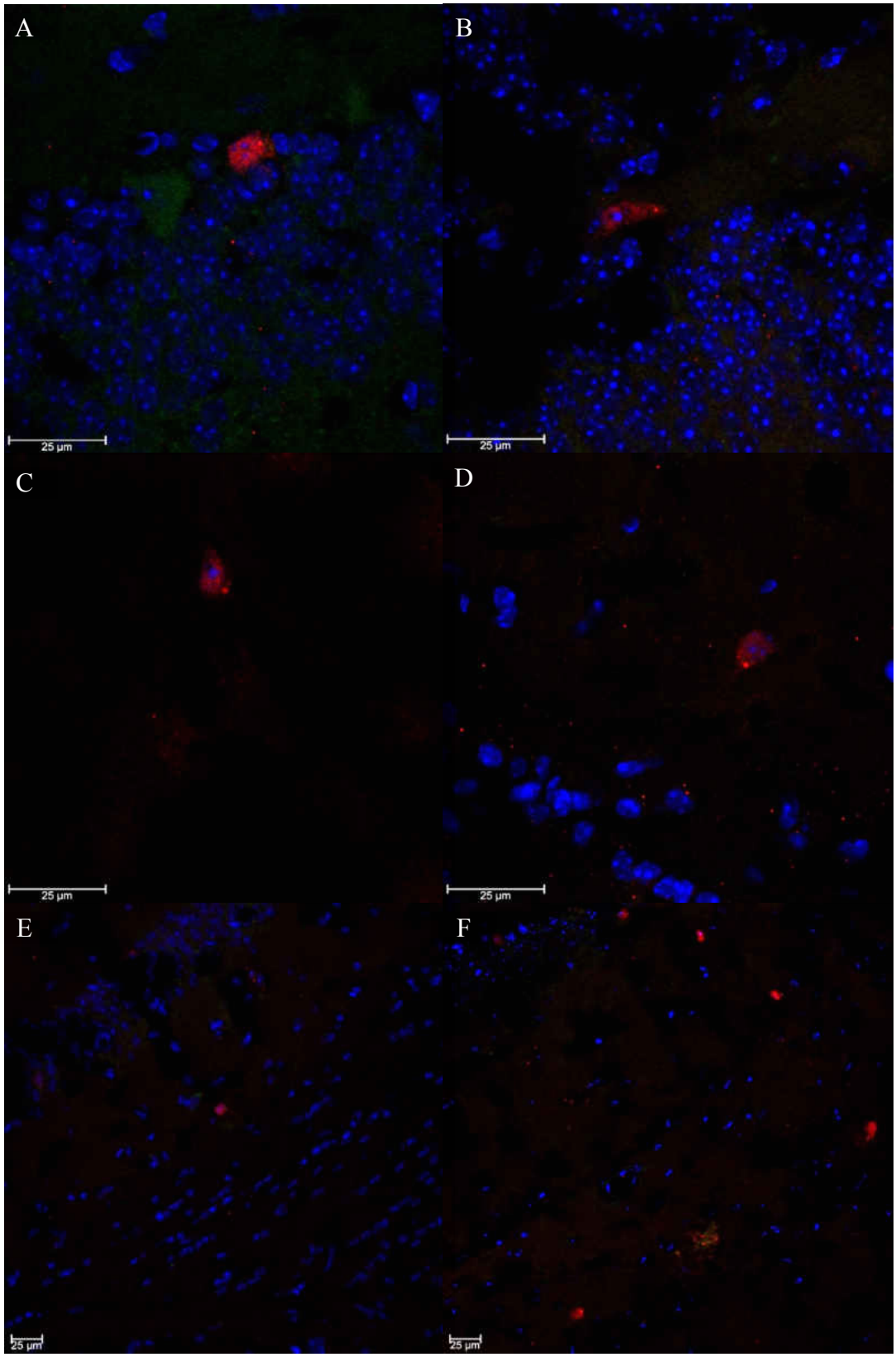
A
B
C
D
E
F
25 µm

Figure 22. Examples of β-Gal Positive Puncta Throughout the Hippocampus. (A) High, 63-by-1.5x, magnification image of a β-Gal positive punctum in the area of the subgranular zone of the *stratum granulosum* of the dentate gyrus. (B) High, 63-by-1.5x, magnification image of a β-Gal positive punctum in the hilus of the dentate gyrus. (C) High, 63-by-1.5x, magnification image of a β-Gal positive punctum in the *stratum oriens* of the CA3a subregion of the hippocampus. (D) High, 63-by-1.5x, magnification image of a β-Gal positive punctum in the *stratum oriens* of the CA1a subregion. (E) High, 20-by-1.5x, magnification image of a β-Gal positive punctum in the *stratum oriens* of the CA1b subregion. (F) Low, 20-by-1.5x, magnification image of several β-Gal positive puncta within the upper hilar layer of the dentate gyrus, the *stratum radiatum* of the CA3c subregion, and the stratum *lacunosum-moleculare* of the CA1b subregion.

Hippocampal Puncta Parvalbumin Immunofluorescence

Throughout the hippocampus, many puncta exhibited fluorescence indicating the presence of only parvalbumin. Figure 23 shows two such examples. The localization of these puncta were consistent with interneurons. On the occasion that a punctum was found in the excitatory cell layers, it was alone and adjacent cells were not exhibiting fluorescence as would be the expectation if observing expression in pyramidal (excitatory) cells. We estimated higher occurrence of parvalbumin-expressing puncta in the *stratum oriens* than in other hippocampal layers.

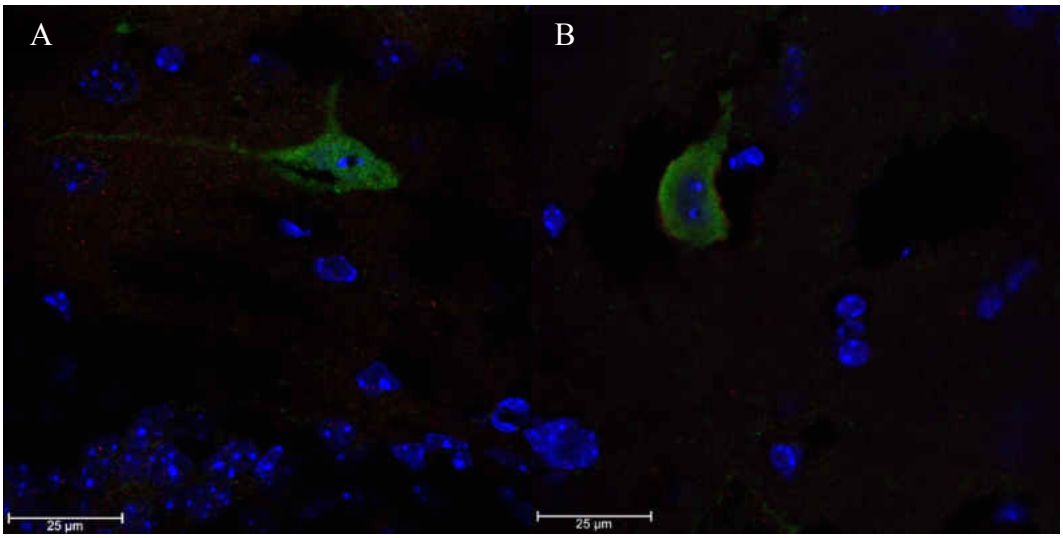

Figure 23. Example Images of Showing Parvalbumin-Positive Puncta in the Mouse Hippocampus. (A) High, 63-by-1.5x, magnification image of a parvalbumin-positive punctum near the stratum radiatum of the CA3c subregion. (B) High, 63-by-1.5x, magnification image of a parvalbumin-positive punctum near in the hilus of the dentate gyrus.

Hippocampal Puncta Co-labelled for α_{1A}-AR Reporter and Parvalbumin Immunofluorescence

Co-localization of the α_{1A}-AR reporter, β-Galactosidase, and parvalbumin was determined by qualitative assessment of relative fluorescence intensity, compared with the adjacent background in each channel, corresponding to the fluorescence emission band for each secondary antibody, and the overlap on a DAPI-positive punctum (Fig. 24).

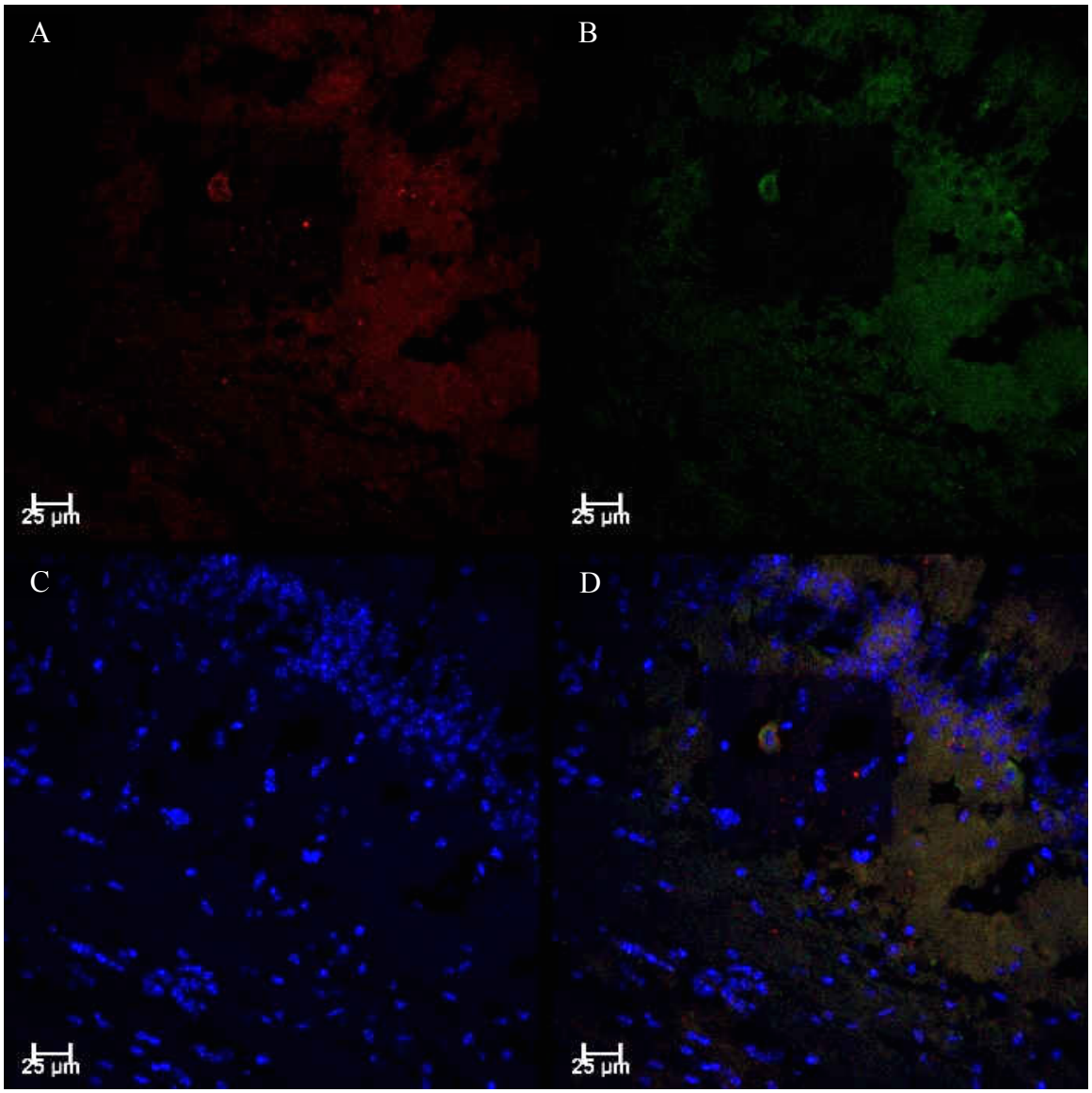

Figure 24. Separated Fluorescence Emission Channels and Combined Overlay. Low (20-by-1.5x) magnification images showing the fluorescence in individual emission channels of a punctum within the stratum oriens of the CA1c sub-region of the mouse hippocampus (also shown at high magnification in Figure 25C). (A) Pseudo-colored representative image of fluorescence emission intensity elicited by laser excitation and corresponding emission filters at 594 nm. This channel corresponds to fluorescence signal from a primary antibody specific to the α_{1A}-AR reporter, β-Galactosidase, and an Alexa Fluor 568 fluorophore-conjugated secondary antibody (B) Pseudo-colored representative image of fluorescence emission intensity elicited by laser excitation and corresponding emission filters at 488 nm. This channel corresponds to fluorescence signal from a primary antibody specific to parvalbumin, and an Alexa Fluor 488 fluorophore-conjugated secondary antibody. (C) Pseudo-colored representative image of

fluorescence emission intensity elicited by laser excitation and corresponding emission filters at 405 nm. This channel corresponds to fluorescence signal from DAPI. (D) Pseudo-colored representative overlay image of all fluorescence emission channels combined.

We observed co-localization on puncta almost exclusively within the regions of Ammon's Horn (CA1-3), with very few puncta apparent within the dentate gyrus. Additionally, the majority of co-labelled puncta seemingly were localized within the *stratum oriens* layer of Ammon's Horn. This may be partially due to the overall low apparent density of parvalbumin-positive puncta within the dentate gyrus and the apparent higher density of these puncta within the *stratum oriens*. That said, we did observe occasional overlap within the *stratum lacunosum-moleculare* (Fig. 25D). Figure 25 shows representative images of several co-labelled puncta indicating the presence of both the α_{1A}-AR reporter, β-Galactosidase, and parvalbumin. The fluorescence intensity from the 488 nm channel (green), parvalbumin, was typically greater than was observed in the 594 nm channel (red), β-Galactosidase. Thus, in overlay images the green tends to be the dominant feature. As mentioned, the likelihood of positive co-localization was determined by the puncta-to-background, fluorescence emission intensity and the presence of DAPI-positive nuclear material; the degree to which puncta were more or less dominated by either marker was not assessed.

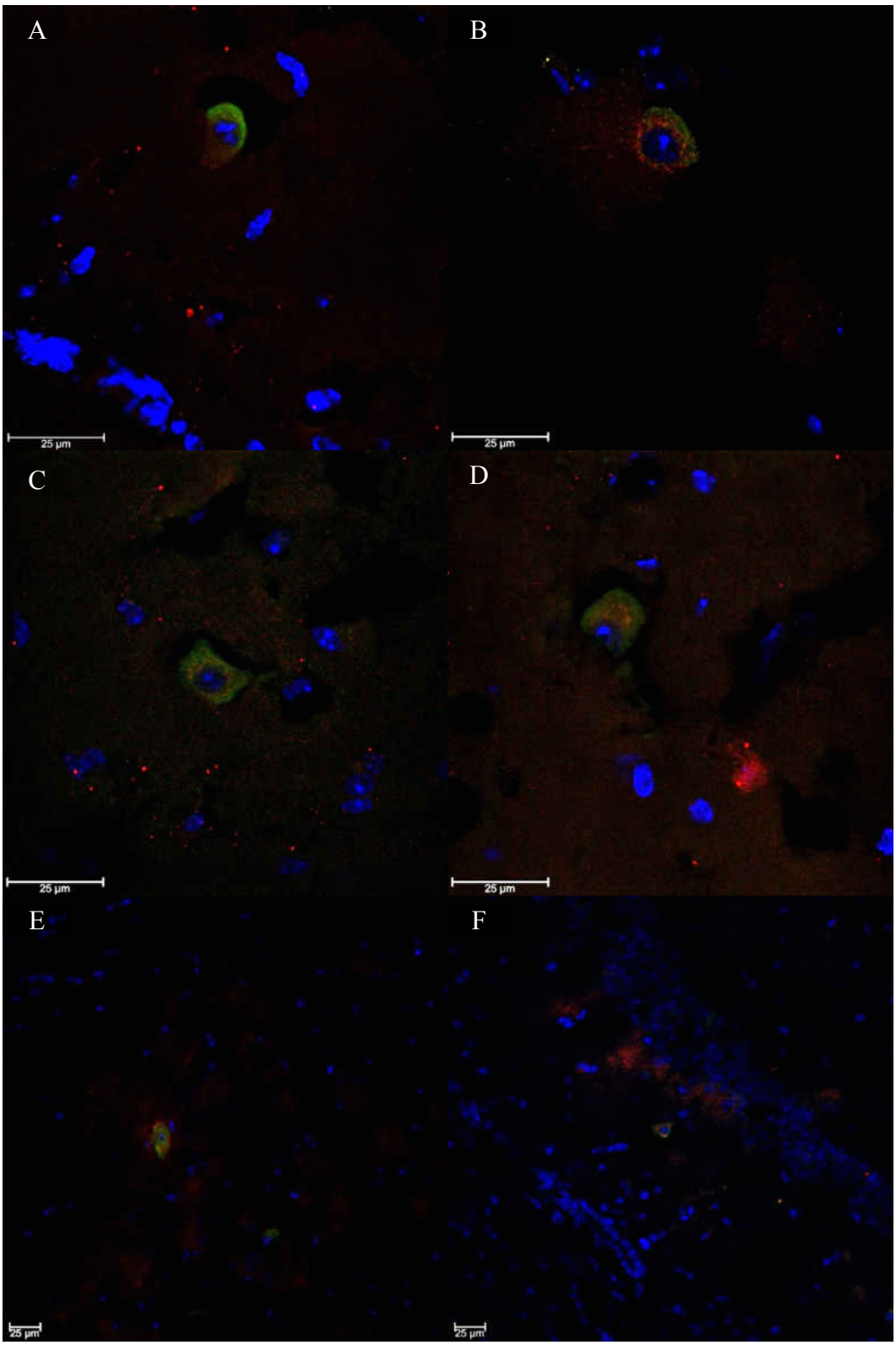
A
B
C
D
E
F
25 µm
25 µm
25 µm
25 µm
25 µm
25 µm

Figure 25. Puncta Showing Co-localization for β-Gal and Parvalbumin in Throughout the Mouse Hippocampus. β-Gal is shown as red and Parvalbumin is shown as green. (A) High (63-by-1.5x) magnification image of a co-labelled cell punctum in the CA1c stratum oriens. (B) High (63-by-1.5x) magnification image of a co-labelled cell punctum in the CA1b stratum oriens. (C) High (63-by-1.5x) magnification image of a co-labelled cell punctum in the CA1c stratum oriens. (D) High (63-by-1.5x) magnification image of a co-labelled cell punctum in the CA3b stratum lacunosum-moleculare. (E) Low (20-by-1.5x) magnification image of a co-labelled cell punctum in the CA3a stratum oriens. (F) Low (20-by-1.5x) magnification image of a co-labelled cell punctum in the CA1c stratum oriens.

Other Observations of Immunofluorescence Outside of the Immediate Purview of this Study

A separate interest of our lab is the potential role of the α_{1A}-AR in adult neurogenesis. Consistent with previous findings, we did find many examples of α_{1A}-AR reporter-positive puncta within the apparent margins of the subgranular zone of the dentate gyrus (Fig. 26). The subgranular zone of the hippocampus, along with the subventricular zone of the rostral migratory stream, are two known areas within the adult brain which maintain active pools of neuronal and glial progenitor cells. Unfortunately, the methodology used in this study did not allow for the assessment of these puncta for the characteristics of hippocampal progenitor cells. However, the prevalence of α_{1A}-AR reporter-positive puncta in this neurogenic area at least lends credence to our hypothesis for future investigations.

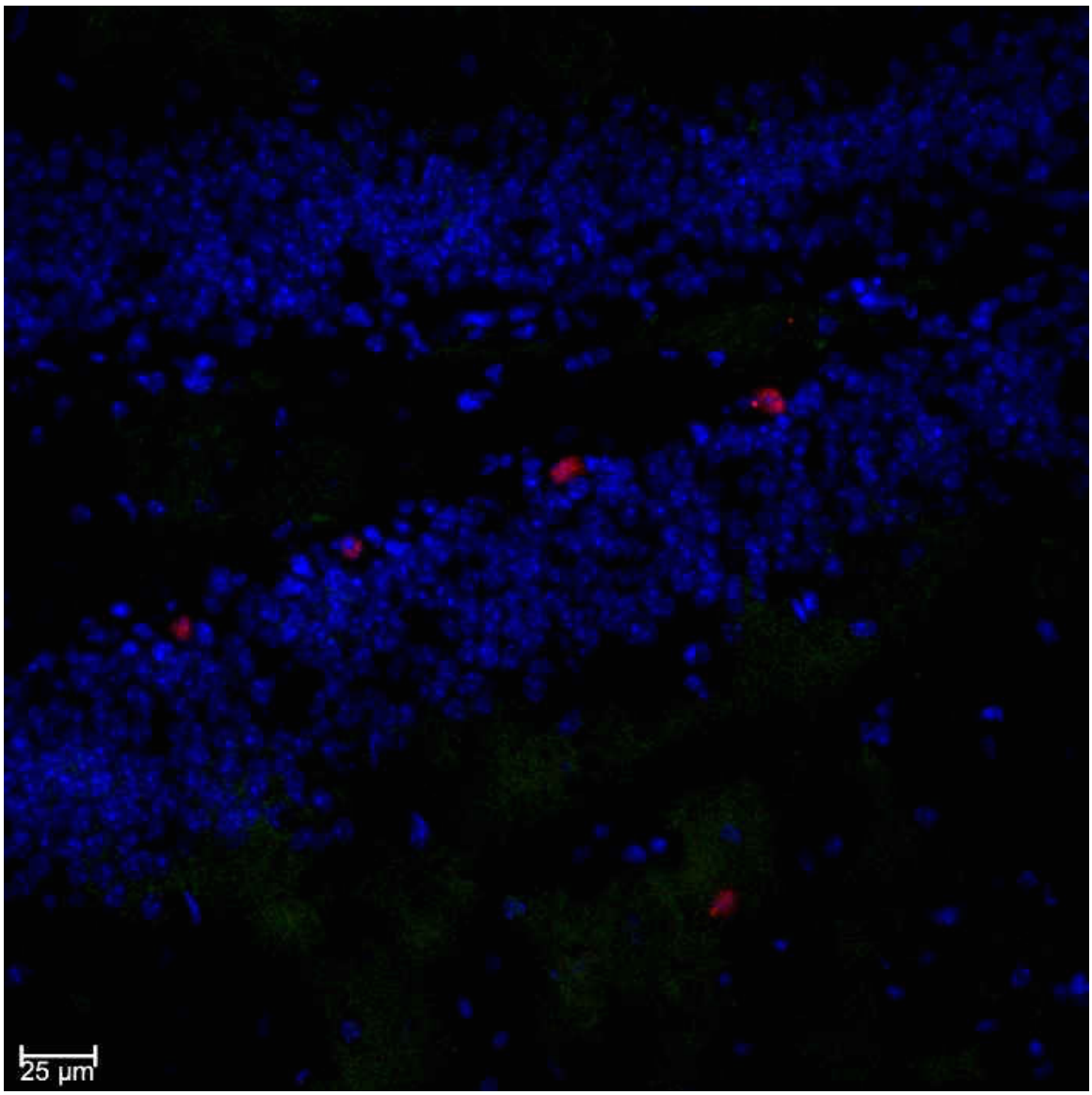

Figure 26. Potential Hippocampal Progenitor Cells Expressing the α_{1A}-AR Reporter. Low (20-by-1.5x) magnification image of α_{1A}-AR reporter-positive puncta within the apparent margins of the subgranular zone of the dentate gyrus of an adult mouse hippocampus.

Negative Controls

To assess antibody cross-reactivity and the possibility of emission spectra overlap, we utilized individual negative no secondary controls, for each antibody, as well

as a double-negative no secondary antibody control with each set of immunofluorescence staining. Following our implementation of antigen retrieval, we were confident that each antibody was labeling specifically, well above background fluorescence intensity.

In no β-Gal secondary antibody control samples, we observed strong staining on puncta throughout all samples (Fig. 27A). Additionally, even at lower magnifications, where higher laser power was required to produce similar puncta intensity, producing some background fluorescence, there was very little, if any, β-Gal excitation channel bleed-though from the parvalbumin secondary antibody emission (Fig. 27B). We did attempt to visualize any bleed-through from the β-Gal excitation channel by tuning the laser to a very high intensity, but only a very low background fluorescence became apparent (Figure not shown). None of this background fluorescence was denser on any puncta.

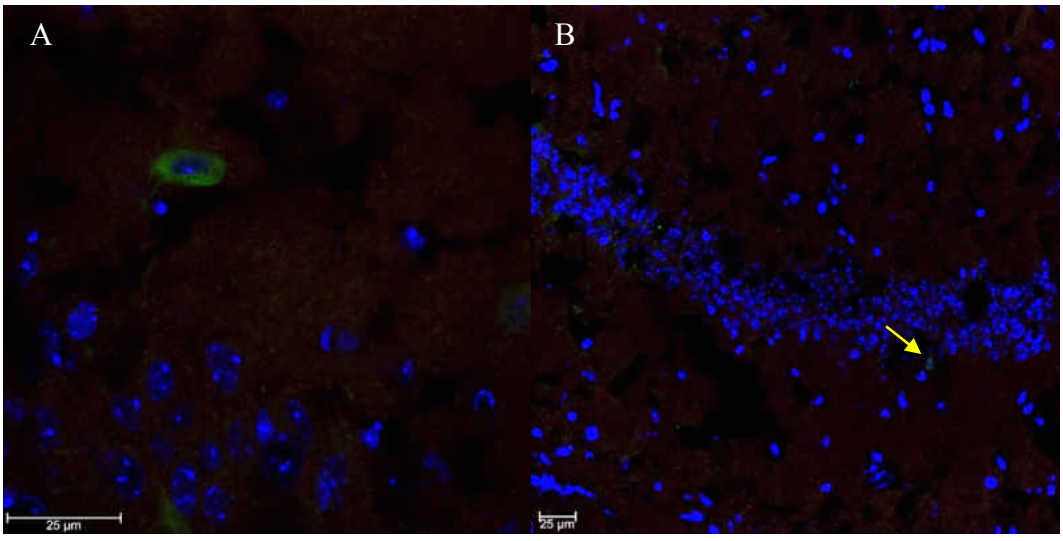

Figure 27. No β-Gal Secondary Antibody Control Samples. (a) High, 63-by-1.5x, magnification image of a no β-Gal secondary control sample with a cell exhibiting fluorescence for parvalbumin, within the *stratum radiatum* layer of the CA1a region of the mouse hippocampus. (b) A low, 20-by-1.5x, magnification image of a no β-Gal secondary control sample showing several cells with fluorescence indicating the presence

of parvalbumin, within the *stratum oriens* layer of the CA1b region of another mouse hippocampus.

Next, we performed the same assessment with a no parvalbumin secondary antibody control. There results were similar to those in the no β-Gal secondary antibody control samples. We did not observe any emission bleed-through from the parvalbumin excitation channel at the laser powers utilized to image puncta, at high or low magnification (Fig. 28). Even at higher laser powers, we observed only very slight fluorescence from the parvalbumin emission channel, which was uniformly distributed equally and did not skew the pseudo-coloration of the β-Gal positive puncta in channel overlaps.

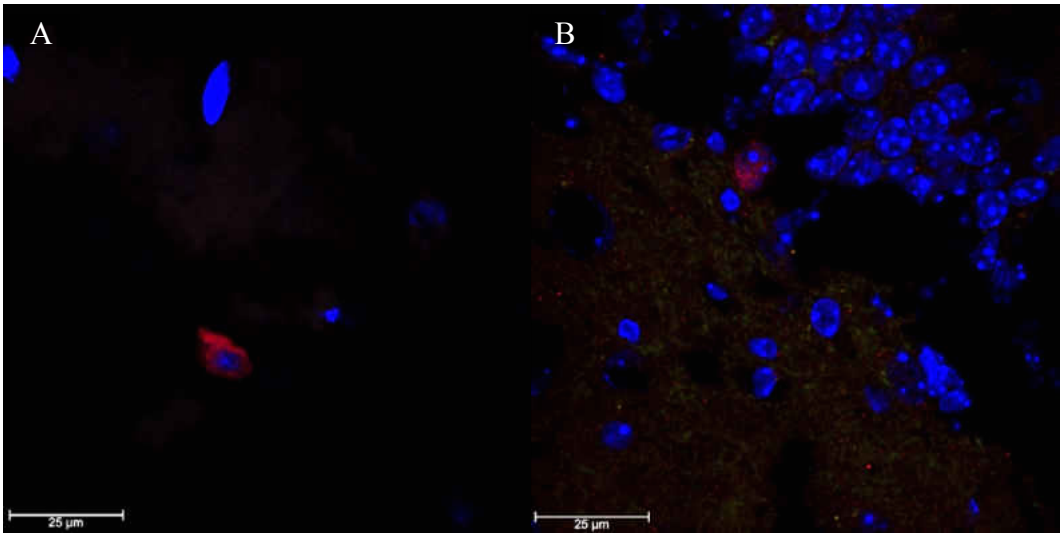

Figure 28. No Parvalbumin Secondary Antibody Control Samples. (a) High, 63-by-1.5x, magnification image of a no parvalbumin secondary control sample with a cell exhibiting fluorescence for β-Gal (red), within the *stratum lacunosum-moleculare* layer of the CA1a region of the mouse hippocampus. (b) A low, 20-by-1.5x, magnification image of a no parvalbumin secondary control sample showing a cell with fluorescence indicating the presence of β-Gal (red), within the hilar layer of the dentate gyrus region, near the lower blade of the *stratum granulosum*, of another mouse hippocampus.

Finally, for each experiment, we performed a double-negative control, which did not contain the secondary antibodies for either primary antibody of interest. We did not observe staining of any cells in these samples (Fig. 29). Similar to previous attempts to visualize any non-specific fluorescence, laser powers well above those used to image cells did not yield fluorescence staining of any puncta (Figure not shown). Generally, only nuclear staining of cell nuclear material, from DAPI, was observable in these samples.

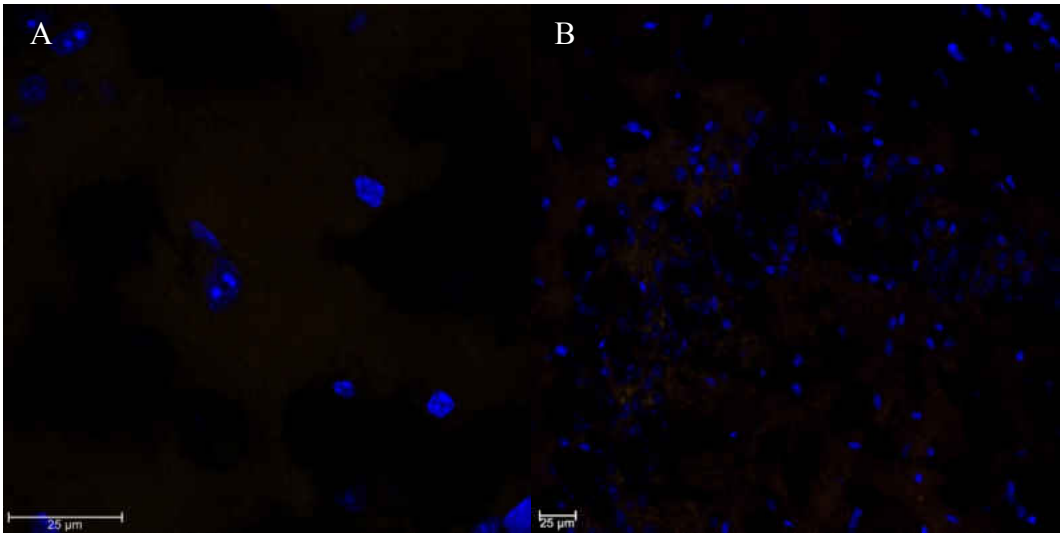

Figure 29. No Secondary Antibody Control Samples. Only DAPI nuclear staining is visible in these images. (a) High, 63-by-1.5x, magnification image of a no secondary control sample with no cell puncta exhibiting fluorescence. This image was taken from within the *stratum oriens* layer of the CA1b region of the mouse hippocampus. (b) A low, 20-by-1.5x, magnification image of a no secondary control sample no cell puncta fluorescence. This image was from the interface between the CA3a and CA3b sub-regions of the same mouse hippocampus.

Discussion

While the research presented here, and previous research from our laboratory and others, have provided a great deal of insight into the functional role of the adrenergic receptors in the hippocampus, the actual location of the receptors has remained somewhat of a mystery. Largely, this has to do with minor variability of the AR subtypes, which is especially true of the α_1-AR class (Hwa *et al*., 1995; 1996). In fact there are very few "selective" ligands that can differentiate α_{1A}-AR and α_{1B}-AR function, and as mentioned earlier, no known commercially-available antibodies for the α_{1A}-AR (Jensen *et al.,* 2009). Several approaches have been attempted to circumvent the visualization issue with mixed success. The laboratory of Dianne Perez attempted to visualize the α_{1A}-AR using an overexpression vector, containing a green-fluorescent protein tag; upon further investigation, we could not find any effects of pharmacological stimulation of the α_{1A}-AR on many of the cell populations and suggested false-positive expression. Others have utilized radiometric imaging of radioisotope-tagged ligands to infer general density of the α_{1A}-AR, in the presence, or absence, of selective antagonists. These methods were very useful for identifying the receptor density in different brain regions and sub-regions, but lacked the resolution necessary to visualize individual cells, or even laminar distribution within a sub-region. Thus, we decided to utilize a technique, in a novel fashion, which had been used for other studies and provided results consistent with physiology studies. Our approach to was to visualize the α_{1A}-AR by using the transgenic α_{1A}-AR knockout mouse that had a LacZ insert, expressed under the control of the endogenous gene promoter. To our knowledge, this study and our collaborators were the first investigators to implement fluorescence microscopy with this model to visualize brain tissue.

Specifically, the goal of this study was to investigate the propensity for co-labelling of the α_{1A}-AR on puncta exhibiting the interneuron marker, parvalbumin.

Our experiments provided support and/or novel insight to many of our questions. First, our hypothesis that the α_{1A}-AR is primarily localized to interneurons seems to be supported by these findings. We observed that the α_{1A}-AR reporter was expressed almost entirely outside of the hippocampal layers where excitatory cells are found. While our hypothesis remains that these cells are inhibitory interneurons, we cannot rule out the possibility that these are excitatory neurons or glial cells. Next, our hypothesis that the α_{1A}-AR is primarily localized on parvalbumin-expressing cells was partially refuted by these experiments. Instead, we observed that the majority of α_{1A}-AR reporter-expressing cells did not co-localize with parvalbumin-positive puncta. This suggests that there are likely other populations of interneurons expressing the α_{1A}-AR within the hippocampus. Our collaborators in the Bergles laboratory have taken more interest in the possibility of α_{1A}-AR expression on glial populations, in the hippocampus and elsewhere. An alternative hypothesis remains, in that previous experiments in our laboratory found gene expression evidence suggesting that α_{1A}-AR expression may be prevalent on somatostatin-expressing interneurons. However, what can be definitively concluded from these experiments is that, unsurprisingly, the hippocampal α_{1A}-AR expression is not as simple as was initially hypothesized.

Our experiments, using LacZ-mediated reporter labelling, provides a framework for investigating the distribution patterns of the α_{1A}-AR so that the mechanism(s) of action can be more precisely defined. Our specific interest in α_{1A}-AR co-expression on

parvalbumin-expressing interneurons is based on the demonstrated role of parvalbumin-expressing interneurons in epilepsy. This cell type has been shown to be especially vulnerable to seizure-induced cell death (Dinocourt *et al*., 2003). Additionally, these experiments were done in conjunction with a collaborator, Dwight Bergles, whose laboratory is developing several cell-type specific, conditional knockout mice; the first of which is the α_{1A}-AR-Parvalbumin knockout. Our results suggested an α_{1A}-AR laminar distribution consistent with hippocampal interneurons and showed that some of these cells did indeed co-label on parvalbumin-expressing cells.

CHAPTER V
DISCUSSION

This dissertation research has revealed several novel findings about the contributions of α_1-AR subtypes to shifting seizure threshold. This work has built significantly upon our previous work identifying hippocampal sites of action for the α_1-AR subtypes and the functional consequences of α_1-AR activation on hippocampal inhibitory tone. Our initial primary challenge was the conversion from studying rats to using mice. Historically, our laboratory has exclusively utilized rats for electrophysiological experiments. Although mice and rats are anatomically similar, the primary challenge with switching to mice revolved around the relatively small scale of the mouse brain, compared with the rat. This presented unique challenges, especially in the fine-tuning of our electrophysiological preparation protocols and with the level of fine-motor skills required to prepare hippocampal slices and surgeries involving EEG head-stage implementation.

The primary advantage of utilizing mice is the broad availability of genetically modified mice, including the existence of transgenic constitutively active mutant and knockout variants of the α_1-AR subtypes. Additionally, we have recently begun a collaboration with the laboratory of Dwight Bergles at the Johns Hopkins University, which is focused on producing several inducible cell-specific knockout mouse lines for studying α_{1A}-AR function in discrete brain cell populations. The value in such a

collaboration is great from both basic science and translational investigation perspectives; cell-specific knockout will allow for an unprecedented level of specificity of the physiological mechanism(s) of α_{1A}-AR function in the brain. Unlike traditional pharmacological approaches, the findings should allow for more comparability between *in vitro* and *in vivo* experiments. Additionally, inducible gene knockout allows for the delineation of knockout consequences to developmental abnormalities versus inherent physiological changes to a normally-developed system; this is a major limitation of our current generation of α_1-AR subtype knockouts, especially when attempting to draw conclusions about our findings pertaining to altered epileptiform frequency and spontaneous, recurrent seizures in α_{1A}-AR knockout mice.

Our findings herein relied heavily on the implementation of α_1-AR subtype knockout mice, which allowed us to differentiate between α_{1A}-AR and α_{1B}-AR contributions, in a highly specific manner, for the first time. In addition to our inclusion of novel methods for assessing AR subtype contribution in models seizure and epilepsy, our development of *in vivo* models provides a robust foundation for testing α_{1A}-AR modulation in a more biomedical-relevant paradigm. The opportunity to implement state-of-the-art synchronized, long-term video and long-term video-EEG recordings into my studies was instrumental to the success in developing these *in vivo* models.

Broadly speaking, our results were significant for showing the antiepileptic properties of the α_{1A}-AR, both in vitro and in vivo; our characterization of detrimental effects of α_{1A}-AR knockout, both in vitro and in vivo; as well as our novel approach to utilizing the α_{1A}-AR knockout as a fluorescence microscopy reporter strain.

Overall, this dissertation research resulted in some exciting discoveries which progressed our depth of knowledge about this topic, a confirmation of previous results, and an evolution to our current hypotheses.

Electrophysiological Findings in Hippocampal Slice

In Chapter 2, we presented results from our work with the hippocampal slices in a magnesium-deprivation model of epileptiform activity. These experiments resulted in several exciting findings. The general conclusion from these findings was that α_{1A}-AR expression and activity was essential for α_1-AR-mediated alterations to epileptiform frequency. Additionally, we found surprising alterations to baseline epileptiform frequency in α_{1A}-AR knockout mice, which may provide exciting insight into the physiological mechanisms underlying *in vivo* observations.

First, we showed that activation of the α_1-AR, via pharmacological manipulation, resulted in similar effects to those seen in rat; these findings were a moderate decrease in hippocampal epileptiform frequency, upon α_1-AR activation. This was important because it suggests that the same physiological mechanisms may be underlying this phenomenon and that the effects are consistent across species. Our laboratory has spent a number of years painstakingly characterizing the effects of AR activation, from the single-cell level, to local neuronal networks (such as inhibitory post-synaptic current and excitatory post-synaptic potential alterations), and at the level of the local field potential. Our experiments focused on experimental measurement of alterations in local field potential.

Observations of local field potential allowed for observations of epileptiform synchronicity and phasic changes to the waveforms and frequencies of the epileptiform population. The downside to local field potential measurements, as opposed to single-cell recordings, is that there is a loss of fidelity as electrical potentials encounter constructive and destructive interference. Generally, local field potential measurements provide a more accurate assessment of the total effect of α_{1A}-AR activation or loss, but does so at decreased resolution of subpopulation differences and other extraneous factors, which may mask effect size. However, ultimately, a seizure is a manifestation of congruent neuronal activity, which makes the local field potential a powerful tool for studying seizures and epilepsy. The hippocampus is of particular interest because it is a highly vulnerable brain structure to seizure activity and is point of origin for the most commonly diagnosed and most commonly medically-intractable focal epilepsy, mesial temporal lobe epilepsy.

Our findings in the mouse hippocampus, suggested that α_{1A}-AR activation results in a consistent, moderate decrease in epileptiform burst frequency, resultant from exposure to both endogenous and synthetic AR agonists. These results were consistent with findings in the rat and extended this effect to the CA3 field of the hippocampus. Previous studies had only measured CA1 hippocampal alterations. We found a consistent efficacy, around 15%, for all ligands. This may not seem impressive without proper context. In the magnesium-deprivation model of epileptiform generation, the lack of magnesium abolishes the magnesium block of NMDA glutamate receptors, but does so nonspecifically. In practice, this means that both excitatory and inhibitory circuits enter a hyperexcitable state. Our hypothesis suggests that the α_{1A}-AR mediates its actions by a

hyperexcitation of inhibitory interneurons. Evidence within the magnesium deprivation model suggests that epileptiform bursts only arise once the more prevalent excitatory neurons overcome the compensatory actions of the inhibitory neurons. Thus, logic dictates that the inhibitory neurons are likely already firing near maximum capacity. This reduction in epileptiform burst frequency strongly suggests increased inhibitory contributions, which without increased excitatory sensitivity (from abolishment of magnesium block), may be sufficient to increase seizure resistance/threshold, reduce seizure prevalence, and/or decrease seizure intensity or duration in epilepsy.

Additionally, we made several novel findings, in this model, with hippocampal slices from α_{1A}-AR and α_{1B}-AR knockout mice. Using these mice, we were able to clearly show that the α_{1A}-AR is the prominent α_1-AR subtype mediating decreases in epileptiform frequency. α_{1A}-AR knockout resulted in complete abolishment of phenylephrine-mediated decreases in epileptiform burst frequency, whereas α_{1B}-AR knockout did not elicit any measurable changes in epileptiform burst frequency when compared to the efficacy measured in hippocampal slices from wild-type control mice.

Another surprising finding with these knockout mice arose from measurements of baseline epileptiform burst frequencies hippocampal slices from wild-type control mice and in α_1-AR subtype knockout mice. While α_{1B}-AR knockout had no measureable difference from the baseline burst frequencies in the wild-type controls, slices from α_{1A}-AR knockouts exhibited baseline epileptiform burst frequencies which were more than 1.5-fold greater than wild-type controls. While the constitutive α_{1A}-AR knockout mouse strain does not allow us to delineate whether this is a developmental consequence or a sign that α_{1A}-AR activity is necessary for normal hippocampal physiology, it does clearly

suggest a difference in excitatory-inhibitory balance in these slices. Further, this finding provides an interesting contextual clue as to the nature of spontaneous seizures observed within α_{1A}-AR knockout mice.

Findings *in vivo*

In Chapter III, we described our findings from experiments performed *in vivo*. Particularly, our experiments investigated the effects of α_{1A}-AR activation in a model of acute *status epilepticus*, as well as a characterization of seizure prevalence and severity in α_{1A}-AR knockout mice, over a 48-hour observation period. To our knowledge, this was one of the first investigations into α_{1A}-AR effects in vivo. Our laboratory has previously performed limited studies into in vivo seizures and α_{1A}-AR manipulation. However, these studies have yet to be published and are only tangentially-related to these studies. The notable exception to this being the observations by Dr. Katie Collette, who performed the initial characterization of α_{1A}-AR knockout mouse seizure prevalence. Our observations are a natural extension of that earlier study. Other attempts at *in vivo* modeling α_{1A}-AR effects in seizure models are discussed, in detail, within Chapter III. Briefly, our attempts have shown results consistent with previous attempts to activated the α_{1A}-AR in acute models of *status epilepticus*. We found that upon α_{1A}-AR activation, there is an increase in latency to initial seizure activity. This consistency suggests a robust effect and lends credence to our findings in hippocampal slices. Further, our findings suggest, together with our *in vitro* findings, that α_{1A}-AR activity is necessary for maintenance of normal seizure threshold and added activation of this receptor subtype results in moderately increased seizure threshold and resistance.

Our first set of experiments investigated the effects of cirazoline-mediated α_{1A}-AR activation on latency to seizure emergence and progression of severity following insult with the chemoconvulsant kainic acid. We found that α_{1A}-AR activation increased the latency to emergence of initial seizure activity. This suggests that α_{1A}-AR activity increased the seizure threshold. However, we did not find any significant alteration to the progression of seizure severity during the course of the acute status epilepticus event, suggesting that α_{1A}-AR activation is insufficient to halt the proliferation of seizure activity as it progresses. Alternatively, because we administed kainic acid systemically, these findings may suggest that α_{1A}-AR activation could be sufficient to prevent or mitigate initial seizure recruitment in especially vulnerable brain regions, but ultimately unsuccessful at preventing generalized brain seizure activity. This possibility is especially interesting because certain areas of the brain are known to be vulnerable to seizure activity, such as the hippocampus, and current evidence does suggest asymmetric distribution of α_{1A}-AR expression throughout the brain. An interesting experiment would be to repeat α_{1A}-AR activation and insult brain areas individually. Initially, we had intended to inject kainic acid locally into the hippocampus and assess these same seizure criteria. However, it was determined that the follow-up required to assessment of injection accuracy and precision, as well as the necessity for refinement of dosage would have significantly limited our experimental throughput. Additionally, even with vehicle injections, it would be difficult to assess whether the invasive procedure of placing an injection needle into a deep-brain structure would exacerbate seizures or alter effects observed.

Our next experiment was to further characterize spontaneous seizure activity in α_{1A}-AR knockout mice. Our observations were specifically designed to observe seizure prevalence in a minimally-stressful environment. This was important because the main goal of this experiment was to observe if the α_{1A}-AR knockout mice exhibited unprovoked, recurrent seizures. We found an extremely high prevalence of spontaneous seizure activity within our sample population. Additionally, we observed several α_{1A}-AR knockout mice exhibited multiple unprovoked seizures. We provide the time of day and level of activity during each seizure event. Interestingly, while previous short-term observations by Dr. Katie Collette (Unpublished) had only found evidence for minimal convulsive activity (Racine's Grade 2 or lower), we observed several instances, in multiple mice, of high grade (Racine's Grade 4-6) seizure activity. Together, we concluded that α_{1A}-AR knockout results in a high prevalence of seizures, which are consistent with the clinical definition of epilepsy in a subset of mice; that is, multiple unprovoked seizures over a period greater than 24-hours. These findings suggest that α_{1A}-AR knockout mice may be a model of epilepsy predisposition in mice. Together, with the conclusions of Dr. Collette, this phenomenon is likely exacerbated with age for unknown reasons.

In both sets of experiments, we repeated the procedures above with the inclusion of cortical video-EEG monitoring. Our sample sizes were not large enough to provide robust conclusions, but were sufficient to make at least one conclusion. Using video-EEG, we were able to conclude that our behavioral categorization of seizure activity was consistent with distinct abnormal and excessive cortical EEG activity, as measured by power, line length, and amplitude. This translates to a confirmation that the spontaneous

seizures, or those induced by kainic acid, were of epileptic nature. This is an important distinction because there is the possibility of non-epileptic convulsions, which are not associated with abnormal brain electrical activity. Thus, our implementation was essential for confirming that our observations and grading of bodily convulsions did correlate with underlying electrical abnormalities, or in general terms, epileptic seizures. Further insight was tantalizingly close; we were particularly interested in measuring the latency to the emergence of abnormal seizure activity, which was not associated with any behavioral manifestation (sub-clinical seizure activity), because this type of seizure activity is usually attributed to sub-cortical structures, such as the hippocampus. Finally, our incorporation of multiple cortical EEG electrodes, in distinct areas across the brain surface could eventually allow for triangulation of particular areas of interest, should the necessary surgical throughput and improvement of surgical outcomes become sufficiently refined. As it stands now, our use of EEG is limited to qualitative assessment, but could be invaluable should refinement of the surgical procedure become sufficiently easier.

Findings from Immunofluorescence α_{1A}-AR Reporter Staining

The final research project of this dissertation, presented in Chapter IV, aimed to elucidate the expression patterns of the α_{1A}-AR in the mouse hippocampus. Traditional methods of visualizing the ARs are unspecific and unreliable due to a high degree of similarities in nearly all AR targeting moieties (Jensen *et al*., 2009). This is especially evident from the publication from the Simpson laboratory showing no reliable antibodies for the α_{1A}-AR. We utilized β-galactosidase protein production, encoded by the LacZ operon imparted in the α_{1A}-AR knockout mouse, to garner representative expression of this receptor. Importantly, the LacZ operon is expressed only under the endogenous α_{1A}-

AR gene promoter and thus is much more likely to exhibit representative patterns of expression than other models which utilize gene amplification and/or add highly transcribed promoters. We have had difficulties in the past confirming physiological function on some populations of neurons that were indicating α_{1A}-AR expression in these other models.

To our knowledge, the β-galactosidase reporter protein in the α_{1A}-AR knockout mouse has only previously been utilized for immunohistochemical staining and assessment of broad patterns of expression in the brain. Thus, it had not been used to investigate co-localization of the α_{1A}-AR on neuronal sub-populations. Our approach used immunofluorescence staining techniques to assess β-galactosidase and parvalbumin expression and co-localization in the mouse hippocampus. We found a small number of puncta expressed both β-galactosidase and parvalbumin. This suggested that a subpopulation α_{1A}-AR-expressing cells does colocalize with parvalbumin; and likewise, that a subpopulation of parvalbumin-expressing cells colocalize with α_{1A}-AR. We were particularly interested in the α_{1A}-AR status on parvalbumin-expressing cells because parvalbumin has been shown to almost exclusively be expressed by inhibitory interneurons (Jiang *et al*., 2016). Also, our results are consistent with the literature in suggestions that parvalbumin-expressing inhibitory interneurons are a heterogenous population, in protein expression, morphology, connectivity, and electrophysiological properties. This is typical of interneurons, once coined "the butterflies of the soul" by Santiago Ramon y Cajal (Jiang, 2018).

A secondary conclusion from these experiments were that the α_{1A}-AR reporter expression was consistent with expression on non-excitatory brain cells. The

hippocampus is a tightly-laminar brain structure, where excitatory cells are almost exclusively constrained to two distinct regions, the granule layer of the dentate gyrus and the pyramidal layer of Ammon's horn. We observed a moderate level of positive puncta for β-galactosidase, with a rough estimate of prevalence of about one-fourth that of parvalbumin-positive cell puncta. Despite this relative commonality, we observed very few occurrences of β-galactosidase-positive puncta in either the granule layer of the dentate gyrus, or the pyramidal layer of Ammon's horn. Importantly, if there was evidence of excitatory cell expression, one would expect diffuse β-galactosidase reporter expression on puncta throughout these layers, due to the high degree of homogeneity typically observed in excitatory cell populations; we did not observe this. This secondary finding may ultimately be more important to supporting our hypothesis that the α_{1A}-AR is modulating seizure activity by altering the excitability of inhibitory interneurons. Consistent with this hypothesis, the pattern of β-galactosidase expression was consistent with the prevalence and laminar organization of inhibitory populations within the hippocampus and does not indicate α_{1A}-AR expression on excitatory cell populations.

Significance

The overarching goal of this dissertation research was to further characterize the contributions of the α_{1A}-AR subtype to the antiepileptic properties of NE. Specifically, we were interested in further characterizing the specific α_{1A}-AR role in altering seizure threshold. While our findings show a potential antiepileptic/anticonvulsant effect upon α_{1A}-AR activation, the effect size was only moderate in our acute seizure models, *in vitro* and *in vivo*. Our identification of epileptiform intensification *in vitro* and the recurrent spontaneous and unprovoked seizures observed *in vivo,* in α_{1A}-AR knockout mice,

suggests an interesting potential for α_{1A}-AR knockout as a potential avenue to model epilepsy. However, very little is known about the prevalence α_{1A}-AR mutation in humans, or the potential ramifications for seizures or epilepsy.

While it is known that the α_{1A}-AR, as well as other ARs, exhibit a fair amount of constitutive activity, very little exists in the literature about whether this might be sufficient to explain the detrimental nature of α_{1A}-AR loss on seizure threshold that we observed. Confirmation studies performed during the construction of the α_{1A}-AR knockout strain did not reveal any compensatory increases in expression in other α_1-AR subtypes, which lends some credence to the constitutive activity hypothesis.

To our knowledge, there have only been a few documented case studies of α_1-AR manipulations and seizure-related consequences in humans. Briere *et al*. (1986) showed reduced α_1-AR density in human hippocampi from patients undergoing surgical resection for drug-resistant epilepsy. Additionally, a more recent case report presented that tamsulosin (Flomax) treatment, an α_1-AR-selective antagonist, exacerbated seizure prevalence in a patient with temporal lobe epilepsy, and that termination of tamsulosin treatment returned seizure prevalence to baseline(Ivanez *et al*., 2006). Both of these studies suggest an interesting potential correlation between α_1-ARs and seizure activity. Collectively, this research and these case studies may suggest the α_{1A}-AR as a potential biomarker in epilepsy.

Genetic testing in epilepsy is a growing but still immature field. While there have long been known specific mutations associated with the development of epilepsy (e.g. CDKL5, GLUT1, PCDH19, etc.) many epilepsies with clear patterns of inheritance

remain poorly understood genetically. Generally, there is little information about α_1-AR subtype gene status in epilepsies, possibly due the difficulties involved with protein quantification unreliability. Additionally, most genetic testing in epilepsy does not yet involve whole-genome sequencing techniques. Rather, most genetic testing in epilepsy is targeted at specific genes likely to be altered in seizure disorders, such as those associated with ion channels and pumps, or metabolic transporters like GLUT1. There are now several ongoing projects with aims to sequence the genomes of large populations of epilepsy patients, but most current available information focuses on broad chromosomal abnormalities. Even so, it is highly likely that genetic patterning in epilepsy will be highly heterogeneous and inconsistent based on the spectral and syndromic nature of the disease. We hope that our findings may encourage clinicians to implement analysis of α_1-AR subtype status in epilepsy.

Conclusions

This dissertation research has made significant contributions to our understanding of the functions and consequences of the α_{1A}-AR, especially pertaining to the role of this receptor to seizures and epilepsy. Our research took a translational approach, focusing on the functional consequences of α_{1A}-AR expression and activity, rather than a purely mechanistic approach. However, our experiments were meticulously planned in method and technique so that they were similar and complementary to our previous efforts to unravel the mechanism(s) of α_{1A}-AR action. We were especially careful to perform experiments which were translatable in vitro and in vivo. Thus, using deductive reasoning, we can build upon our previous conclusions to expand our current working hypothesis: α_{1A}-AR activation elicits antiepileptic effects, particularly a shift in seizure

threshold, likely mediated by increased resting membrane potential and increased rate of action potentials in hippocampal inhibitory interneurons, mediated via increased conductance of potassium channels and funny current. Put more simply, our observations suggest that α_{1A}-AR activity is critical for maintenance and modulation of excitatory-inhibitory balance in the brain, with measurable consequences for epileptic seizures.

More broadly, this research has significantly contributed to our understanding of the central noradrenergic system. We have developed novel methodologies for selectively measuring the contributions AR subtypes to NE action. The applicability of the findings in this dissertation are not limited only to seizures and should be easily transferable to other experimental paradigms. If not directly useful to a researcher, the techniques and methodologies used here clearly show the value of combining multiple approaches to understand a research question; for our experimental paradigm, the implementation of transgenics has become a necessity to further elucidate the mechanisms and functionality of the α_{1A}-AR. Eventually, it may become possible to selectively target and characterize the α_{1A}-AR using conventional methods, but current pharmacological ligand and antibody selectivity do not allow for the necessary accuracy and reproducibility to garner useful information. Interestingly, but not surprisingly, the efforts of our laboratory and those of our collaborators closely mimic the path of historic progression that has led the researchers of NE and the ARs to be so influential for the development of receptor theory, pharmacology, and many other fields. The noradrenergic system is extremely complex, but necessity is the mother of invention, or so they say.

Clinically, this research has significance in furthering our understanding of seizures, seizure threshold, and the potential of interneuron-based therapies in epilepsy. Our research showed the specific contributions of α_{1A}-AR activation to noradrenergic antiepileptic effects in multiple models of epilepsy. We showed evidence suggesting that α_{1A}-AR activation can partly mitigate actively-elicited epileptiform and seizure activity. While more difficult to measure and control for extraneous variables, the α_{1A}-AR may prove more efficacious in chronic models of epilepsy, where a shift in inhibitory threshold may be more consequential in the prevention of ictogenesis. These results seems especially worthwhile when considering our previous findings about the neurocognitive benefits of α_{1A}-AR activation; this presents a possibility that an α_{1A}-AR-based therapy may be dually beneficial as a seizure treatment with minimal, or possibly beneficial, neurocognitive consequences. Another fascinating contribution of this research were our findings which assessed the detrimental effect of α_{1A}-AR knockout on exacerbation of epileptiform characteristics and to spontaneous, recurrent epileptic seizures observed *in vivo*. While genetic and transcriptome analysis is still an emerging field in epilepsy, our findings strongly suggest that deleterious α_{1A}-AR mutations may increase vulnerability to ictogenesis.

Collectively, these results suggest potential clinical potential for the α_{1A}-AR both as an epilepsy therapy and potential biomarker. Finally, these results may also be applicable to neurocognitive disorders other than epilepsy. Our findings, and those of previous researchers, suggest that both α_{1A}-AR activation and loss-of-function has physiological consequences for neural circuit function. Thus, these findings may

translatable to many neurocognitive disorders which involve neurophysiological imparement.

References

Abel, J. J. (1899). Ueber den blutdruckerregenden Bestandtheil der Nebenniere, das Epinephrin. *Hoppe-Seyler's Zeitschrift Fur Physiologische Chemie*. 28(3-4).

Ahlquist, R. P. (1948). A STUDY OF THE ADRENOTROPIC RECEPTORS. *American Journal of Physiology*, *153*(3), 586–600.

Ahlquist, R. P. (1973). Adrenergic Receptors: A Personal and Practical View. *Perspectives in Biology and Medicine*, *17*(1), 119–122.

Akam, T., & Kullmann, D. M. (2010). Oscillations and filtering networks support flexible routing of information. *Neuron*, *67*(2), 308–320.

American Epilepsy Society (Ed.). (2019). FAQs. Retrieved October 31, 2019, from https://www.aesnet.org/clinical_resources/faqs.

Arnold P.S., Racine R.J., Wise P.A. (1973) Effects of atropine, reserpine, 6-hydroxydopamine and handling on seizure development in the rat. *Exp Neurol* 40, 457–70.

Arthur, G. (2015) Epinephrine: a short history. *Lancet Respiratory Med.* 3(5), 350-351.

Ashwin, P., Coombes, S., & Nicks, R. (2016). Mathematical Frameworks for Oscillatory Network Dynamics in Neuroscience. *Journal of Mathematical Neuroscience*. 6(1), 2

Aston-Jones G., Bloom F.E. (1981) Activity of norepinephrine-containing locus coeruleus neurons in behaving rats anticipates fluctuations in the sleep–waking cycle. *J Neurosci*. 1, 876–86.

Aston-Jones G., Chiang C., Alexinski T. (1991) Discharge of noradrenergic locus coeruleus neurons in behaving rats and monkeys suggests a role in vigilance. In: Barnes CD, Pompeiano O, editors. Progress in Brain Research, vol. 88. Amsterdam: Elsevier; 1991, pp. 501–520.

Aston-Jones G., Rajkowski J., Kubiak P., Alexinski, T. (1994) Locus coeruleus neurons in monkey are selectively activated by attended cues in a vigilance task. *J Neurosci*. 14, 4467–80.

Aston-Jones, G., & Cohen, J. D. (2005). AN INTEGRATIVE THEORY OF LOCUS COERULEUS-NOREPINEPHRINE FUNCTION: Adaptive Gain and Optimal Performance. *Annual Review of Neuroscience*.

Aston-Jones, G., & Waterhouse, B. (2016). Locus coeruleus: From global projection system to adaptive regulation of behavior. *Brain Research*.

Augustinack, J. C., van der Kouwe, A. J. W., Salat, D. H., Benner, T., Stevens, A. A., Annese, J., … Corkin, S. (2014). H.M.'s contributions to neuroscience: A review and autopsy studies. *Hippocampus*. 24(11), 1267-1286.

Bancaud, J., Henriksen, O., Rubio-Donnadieu, F., … , Penry, J.K. (1981) Proposal for Revised Clinical and Electroencephalographic Classification of Epileptic Seizures. *Epilepsia.* 22(4), 489-501.

Barzel, B., Sharma, A., & Barabási, A. L. (2013). Graph Theory Properties of Cellular Networks. In *Handbook of Systems Biology*.

Bayliss, A., & Evans, P. D. (2013). Characterisation of AmphiAmR4, an amphioxus (Branchiostoma floridae) α2-adrenergic-like G-protein-coupled receptor. *Invertebrate Neuroscience*. 13(1), 71-84.

Bean, B. P. (2007). The action potential in mammalian central neurons. *Nature Reviews Neuroscience*. 8(6), 461-465.

Beggs, J. M. (2008). The criticality hypothesis: How local cortical networks might optimize information processing. *Philosophical Transactions of the Royal Society A: Mathematical, Physical and Engineering Sciences*. 366(1864), 329-343.

Beggs, J. M., & Timme, N. (2012). Being critical of criticality in the brain. *Frontiers in Physiology*.

Ben-Ari, Y., & Cossart, R. (2000). Kainate, a double agent that generates seizures: Two decades of progress. *Trends in Neurosciences*. 23(11), 580-587.

Berényi, A., Belluscio, M., Mao, D., & Buzsáki, G. (2012). Closed-loop control of epilepsy by transcranial electrical stimulation. *Science*. 337(6095), 735-737.

Bergles, D. E., Doze, V. a, Madison, D. V, & Smith, S. J. (1996). Excitatory actions of norepinephrine on multiple classes of hippocampal CA1 interneurons. *The Journal of Neuroscience : The Official Journal of the Society for Neuroscience*, *16*(2), 572–585.

Bernard, C., Cossart, R., Hirsch, J. C., Esclapez, M., & Ben-Ari, Y. (2000). What is GABAergic Inhibition? How Is it Modified in Epilepsy? *Epilepsia*. Suppl 6, S90-95.

Black, A. R., & Black, J. D. (2012). Protein kinase C signaling and cell cycle regulation. *Frontiers in Immunology*. 3, 423.

Brière, R., Sherwin, A. L., Robitaille, Y., Olivier, A., Quesney, L. F., & Reader, T. A. (1986). α-1 Adrenoceptors are decreased in human epileptic foci. *Annals of Neurology*. 19(1), 26-30.

Buzsáki, G., Draguhn, A. (2004) Neuronal Oscillations in Cortical Networks. *Science.* June, 2004, 1926-1929.

Bylund, D.B. (2006). Adrenergic Receptors: Historical Perspectives from the 20th Century In D.M. Perez (1st Edition), The Receptors: The Adrenergic Receptors: In the 21st Century (pp. 3-21). Totowa, NJ: Humana Press.

Bylund, D. B., Eikenberg, D. C., Hieble, J. P., Langer, S. Z., Lefkowitz, R. J., Minneman, K. P., … Trendelenburg, U. (1994). IV. International union of pharmacology nomenclature of adrenoceptors. *Pharmacological Reviews*. 46(2), 121-136.

Cavalli, A., Lattion, A. L., Hummler, E., Nenniger, M., Pedrazzini, T., Aubert, J. F., … Cotecchia, S. (1997). Decreased blood pressure response in mice deficient of the α1b-adrenergic receptor. *Proceedings of the National Academy of Sciences of the United States of America*. 94(21), 11589-11594.

Chan, A. Y., Knowlton, R. C., Chang, E. F., & Rao, V. R. (2018). Seizure localization by chronic ambulatory electrocorticography. *Clinical Neurophysiology Practice*. 21(3), 174-176.

Choi, H., Sell, R. L., Lenert, L., Muennig, P., Goodman, R. R., Gilliam, F. G., & Wong, J. B. (2008). Epilepsy surgery for pharmacoresistant temporal lobe epilepsy: A decision analysis. *JAMA - Journal of the American Medical Association*. 3(300), 2497-2505.

Comin, C. H., & da Fontoura Costa, L. (2013). Shape, connectedness and dynamics in neuronal networks. *Journal of Neuroscience Methods*. 220(2), 100-115.

Copik, A. J., Baldys, A., Nguyen, K., Sahdeo, S., Ho, H., Kosaka, A., … Milla, M. E. (2015). Isoproterenol acts as a biased agonist of the alpha-1A-adrenoceptor that selectively activates the MAPK/ERK Pathway. *PLoS ONE*. 10(1), e0015701

Corcoran M.E., Mason S.T. (1980) Role of forebrain catecholamines in amygdaloid kindling. *Brain Res.* 190, 473–84.

Cotecchia, S., Schwinn, D. A., Randall, R. R., Lefkowitz, R. J., Caron, M. G., & Kobilka, B. K. (1988). Molecular cloning and expression of the cDNA for the hamster α1-adrenergic receptor. *Proceedings of the National Academy of Sciences of the United States of America*. 85(19), 7159-7163.

Crespo, P., Cachero, T. G., Xu, N., & Gutkind, J. S. (1995). Dual effect of β-adrenergic receptors on mitogen-activated protein kinase. Evidence for a βγ-dependent activation and a Gα(s)-cAMP-mediated inhibition. *Journal of Biological Chemistry*. 270 (42), 25259-25265.

Currie, K. P. M. (2010). Inhibition of Ca2+ channels and adrenal catecholamine release by G protein coupled receptors. *Cellular and Molecular Neurobiology*. 30(8), 1201-1208.

Dale, H. H. (1906). On some physiological actions of ergot. *The Journal of Physiology*. 34(3), 163-206.

DeGraff, J. L., Gagnon, A. W., Benovic, J. L., & Orsini, M. J. (1999). Role of arrestins in endocytosis and signaling of α 2 -adrenergic receptor subtypes. *Journal of Biological Chemistry*. 274(16), 11253-11259.

Dinocourt, C., Petanjek, Z., Freund, T. F., Ben-Ari, Y., & Esclapez, M. (2003). Loss of interneurons innervating pyramidal cell dendrites and axon initial segments in the CA1 region of the hippocampus following pilocarpine-induced seizures. *Journal of Comparative Neurology*. 459(4), 407-425.

Doze, V. A., Papay, R. S., Goldenstein, B. L., Gupta, M. K., Collette, K. M., Nelson, B. W., … Perez, D. M. (2011). Long-term α 1A-adrenergic receptor stimulation improves synaptic plasticity, cognitive function, mood, and longevity. *Molecular Pharmacology*. 80(4), 747-758.

Eisenhofer, G., Kopin, I. J., & Goldstein, D. S. (2004). Catecholamine metabolism: A contemporary view with implications for physiology and medicine. *Pharmacological Reviews*. 56(3), 331-349.

Engel, J., Wiebe, S., French, J., Sperling, M., Williamson, P., Spencer, D., … Enos, B. (2007). Appendix E: Practice parameter: Temporal lobe and localized neocortical resections for epilepsy: Report of the Quality Standards Subcommittee of the American Academy of Neurology, in Association with the American Epilepsy Society and the American Association of Neurological Surgeons. *CONTINUUM Lifelong Learning in Neurology*.

Englot, D. J., Birk, H., & Chang, E. F. (2017). Seizure outcomes in nonresective epilepsy surgery: an update. *Neurosurgical Review*. 40(2), 181-194.

Finch, A.M., Sarramegna, V., & Graham, R.M. (2006). Ligand Binding, Activation, and Agonist Trafficking In D.M. Perez (1st Edition), The Receptors: The

Adrenergic Receptors: In the 21st Century (pp. 25-85). Totowa, NJ: Humana Press.

Fisher, R. S., Cross, J. H., French, J. A., Higurashi, N., Hirsch, E., Jansen, F. E., … Zuberi, S. M. (2018). Operational classification of seizure types by the International League Against Epilepsy: position paper of the ILAE Commission for Classification and Terminology. *Epilepsia.* 58(4), 522-530.

Foote, S. L., Bloom, F. E., & Aston Jones, G. (1983). Nucleus locus ceruleus: New evidence of anatomical and physiological specificity. *Physiological Reviews*. 63(3), 844-914.

Fornito, A., Zalesky, A., & Bullmore, E. T. (2016). An Introduction to Brain Networks In Fundamentals of Brain Network Analysis. *Elsevier.*

Furchgott, R. (1967). The pharmacological differentiation of adrenergic receptors. *Ann NY Acad Sci*. 139(3), 553-570.

García-Sáinz, J. A., & Torres-Padilla, M. E. (1999). Modulation of basal intracellular calcium by inverse agonists and phorbol myristate acetate in rat-1 fibroblasts stably expressing α(1d)-adrenoceptors. *FEBS Letters*.

Giorgi, F. S., *et al*. (2004) The role of norepinephrine in epilepsy: from the bench to the bedside. *Neurosci. Biobehav. Rev.* 28, 507–524.

Gisbert, R., Noguera, M. A., Ivorra, M. D., & D'Ocon, P. (2000). Functional evidence of a constitutively active population of α(1D)-adrenoceptors in rat aorta. *Journal of Pharmacology and Experimental Therapeutics*. 443(3), 277-281.

Goldenstein, B. L., Nelson, B. W., Xu, K., Luger, E. J., Pribula, J. A., Wald, J. M., … Doze, V. A. (2009). Regulator of G protein signaling protein suppression of Gαo protein-mediated α2A adrenergic receptor inhibition of mouse hippocampal CA3 epileptiform activity. *Molecular Pharmacology*. 75(5), 1222-1230.

Guldberg CM, Waage P. (1879) Concerning chemical affinity. *Erdmann's J Prac Chem*. 127, 69-114.

Granneman, J. G. (2001). The putative b4-adrenergic receptor is a novel state of the b1-adrenergic receptor. *American Journal of Physiology - Endocrinology and Metabolism*. 280(2), E199-202.

Grubbs, D. S., & Worley, D. S. (1983). New technique for reducing the impedance of silver-silver chloride electrodes. *Medical & Biological Engineering & Computing*. 21(2), 232-234.

Halls, M. L., & Cooper, D. M. F. (2017). Adenylyl cyclase signalling complexes – Pharmacological challenges and opportunities. *Pharmacology and Therapeutics*. 172, 171-180.

Hein, P., & Michel, M. C. (2007). Signal transduction and regulation: Are all α1-adrenergic receptor subtypes created equal? *Biochemical Pharmacology*. 73(8), 1097-1106.

Hellier, J. L., Patrylo, P. R., Buckmaster, P. S., & Dudek, F. E. (1998). Recurrent spontaneous motor seizures after repeated low-dose systemic treatment with kainate: Assessment of a rat model of temporal lobe epilepsy. *Epilepsy Research*. 31(1), 73-84.

Hesse, J., & Gross, T. (2014). Self-organized criticality as a fundamental property of neural systems. *Frontiers in Systems Neuroscience*. 23(8),166.

Hieble, J. P., Bylund, D. B., Clarke, D. E., Eikenburg, D. C., Langer, S. Z., Lefkowitz, R. J., … Ruffolo, R. R. (1995). International union of pharmacology. X. Recommendation for nomenclature of α1-adrenoceptors: Consensus update. *Pharmacological Reviews*. 47(2), 267-270.

Hillman, K. L., Doze, V. A., & Porter, J. E. (2005). Functional characterization of the β-adrenergic receptor subtypes expressed by CA1 pyramidal cells in the rat hippocampus. *Journal of Pharmacology and Experimental Therapeutics*. 314(2), 561-567.

Hillman, K. L., Doze, V. A., & Porter, J. E. (2007). α1A-adrenergic receptors are functionally expressed by a subpopulation of cornu ammonis 1 interneurons in rat hippocampus. *Journal of Pharmacology and Experimental Therapeutics*. 321(3), 1062-1068.

Hillman, K. L., Lei, S., Doze, V. A., & Porter, J. E. (2009). Alpha-1A adrenergic receptor activation increases inhibitory tone in CA1 hippocampus. *Epilepsy Research*. 84(2-3), 97-109.

Hirtz, D., Thurman, D. J., Gwinn-Hardy, K., Mohamed, M., Chaudhuri, A. R., & Zalutsky, R. (2007). How common are the "common" neurologic disorders? *Neurology*, *68*(5), 326–337.

Hodgkin, A. L. & Huxley, A. F. (1952) A quantitative description of membrane current and its application to conduction and excitation in nerve. *J. Physiol.* **117**, 500–544.

Hwa, J., Graham, R. M., & Perez, D. M. (1995). Identification of critical determinants of α1-adrenergic receptor subtype selective agonist binding. *Journal of Biological Chemistry*. 270(39), 23189-23195.

Hwa, J., Graham, R. M., & Perez, D. M. (1996). Chimeras of α1-adrenergic receptor subtypes identify critical residues that modulate active state isomerization. *Journal of Biological Chemistry*. 271(14), 7956-7964.

International League Against Epilepsy (2003) The Effects of Medication on Quality of Life. *Epilepsia.* 44, s60.

Isaev, D., Ivanchick, G., Khmyz, V., Isaeva, E., Savrasova, A., Krishtal, O., … Maximyuk, O. (2012). Surface charge impact in low-magnesium model of seizure in rat hippocampus. *Journal of Neurophysiology*. 107(1), 417-423.

Iváñez, V., & Ojeda, J. (2006). Exacerbation of seizures in medial temporal lobe epilepsy due to an α1-adrenergic antagonist. *Epilepsia*. 47(10), 1741-1742.

Jensen, B. C., Swigart, P. M., & Simpson, P. C. (2009). Ten commercial antibodies for alpha-1-adrenergic receptor subtypes are nonspecific. *Naunyn-Schmiedeberg's Archives of Pharmacology*. 379(4), 409-412.

Jiang, X., Lachance, M., & Rossignol, E. (2016). Involvement of cortical fast-spiking parvalbumin-positive basket cells in epilepsy. In *Progress in Brain Research*. 226, 81-126.

Jiang, K. (2018). Butterflies of the Soul. Retrieved October 31, 2019, from https://hms.harvard.edu/news/butterflies-soul.

Jimenez-Rivera C., Voltura A., Weiss G.K. (1986) Effect of locus coeruleus stimulation on the development of kindled seizures. *Exp Neurol*. 95, 13–20.

Jirsa, V. K., Stacey, W. C., Quilichini, P. P., Ivanov, A. I., & Bernard, C. (2014). On the nature of seizure dynamics. *Brain*. 137(Part 8), 2210-2230.

Jobst, B. C., Kapur, R., Barkley, G. L., Bazil, C. W., Berg, M. J., Bergey, G. K., … Morrell, M. J. (2017). Brain-responsive neurostimulation in patients with medically intractable seizures arising from eloquent and other neocortical areas. *Epilepsia*. 58(6), 1005-1014.

Jurgens, C. W. D., Boese, S. J., King, J. D., Pyle, S. J., Porter, J. E., & Doze, V. A. (2005). Adrenergic receptor modulation of hippocampal CA3 network activity. *Epilepsy Research*. 66(1-3), 117-128.

Jurgens, C. W. D., Rau, K. E., Knudson, C. A., King, J. D., Carr, P. A., Porter, J. E., & Doze, V. A. (2005b). β1 adrenergic receptor-mediated enhancement of hippocampal CA3 network activity. *Journal of Pharmacology and Experimental Therapeutics*. 314(2), 552-560.

Jurgens, C. W. D., Hammad, H. M., Lichter, J. A., Boese, S. J., Nelson, B. W., Goldenstein, B. L., … Doze, V. A. (2007). α2A adrenergic receptor activation

inhibits epileptiform activity in the rat hippocampal CA3 region. *Molecular Pharmacology*. 71(6), 1572-1581.

Kaufman, S., Friedman, S. (1965) DOPAMINE-β-HYDROXYLASE. *Pharmacological Reviews*. 17(2), 71-100.

Kenakin, T. (2016) The Mass Action Equation in Pharmacology. *Br J Clin Phamacol*. 81(1), 41-51.

Kepecs, A., & Fishell, G. (2014). Interneuron Cell Types are Fit to Function. *Nature*. 505(7483), 318-326.

Knudson, C.A. (2007) Characterization of Adrenergic Receptor Subtypes in the Rodent Hippocampus. University of North Dakota Doctoral Dissertation. Ann Arbor, MI. ProQuest, LLC.

Kobilka B.K. (2013) Brian Kobilka – Biographical. NobelPrize.org. Nobel Media AB 2019. October 2019.

Kobilka, B. K., Matsui, H., Kobilka, T. S., Yang-Feng, T. L., Francke, U., Caron, M. G., … Regan, J. W. (1987). Cloning, sequencing, and expression of the gene coding for the human platelet α2-adrenergic receptor. *Science*. 238(4827), 650-656.

Koch, W. J., Hawes, B. E., Allen, L. F., & Lefkowitz, R. J. (1994). Direct evidence that G(i)-coupled receptor stimulation of mitogen- activated protein kinase is mediated by G(βγ) activation of p21(ras). *Proceedings of the National Academy of Sciences of the United States of America*. 91(26), 12706-12710.

Krook-Magnuson, E., Gelinas, J. N., Soltesz, I., & Buzsáki, G. (2015). Neuroelectronics and biooptics: Closed-loop technologies in neurological disorders. *JAMA Neurology*. 72(7), 823-829.

Le Duigou, C., Simonnet, J., Teleñczuk, M. T., Fricker, D., & Miles, R. (2014). Recurrent synapses and circuits in the CA3 region of the hippocampus: An associative network. *Frontiers in Cellular Neuroscience*. 8(7), 262.

Lefkowitz, R. J. (2007). Seven transmembrane receptors: Something old, something new. In *Acta Physiologica*. 190(1), 9-19.

Lefkowitz, R. J. (2013). A brief history of G-protein coupled receptors (Nobel Lecture). *Angewandte Chemie - International Edition*.

Lefkowitz, R. J., & Shenoy, S. K. (2005). Transduction of receptor signals by β-arrestins. *Science*. 308(5721), 512-517.

Lefkowitz, R.J. (1979) Direct Binding Studies of Adrenergic Receptors: Biochemical, Physiologic, and Clinical Implications. *Ann Intern Med.* 91, 450–458.

Lomasney, J. W., Cotecchia, S., Lorenz, W., Leung, W. Y., Schwinn, D. A., Yang-Feng, T. L., … Caron, M. G. (1991). Molecular cloning and expression of the cDNA for the α(1A)-adrenergic receptor: The gene for which is located on human chromosome 5. *Journal of Biological Chemistry*. 266(10), 6365-6369.

Lymperopoulos, A., Brill, A., & McCrink, K. A. (2016). GPCRs of adrenal chromaffin cells & catecholamines: The plot thickens. *International Journal of Biochemistry and Cell Biology*. 77(Pt B), 213-219.

Magiorkinis, E., Diamantis, A., Sidiropoulou, K., & Panteliadis, C. (2014). Highights in the History of Epilepsy: The Last 200 Years. *Epilepsy Research and Treatment*. 2014, 582039.

McCormick, D.A. (2008). Membrane Potential and Action Potential In L. Squire (3rd Edition), Fundamental Neuroscience (pp. 15-22). San Diego, CA: Elsevier.

McCune, D. F., Edelmann, S. E., Olges, J. R., Post, G. R., Waldrop, B. A., Waugh, D. J. J., … Piascik, M. T. (2000). Regulation of the cellular localization and signaling properties of the α(1B)- and α(1D)-adrenoceptors by agonists and inverse agonists. *Molecular Pharmacology*. 57(4), 659-666.

McIntyre D.C., Edson N., Chao G., Knowles V. (1982) Differential effect of acute vs chronic desmethylimipramine on the rate of amygdala kindling in rats. *Exp Neurol*. 78, 158–166.

McIntyre D.C., Saari M., Pappas B.A. (1979) Potentiation of amygdala kindling in adult or infants rats by injections of 6-hydroxydopamine. *Exp Neurol*. 63, 527–544.

McIntyre D.C., Wong R.K. (1986) Cellular and synaptic properties of amygdala-kindled piriform cortex in vitro. *J Neurophysiol*. 55, 1295–1307.

McIntyre D.C. (1981) Catecholamines involvement in amygdala kindling of the rat. In: Wada JA, editor. Kindling. New York: Raven Press; pp. 67–80.

Miles, R., & Wong, R. K. (1986). Excitatory synaptic interactions between CA3 neurones in the guinea-pig hippocampus. *The Journal of Physiology*. 373, 397-418.

Miles, R., & Wong, R. K. S. (1983). Single neurones can initiate synchronized population discharge in the hippocampus. *Nature*. 306(5941), 371-373.

Miles, R., & Wong, R. K. S. (1987). Latent synaptic pathways revealed after tetanic stimulation in the hippocampus. *Nature*. 329(6141), 724-726.

Millett, D. (2009). Chapter 26 A history of seizures and epilepsies. From the falling disease to dysrhythmias of the brain. In *Handbook of Clinical Neurology*.

Mishra P.K., Burger R.L., Bettendorf A.F., Browning R.A., Jobe P.C. (1994) The role of norepinephrine in forebrain and brainstem seizures: chemical lesioning of locus coeruleus with DSP4. *Exp Neurol*. 125, 58–64.

Molnoff, P. & Axelrod, J. (1971) Biochemistry of Catecholamines. *Annual Review of Biochemistry*. 40, 465-500.

Muramatsu, I., Murata, S., Isaka, M., Piao, H. L., Zhu, J., Suzuki, F., … Taniguchi, T. (1998). α1-adrenoceptor subtypes and two receptor systems in vascular tissues. In *Life Sciences*. 62(17-18), 1461-1465.

Nagaraj, V., Lee, S. T., Krook-Magnuson, E., Soltesz, I., Benquet, P., Irazoqui, P. P., & Netoff, T. I. (2015). Future of seizure prediction and intervention: Closing the loop. *Journal of Clinical Neurophysiology*. 32(3), 194-206.

Nagatsu, T., Levitt, M., & Udenfriend, S. (1964). TYROSINE HYDROXYLASE. THE INITIAL STEP IN NOREPINEPHRINE BIOSYNTHESIS. *The Journal of Biological Chemistry*. 239, 2910-2917.

Ovsepian, S. V. (2019). The dark matter of the brain. *Brain Structure and Function*. 224(3), 973-983.

Papay, R., Gaivin, R., Jha, A., McCune, D. F., McGrath, J. C., Rodrigo, M. C., … Perez, D. M. (2006). Localization of the mouse α 1A-adrenergic receptor (AR) in the brain: α 1AAR is expressed in neurons, GABAergic interneurons, and NG2 oligodendrocyte progenitors. *Journal of Comparative Neurology*. 497(2), 209-222.

Parascandola, J. (2010). Abel, Takamine, and the isolation of epinephrine. *The Journal of Allergy and Clinical Immunology*. 125(2), 514-517.

Petersen, B., Walker, M.L., Runge, U., Kessler, C. (1998) Quality of life in patients with idiopathic, generalized epilepsy. *Journal of Epilepsy.* 11, 306-13.

Piascik, M.T., Garcia-Cazarin, M.L., & Post, S.R. (2006). Regulation of the Cellular Localization and Trafficking of the Adrenergic Receptors In D.M. Perez (1st Edition), The Receptors: The Adrenergic Receptors: In the 21st Century (pp. 107-128). Totowa, NJ: Humana Press.

Pizzanelli, C. *et al*. (2009) Lack of α1b-adrenergic receptor protects against epileptic seizures. *Epilepsia.* 50, 59-64.

Poil, S. S., Van Ooyen, A., & Linkenkaer-Hansen, K. (2008). Avalanche dynamics of human brain oscillations: Relation to critical branching processes and temporal correlations. *Human Brain Mapping*. 29(7), 770-777.

Pupo, A. S., & Minneman, K. P. (2003). Specific Interactions Between gC1qR and α1-Adrenoceptor Subtypes. *Journal of Receptors and Signal Transduction*. 23(2-3), 185-195.

Ramani, R. (2008). Vagus nerve stimulation therapy for seizures. *Journal of Neurosurgical Anesthesiology*. 20(1), 29-35.

Rasmussen, S. G. F., Choi, H. J., Rosenbaum, D. M., Kobilka, T. S., Thian, F. S., Edwards, P. C., … Kobilka, B. K. (2007). Crystal structure of the human β2 adrenergic G-protein-coupled receptor. *Nature*. 450(7168), 383-387.

Rasmussen, S. G., DeVree, B. T., Zou, Y., Kruse, A. C., Chung, K. Y., Kobilka, T. S., … Kobilka, B. K. (2011). Crystal structure of the β2 adrenergic receptor-Gs protein complex. *Nature*, *477*(7366), 549–555.

Riss, J., Cloyd, J., Gates, J., & Collins, S. (2008). Benzodiazepines in epilepsy: Pharmacology and pharmacokinetics. *Acta Neurologica Scandinavica*. 118(2), 69-86.

Roberts, J. A., Boonstra, T. W., & Breakspear, M. (2015). The heavy tail of the human brain. *Current Opinion in Neurobiology*. 31, 164-172.

Rokosh, D. G., & Simpson, P. C. (2002). Knockout of the α1A/C-adrenergic receptor subtype: The α1A/C is expressed in resistance arteries and is required to maintain arterial blood pressure. *Proceedings of the National Academy of Sciences of the United States of America*. 99(14), 9474-9479.

Sampaio, L. P. de B. (2016). Ketogenic diet for epilepsy treatment. *Arquivos de Neuro-Psiquiatria*. 74(10), 842-848.

Schachter, Steven C. "What Causes Epilepsy and Seizures?" Epilepsy Foundation, www.epilepsy.com/learn/about-epilepsy-basics/what-causes-epilepsy-and-seizures.

Schevon, C. A., Weiss, S. A., McKhann, G., Goodman, R. R., Yuste, R., Emerson, R. G., & Trevelyan, A. J. (2012). Evidence of an inhibitory restraint of seizure activity in humans. *Nature Communications*. 3, 1060.

Schild, H.O. (1997) Dale and the Development of Pharmacology. *Br J Pharm*. 120(Suppl 1): 504–508.

Segal, M., & Bloom, F. E. (1974). The action of norepinephrine in the rat hippocampus. I. Iontophoretic studies. *Brain Research*.

Shafer, P. (2015) Epilepsy statistics. *Epilepsy Foundation*.

Shoham, S., O'Connor, D. H., & Segev, R. (2006). How silent is the brain: Is there a "dark matter" problem in neuroscience? *Journal of Comparative Physiology A: Neuroethology, Sensory, Neural, and Behavioral Physiology*. 192(8), 777-784.

Shorvon, S. D. (2009). Drug treatment of epilepsy in the century of the ILAE: The first 50 years, 1909-1958. *Epilepsia*. 50(Suppl 3), 69-92.

Shorvon, S. D. (2009b). Drug treatment of epilepsy in the century of the ILAE: The second 50 years, 1959-2009. *Epilepsia*. 50(Suppl 3), 93-130.

Simpson, P.C. (2006). The a_1-Adrenergic Receptors: Lessons From Knockouts In D.M. Perez (1st Edition), The Receptors: The Adrenergic Receptors: In the 21st Century (pp. 207-240). Totowa, NJ: Humana Press.

Simpson, K.L., Lin, R.C.S. (2007). Neuroanatomical and Chemical Organization of the Locus Coeruleus In G.A. Ordway (1st Edition), Brain Norepinephrine (pp. 9-52). Cambridge, NY: Cambridge University Press.

Sporns, O. (2018). Graph theory methods: applications in brain networks. *Dialogues in Clinical Neuroscience*. 20(2), 111-121.

Stief, F., Zuschratter, W., Hartmann, K., Schmitz, D., & Draguhn, A. (2007). Enhanced synaptic excitation-inhibition ratio in hippocampal interneurons of rats with temporal lobe epilepsy. *European Journal of Neuroscience*. 25(2), 519-528.

Swanson, L.W. (2008). Basic Plan of the Nervous System In L. Squire (3rd Edition), Fundamental Neuroscience (pp. 15-22). San Diego, CA: Elsevier.

Szilagyi, T., Szava, I., Metz, E.J., Mihaly, I. & Orban-Kis, K. (2014) Untangling the pathomechanisms of temporal lobe epilepsy-The promise of epileptic biomarkers and novel therapeutic approaches. *Brain Research Bulletin.* 109, 1-12.

Takamine, J. (1901) Adrenalin the Active Principle of the Suprarenal Glands and Its Mode of Preparation. *Am J Pharm*. Periodicals Series II Nov 1901: 523.

Tang, Y., Hu, L. A., Miller, W. E., Ringstad, N., Hall, R. A., Pitcher, J. A., … Lefkowitz, R. J. (1999). Identification of the endophilins (SH3p4/p8/p13) as novel binding partners for the β1-adrenergic receptor. *Proceedings of the National Academy of Sciences of the United States of America*. 96(22), 12559-12564.

Traub, R. D., & Wong, R. K. S. (1982). Cellular mechanism of neuronal synchronization in epilepsy. *Science*. 216(4547), 745-747.

Traub, R. D., Cunningham, M. O., & Whittington, M. A. (2014). What is a seizure network? Very fast oscillations at the interface between normal and epileptic brain. *Advances in Experimental Medicine and Biology*. 813, 71-80.

Trevelyan, A. J., Sussillo, D., Watson, B. O., & Yuste, R. (2006). Modular propagation of epileptiform activity: Evidence for an inhibitory veto in neocortex. *Journal of Neuroscience*. 26(48), 12447-12455.

Tse, K., Puttachary, S., Beamer, E., Sills, G. J., & Thippeswamy, T. (2014). Advantages of repeated low dose against single high dose of kainate in C57BL/6J mouse model of status epilepticus: Behavioral and electroencephalographic studies. *PLoS ONE*. 9(5), e96622.

Ułamek-Kozioł M., Czuczwar S.J., Januszewski S., Pluta R. (2019) Ketogenic Diet and Epilepsy. *Nutrients*. 11(10), E2510.

Vossler, D.G., Weingarten, M., Gidal, B.E. (2018) Summary of Antiepileptic Drugs Available in the United States of America. American Epilepsy Society.

Wang, Q., & Limbird, L. E. (2002). Regulated interactions of the α2A adrenergic receptor with spinophilin, 14-3-3ζ, and arrestin 3. *Journal of Biological Chemistry*. 277(52), 50589-50596.

Weinshenker, D., & Szot, P. (2002). The role of catecholamines in seizure susceptibility: New results using genetically engineered mice. *Pharmacology and Therapeutics*. 94(3), 213-233.

Weinshilboum, R., & Axelrod, J. (1971). Serum dopamine-beta-hydroxylase activity. *Circulation Research*. 28(3), 307-315.

Weiss, S. A., McKhann, G., Goodman, R., Emerson, R. G., Trevelyan, A., Bikson, M., & Schevon, C. A. (2013). Field effects and ictal synchronization: Insights from in homine observations. *Frontiers in Human Neuroscience*. 7, 828.

Werner, G. (2007). Brain dynamics across levels of organization. *Journal of Physiology Paris*. 101(4-6), 273-279.

Westfield, G. H., Rasmussen, S. G., Su, M., Dutta, S., DeVree, B. T., Chung, K. Y., … Skiniotis, G. (2011). Structural flexibility of the G alpha s alpha-helical domain in the beta2-adrenoceptor Gs complex. *Proceedings of the National Academy of Sciences of the United States of America*, *108*(38), 16086–16091.

Wick, J. Y. (2013). The history of benzodiazepines. *Consultant Pharmacist*. 28(9), 538-548.

Wirrell, E. (2019). Epilepsy Due to Specific Causes. Retrieved October 31, 2019, from https://www.epilepsy.com/learn/epilepsy-due-specific-causes.

Wisler, J. W., Rockman, H. A., & Lefkowitz, R. J. (2018). Biased G Protein-Coupled Receptor Signaling: Changing the Paradigm of Drug Discovery. *Circulation*, *137*(22), 2315–2317.

Wolf, P. (2014). History of epilepsy: Nosological concepts and classification. *Epileptic Disorders*. 16(3), 261-269.

Xu, Z., Hirasawa, A., Shinoura, H., Tsujimoto, G. (1999) Interaction of the alpha(1B)-adrenergic receptor with gC1q-R, a multifunctional protein. *J Biol Chem*. 274(30):21149-54.

Yin, Y. H., Ahmad, N. & Makmor-Bakry, M. (2013) Pathogenesis of epilepsy: Challenges in animal models. *Iran. J. Basic Med. Sci.* 16, 1119–1132.

Zhang, M., Ladas, T. P., Qiu, C., Shivacharan, R. S., Gonzalez-Reyes, L. E., & Durand, D. M. (2014). Propagation of epileptiform activity can be independent of synaptic transmission, gap junctions, or diffusion and is consistent with electrical field transmission. *Journal of Neuroscience*. 34(4), 1409-1419.

Zuscik, M. J., Sands, S., Ross, S. A., Waugh, D. J., Gaivin, R. J., Morilak, D., & Perez, D. M. (2000). Overexpression of the alpha1B-adrenergic receptor causes apoptotic neurodegeneration: multiple system atrophy. *Nature Medicine*, *6*(12), 1388–1394.